Two-Dimensional Modeling of the Effect of Relative Humidity on Volatile Organic Compounds Adsorption in a Fixed Bed Adsorber

by

Imranul Islam Laskar

A thesis submitted in partial fulfillment of the requirements for the degree of

Master of Science

in

Environmental Engineering

Department of Civil and Environmental Engineering

University of Alberta

ABSTRACT

Water vapor can affect adsorption of volatile organic compound (VOC) onto activated carbon. In this research, a two-dimensional heterogenous computational fluid dynamics model was developed and validated to understand the mechanism and kinetics during competitive adsorption between VOC and water vapor in a beaded activated carbon (BAC) fixed-bed adsorber. The model comprised of a VOC-water vapor multicomponent competitive adsorption isotherm and governing transport phenomena equations. The multicomponent competitive adsorption isotherm was based on Manes method, which requires only single-component adsorption isotherms of adsorbates as inputs. Consequently, a modified Dubinin-Radushkevich (MDR) isotherm equation and Qi-Hay-Rood (QHR) isotherm equation were used to describe the pure single-component adsorption equilibrium of VOC (type I) and water vapor (type V), respectively. The MDR and QHR isotherm equations fitted the experimental data of pure VOC adsorption and water vapor adsorption on BAC with an overall r^2 value of 0.998 and 0.999 respectively. The governing transport phenomena component of the model consists of macroscopic mass, momentum, and energy conversation equations. The model predicted the competitive adsorption isotherms, breakthrough and bed temperature profiles of selected VOCs (2-propanol, acetone, toluene, n-butanol, 1,2,4-trimethylbenzene) with a mean relative absolute error (MRAE) of 3.6%, 15.4% and 2.2% respectively. Sensitivity analysis was also conducted to test the robustness of the model in detecting the impact of relative humidity (RH) on VOC adsorption with change in adsorption temperature and inlet adsorbate concentration; and an overall MRAE of 6.6% was observed between the experimental and simulated results. The model, hence, can be used for optimizing adsorber design and operating conditions to minimize the impact of RH during adsorption of contaminants from gas streams.

I dedicate this dissertation to my beloved parents, Saleha and Ashraful-Haque, my dearest grandparents, Abdul-Latif and Aklasun-Nessa, and my adorable sister, Sabina. They have been a constant source of support, motivation, and perseverance for me throughout my life.

ACKNOWLEDGEMENTS

First and foremost, I would like to express my deepest gratitude to my supervisor, Dr. Zaher Hashisho, for his supervision, guidance and generous support throughout my course work and research. I highly appreciate his invaluable comments and continuous feedback throughout my MSc research. This work could not have been accomplished without his profound knowledge, guidance and passion.

I would like to acknowledge the financial support from the Ford Motor Company, and the Natural Sciences and Engineering Research Council (NSERC) of Canada.

I would also like to thank my colleagues in Air Quality Characterization Lab, for their suggestions and assistance in my experiments.

I am grateful to the technicians in the Department of Civil and Environmental Engineering, Chen Liang and David Zhao, for their help and support during this research work.

Finally, I would like to thank my friends and anyone who directly or indirectly have lent their helping hands in this research.

TABLE OF CONTENTS

ABSTRACT ii

ACKNOWLEDGEMENTS v

TABLE OF CONTENTS vi

LIST OF TABLES ix

LIST OF FIGURES x

LIST OF ACRONYMS xii

CHAPTER 1 INTRODUCTION 1

- 1.1 Background 2
    - 1.1.1 Volatile Organic Compounds (VOCs) 2
    - 1.1.2 Sources of VOCs emissions 2
    - 1.1.3 Impact of VOCs on Human Health and Environment 3
    - 1.1.4 Methods and Techniques to Curb VOCs Emissions 4
    - 1.1.5 Importance of Mathematical Modeling in Adsorption 5
- 1.2 Problem Statement 6
- 1.3 Research Objectives 7
- 1.4 Research Significance 8
- 1.5 Thesis Outline 9
- 1.6 References 10

CHAPTER 2 LITERATURE REVIEW 16

- 2.1 Competitive Adsorption of Water Vapor and VOCs 17
    - 2.1.1 Special Behaviour of Water Vapor on Activated Carbon 17
    - 2.1.2 Impact of Relative Humidity on Adsorption Capacity for VOCs 19
- 2.2 Adsorption Isotherm Models for Predicting Equilibria 21
    - 2.2.1 Single-Component Adsorption Isotherm Models for VOCs 22
        - 2.2.1.1 Langmuir Isotherm Model 22
        - 2.2.1.2 Freundlich Isotherm Model 23
        - 2.2.1.3 Brunauer-Emmett-Teller Isotherm Model 23
        - 2.2.1.4 Toth Isotherm Model 24
        - 2.2.1.5 Dubinin-Radushkevich Isotherm Model 25
        - 2.2.1.6 Dubinin-Astakhov Isotherm Model 27
        - 2.2.1.7 Modified Dubinin-Radushkevich Isotherm Model 27
    - 2.2.2 Single-Component Adsorption Isotherm Models for Water Vapor 29

2.2.2.1 Modified Dubinin-Astakhov Isotherm Model 29
2.2.2.2 Dubinin-Serpinski Isotherm Model 30
2.2.2.3 Qi-Hay-Rood Isotherm Model 31
2.2.2.4 Talu-Meunier Isotherm Model 33
2.2.2.5 Qi-LeVan Isotherm Model 34
2.2.2.6 Do and Do Isotherm Model 35
2.2.3 Multicomponent Competitive Adsorption Isotherm Models 36
2.2.3.1 Jain and Snoeyink's Extended Langmuir Isotherm Model 36
2.2.3.2 Ideal Adsorbed Solution Theory 39
2.2.3.3 Real Adsorbed Solution Theory 42
2.2.3.4 Vacancy Solution Model 44
2.2.3.5 Method of Chou and Chiou 45
2.2.3.6 Virial Mixture Coefficient Method 46
2.2.3.7 Method of Doong and Yang 48
2.2.3.8 Method of Okazaki, Tamon and Toei 50
2.2.3.9 Method of Manes 52
2.3 Summary and Conclusions 55
2.4 References 62
Chapter 3 MATERIALS AND METHODS 69
3.1 Experimental Setup and Method 70
3.2 Model Development 74
3.2.1 Physical Model 74
3.2.2 VOC-Water Vapor Multicomponent Adsorption Isotherm Formulation 81
3.2.2.1 Input Parameters for Manes Method 83
3.2.2.1.1 Pure Single-Component VOC Adsorption Isotherm 83
3.2.2.1.2 Pure Single-Component Water Vapor Adsorption Isotherm 83
3.2.2.2 Solving Manes Method 84
3.2.3 Transport Phenomena Formulation 90
3.2.3.1 Governing Transport Phenomena 90
3.2.3.1.1 Gas-Phase Mass Balance 90
3.2.3.1.2 Adsorbed-Phase Mass Balance 92
3.2.3.1.3 Momentum Balance 93
3.2.3.1.4 Energy Balance 94

3.2.3.2 Variable and Parameters Definition 95
3.2.3.3 Initial and Boundary Conditions 96
3.2.3.4 Solution Method 96
3.3 Model Validation Method 97
3.4 References 100
Chapter 4 RESULTS AND DISCUSSION 104
4.1 Validation of Pure Single-Component Isotherms 105
4.2 Validation of VOC-Water Vapor Multicomponent Competitive Adsorption Isotherm 109
4.3 Validation of Adsorption Breakthrough Profiles 116
4.4 Absorbed-Phase Concentration Distribution 120
4.5 Absorber Bed Temperature Distribution 123
4.5 Sensitivity Analysis 127
4.5.1 Effect of Adsorption Temperature 127
4.5.2 Effect of Inlet Gas Concentration 128
4.6 References 131
Chapter 5 CONCLUSIONS AND RECOMMENDATIONS 133
5.1 Thesis Overview 134
5.2 Conclusions 135
5.3 Recommendations for Future Work 137
5.4 References 139
WORKS CITED 140
APPENDIX A MATLAB CODE FOR MANES METHOD 153

LIST OF TABLES

Table 2-1. Advantages and disadvantages of the commonly used adsorption isotherms........... 57
Table 3-1. Model variables and parameters 76
Table 3-2. Initial and boundary conditions... 96
Table 4-1. Multitemperature fitting parameters of MDR isotherms for adsorption of pure VOCs on BAC at 298.15 K 105
Table 4-2. Multitemperature fitting parameters of QHR isotherm for adsorption of pure water vapor on BAC at 298.15 K 109
Table 4-3. Physical properties of the selected adsorbates (Haynes, 2017) 114
Table 4-4. Surface diffusion, pore diffusion, and external mass transfer coefficient of the selected adsorbates at 298.15 K 117

LIST OF FIGURES

Figure 3-1. Bench-scale experimental setup for competitive adsorption between VOC and water vapor. 72

Figure 3-2. Simplification of the simulated adsorption unit into an 2D axisymmetric geometry. 75

Figure 3-3. Flowchart describing the procedure to numerically solve Manes-method and its extension for water-miscible VOCs. 88

Figure 4-1. Experimental and fitted MDR isotherms for (a) toluene, (b) n-butanol, (c) 1,2,4-TMB, (d) acetone, (e) 2-propanol adsorption onto BAC at 298.15 K. 107

Figure 4-2. Experimental and fitted QHR isotherm for water adsorption onto BAC at 298.15 K. 108

Figure 4-3. Polar versus non-polar VOC: comparison of experimental and modeled equilibrium adsorption capacities of (a) VOC and (b) water vapor during their competitive adsorption on BAC at 298.15 K. 111

Figure 4-4. 2D competitive adsorption isotherm for water vapor and non-polar VOC at 298.15 K on BAC: Amount of (a) toluene, (b) water vapor adsorbed in toluene-water vapor system; (c) n-butanol, (d) water vapor adsorbed in n-butanol-water vapor system; (e) 1,2,4-TMB, (f) water vapor adsorbed in 1,2,4-TMB-water vapor system. 115

Figure 4-5. 2D competitive adsorption isotherm for water vapor and polar VOC at 298.15 K on BAC: Amount of (a) acetone, (b) water vapor adsorbed in acetone-water vapor system; (c) 2-propanol, (d) water vapor adsorbed in 2-propanol-water vapor system. 116

Figure 4-6. Comparison of experimental and modeled breakthrough curves during competitive adsorption of water vapor with (a) 2-propanol, (b) acetone, (c) n-butanol, (d) toluene, and (e) 1,2,4-TMB on BAC at 298.15 K. 119

Figure 4-7. 2D adsorbed-phase concentration distribution of 2-propanol during competitive adsorption with water vapor on BAC at 298.15 K. 122

Figure 4-8. Comparison of experimental and modeled BAC-bed temperature profiles at the centre of the reactor (r = 0.0 cm, z = 7.5 cm) during competition adsorption of water vapor with (a) 2-propanol, (b) acetone, (c) n-butanol, (d) toluene, (e) 1,2,4-TMB. 124

Figure 4-9. 2D adsorber bed temperature distribution during competitive adsorption of 2-propanol with water vapor at 298.15 K. 126

Figure 4-10. Comparison of experimental and modeled breakthrough curves during competition adsorption of water vapor with 2-propanol on BAC at 298.15 K and 305.15 K. 128

Figure 4-11. Competitive adsorption of water vapor and 1,2,4-TMB on BAC at 298.15 K: (a) comparison of experimental and modeled breakthrough curves; (b) comparison of experimental equilibrium adsorption capacity with modeled results. 130

LIST OF ACRONYMS

1,2,4-TMB	1,2,4-Trimethylbenzene
2D	Two-Dimensional
AC	Activated Carbon
ACC	Activated Carbon Cloth
BAC	Beaded Activated Carbon
BDDT	Brunauer-Deming-Deming-Teller
BET	Brunauer-Emmett-Teller
DA	Dubinin-Astakhov
DAC	Data Acquisition and Control
DR	Dubinin-Radushkevich
DS	Dubinin-Serpinski
FID	Flame Ionization Detector
GAC	Granular Activated Carbon
HTZ	Heat Transfer Zone
IAST	Ideal Adsorbed Solution Theory
LDF	Linear Driving Force
MDA	Modified Dubinin-Astakhov
MDR	Modified Dubinin-Radushkevich
MRAE	Mean Relative Absolute Error
MTZ	Mass Transfer Zone
NRMSE	Normalized Root-Mean-Square Error
PDE	Partial Differential Equation

QHR	Qi-Hay-Rood
QLV	Qi-LeVan
RAST	Real Adsorbed Solution Theory
RH	Relative Humidity
RMSE	Root-Mean-Square Error
SLPM	Standard Liters Per Minute
TCE	Trichloroethylene
TM	Talu-Meunier
UNIQUAC	UNIversal QUAsiChemical
VMC	Virial Mixture Coefficient
VOC	Volatile Organic Compound
VSM	Vacancy Solution Model
WHO	World Health Organization

CHAPTER 1 INTRODUCTION

1.1 Background

1.1.1 Volatile Organic Compounds (VOCs)

Volatile organic compounds (VOCs) are among the most common environmental contaminants that can negatively impact human health and wellness (Khan and Ghoshal, 2000; Pramar and Rao, 2009). Environment and Climate Change Canada defines VOCs as “organic compounds containing one or more carbon atoms that evaporate readily to the atmosphere, and do not include photochemically non-reactive compounds such as methane, ethane and the chlorofluorocarbons” (Environment and Climate Change Canada, 2016). Similarly, according to the United States Environmental Protection Agency, VOC means “any compound of carbon, excluding carbon monoxide, carbon dioxide, carbonic acid, metallic carbides or carbonates and ammonium carbonate, which participates in atmospheric photochemical reactions” (United States Environmental Protection Agency, 2017). VOCs are sometimes classified by their boiling points. For example, the European Union defines VOCs as “organic compounds having an initial boiling point less than or equal to 250 °C measured at a standard atmospheric pressure of 101.3 kPa” (The European Union, 2004). The World Health Organization (WHO) also categorizes VOCs based on their boiling point. They classify VOCs as organic compounds with boiling point ranging from (50 - 100 °C) to (240 - 260 °C) (WHO, 1989).

1.1.2 Sources of VOCs emissions

VOCs are released to the atmosphere from both natural and anthropogenic sources. Natural sources are wetlands, forests, oceans, and volcanoes (Guenther, 1995). Man-made or anthropogenic sources of VOCs include vehicular emissions, oil refineries, chemical process facilities, commercial, and household products (Piccot et al., 1992;

United States Environmental Protection Agency, 2016). In 2014, the total VOC emissions in Canada were 2.157 megatonnes, which is an increase of 1% from 2013 levels. The largest contributors were the oil and gas sector (34%), industries handling paints and solvents (15%), and agricultural activities (12%). By province, Alberta emitted the highest percentage of national emissions (35%), followed by Ontario (18%), and Quebec (14%) (Environment and Climate Change Canada, 2016). In North America, automotive painting operations are one of the major sources of VOC emissions with an estimated usage of about 6.58 kg VOCs as paint solvents per vehicle in a typical automobile manufacturing plant (Kim, 2011; Papasavva et al., 2001). Such emission streams contain a mixture of low and high molecular weight organic compounds such as aromatic hydrocarbons, aliphatic hydrocarbons, alcohols, esters, ethers, ketones, polyaromatic hydrocarbons, etc. (Kim, 2011).

1.1.3 Impact of VOCs on Human Health and Environment

Due to their volatility and photochemical reactivity, VOCs are the main precursors to the formation of ground-level ozone in the atmosphere, giving rise to photochemical smog (Kim, 2011; Pramar and Rao, 2009). Such type of air pollution is known to have adverse effects on human health and environment (Environment and Climate Change Canada, 2016). Exposure to VOCs could lead to eye, nose and throat irritation, nausea, dizziness, headaches, and damage to lungs, kidney, liver and central nervous system (Leslie, 2000; Kampa and Castanas, 2008). Some VOCs are also listed as human carcinogens by the National Toxicology Program, and may react in the atmosphere to form mutagenic or carcinogenic species (National Toxicology Program, 2016; Fletcher et al., 2006). Moreover, VOCs are detrimental to the environment, since their exposure to crops and forests could lead to reduced yields, growth, and increased susceptibility of plants to diseases, pests, and severe weather (Environment and Climate Change Canada, 2016). Because of the effects mentioned above, environmental legislations to limit and ultimately reduce air pollution have been introduced in recent years by several governments and intergovernmental organizations (Fletcher et al., 2006). Hence, enhanced and efficient abatement methods are a necessity, especially for the treatment of VOC laden streams.

1.1.4 Methods and Techniques to Curb VOCs Emissions

Technologies mainly used to control VOCs emissions include adsorption, absorption, condensation, oxidation, incineration, catalytic and thermal oxidation, and biofiltration, and membrane separation (Pramar and Rao, 2009; Leethochawalit et al., 2001). Adsorption is one of the most commonly used methods for the treatment of waste gaseous and aqueous streams because of its low operation and maintenance costs, high removal efficiency at low contaminant concentrations, adsorbent reusability, and the possibility of adsorbate recovery and reuse (Dabrowski et al., 2005; Efremenko and Sheintuch, 2006; Gupta and Verma, 2002; Hung and Bai, 2008; Lapkin et. al., Joyce and Crittenden, 2004; Pelekani and Snoeyink, 1999; Ramos et al., 2010; Shonnard and Hiew, 2000). Out of the many commercially available adsorbents, activated carbon is the most widely used adsorbent for such treatment processes. It is inexpensive, has large surface area, high adsorption capacity for organics, and can have its physical and chemical properties tailored to suit process conditions (Aktas and Cecen, 2006, 2007; Alvarez et al., 2005; Dabrowski et al., 2005; Hashisho et al., 2005, 2008; Kawasaki et al., 2004; Popescu et al., 2003; Yang, 2003). Activated carbon is also available in many forms such as fibres, beads, powders, monoliths, and granules, and therefore, has a wide range of applications (Yang, 2003). Such advantages make activated carbon adsorption systems very attractive, and they are mostly carried out in a fixed bed configuration. Fixed bed adsorption processes are omnipresent throughout the chemical process industry and are frequently used for small-scale and industrial-scale air pollution control processes (Calvert and Englund, 1984). However, optimization of the design and process parameters such as adsorption capacity, breakthrough time, etc., are critical to a highly efficient, economical and environmentally sustainable fixed bed adsorption system for VOCs emissions control (Yang, 1987).

1.1.5 Importance of Mathematical Modeling in Adsorption

Adsorption process and design parameters have been conventionally based on the experimental results from laboratory and pilot-plant tests. But such experiments only help in predicting the parameters specifically tested, and are not suitable for extrapolating other non-tested variables or parameters. Also for holistic design of processes such as adsorption several runs of experiments are required, which put significant amount of stress on resources from an economics and environment protection point of view (Thomas and Crittenden, 1998; Weber and Smith, 1987). However, verified mathematical models can be used to facilitate optimization of an adsorber by drastically reducing the number of tests required to evaluate various operating conditions and design parameters (Thomas and Crittenden, 1998). Such models are generally validated from few simple and well-controlled bench-scale experiments. Once verified, a mathematical model can be utilized to predict non-tested process variables and conduct sensitivity analysis. It can also be used to evaluate and enhance the performance of an adsorber at a variety of operating conditions, in addition to those that were experimented at (Weber and Smith, 1987; Xu et al., 2013). The aforementioned sentences signify the many advantages of mathematical modelling.

1.2 Problem Statement

Water vapor is typically present in VOC-laden streams and ambient air directed to fixed bed adsorption columns for separation, purification, and recovery. In such scenarios, water vapor would compete with VOCs for adsorption sites on the surface of the adsorbent, and even reduce the adsorption capacity for VOCs and service life of a fixed bed adsorber (Nastaj et al., 2016; Huggahalli and Fair, 1996; Linders et al., 2001; Qi et al., 2000; Cal et al., 1996; Ye et al., 2003; Taqvi et al., 1999; Li et al., 2010). Therefore, it is imperative to understand the effects of water vapor on the fixed bed adsorption of VOCs. This would require an accurate prediction of multicomponent coadsorption equilibria and kinetics of water vapor and VOCs, which can serve as a reference for designing and operating fixed bed adsorbers to control VOC emissions (Yang, 1987).

Most mathematical models involving competitive adsorption do not account for water vapor due to the difficulty in modeling the behavior of competing water molecules. In addition, the majority of the models are one-dimensional and focus only on axial variation of adsorption process parameters. They fail to analyse important factors such as radial dispersion and channeling effects in an adsorber column, and therefore have limitations in comprehensively simulating a fixed bed adsorption process (Fournel et al., 2010; Joly and Perrard, 2009; Murillo et al., 2004; Chuang et al., 2003; Puértolas et al., 2010). In recent years, there were a few studies which carried out two-dimensional (axial and radial) mathematical modeling to predict the transport processes (mass, momentum, and energy) in a fixed bed adsorber, and had good accuracy (Tefera et al., 2014, 2013; Schlüter et al., 2016; Coker et al., 2015). However, these models do not consider the impact of water vapor on the adsorption process. As mentioned earlier, water vapor or relative humidity (RH) (amount of water vapor in air at a given temperature and pressure) significantly affects the equilibrium and kinetics of adsorption processes used for the control of VOCs emissions from waste gas streams, especially at low concentrations (Nastaj et al., 2016). Unfortunately, research on multicomponent competitive adsorption equilibrium between water vapor and VOCs have been very rare, and very few reports exist in literature. The existing models for predicting competitive adsorption equilibrium between organics and water vapor are generally empirical or semi-empirical, and their solution methods being either graphical or numerical (Appel et al., 1998; Do, 1998; Gun'ko et al., 2008; Linders et al., 2001; Manes, 1984; Nastaj et al., 2016; Okazaki et al., 1978; Qi and LeVan, 2005a; Qi et al., 2000). A few of them have fairly good accuracy but are thermodynamically inconsistent (Nastaj et al., 2016). But in all cases, application of these equilibria models for predicting a dynamic fixed bed adsorber operation is extremely tedious and difficult, and is considerably incompatible with simulation (Tien, 2013). Therefore, there is a need for thermodynamically consistent and simulation-friendly multicomponent competitive adsorption equilibria for organics-water vapor systems.

1.3 Research Objectives

The goal of this research work is to study, develop, and validate a two-dimensional (2D) mathematical model for predicting the effects of carrier gas relative humidity on adsorption of VOCs mainly emitted from automotive painting operations, on a fixed bed of beaded activated carbon (BAC). The main objectives can be described as given below:

- Modeling and validation of a 2D multicomponent competitive adsorption isotherm which clearly describes the equilibria between the amount of water vapor and VOCs adsorbed, and the amount of water vapor and VOCs in the bulk gas phase. The isotherm will cover all ranges of concentrations of the components involved.
- 2D modeling and verification of the transport phenomena in a fixed bed adsorber during coadsorption of VOCs and water vapor. The multicomponent adsorption isotherm is taken as an input for simultaneously solving the mass, momentum, and energy transfer equations in the adsorber. The model will then be used to perform sensitivity analysis of the fixed bed adsorber.
- Experiments for model validation will be carried out in a small-scale fixed bed adsorber setup, and their results will be compared to the modeled results for the same set of design and operating conditions.

1.4 Research Significance

This study will investigate the impact of water vapor on competitive adsorption by investigating, suggesting, and developing a suitable thermodynamically consistent model which will coherently predict the multi-component adsorption equilibria and transport phenomena of all the components involved. The model will be able to analyse both radial and axial variations in adsorption parameters and will also be sensitive to changes in operational conditions. This will contribute to a better understanding of the mechanism of the competing water vapor and VOC molecules during competitive adsorption. The model developed in this study will help the industry in optimizing adsorber design and operation conditions to minimize the severe impact of RH during adsorption of contaminants from gas streams.

1.5 Thesis Outline

This thesis consists of five chapters. Critical literature reviews of existing studies on the impact of relative humidity on adsorption of VOCs and other gases, as well as available multicomponent competitive adsorption isotherm models are provided in Chapter 2. Chapter 3 provides details on the materials and methods applied to develop and experimentally validate two-dimensional mathematical model for multicomponent competitive adsorption of water vapor with VOCs. Chapter 4 focuses on the results of the mathematical modelling, their discussions, and verifications. Finally, a summary of the findings of this study, the main conclusions, and recommendations for future works are presented in Chapter 5.

1.6 References

Aktas, O., & Cecen, F. (2006). Effect of type of carbon activation on adsorption and its reversibility. *J. Chem. Technol. Biot., 81*, 94-101.

Aktas, O., & Cecen, F. (2007). Competitive adsorption and desorption of a bi-solute mixture: Effect of activated carbon type. *Adsorption, 13*, 159-169.

Alvarez, P., Garcia-Araya, J., Beltran, F., Masaa, F., & Medina, F. (2005). Ozonation of activated carbons: Effect on the adsorption of selected phenolic compounds from aqueous solutions. *J. Colloid Interf. Sci., 283*, 503-512.

Appel, W., LeVan, M., & Finn, J. (1998). Nonideal adsorption equilibria described by pure component isotherms and virial mixture coefficients. *Ind. Eng. Chem. Res., 37*, 4774-4782.

Cal, M., Rood, M., & Larson, S. (1996). Removal of VOCs from humidified gas streams using activated carbon cloth. *Gas Sep. Purif., 10*, 117-121.

Calvert, S., & Englund, H. (1984). *Handbook of Air Pollution Technology*. New York: John Wiley & Sons, Inc.

Chuang, C., Chiang, P., & Chang, E. (2003). Modeling VOCs adsorption onto activated carbon. *Chemosphere, 53*, 17-27.

Coker, R., Gomez, C., & Schunk, G. (2015). Multi-Dimensional Adsorption Model of CO2/H2O Sorbent Bed. *COMSOL Conference*. Boston: COMSOL.

Dabrowski, A., Podkoscielny, P., Hubicki, Z., & Barczak, M. (2005). Adsorption of phenolic compounds by activated carbon - A critical review. *Chemosphere, 58*, 1049-1070.

Do, D. (1998). *Adsorption Analysis: Equilibria and Kinetics*. London: Imperial College Press.

Efremenko, I., & Sheintuch, M. (2006). Predicting solute adsorption on activated carbon: phenol. *Langmuir, 22*, 3614-3621.

Environment and Climate Change Canada . (2016). *Volatile Organic Compounds in Consumer and Commercial Products*. Retrieved from http://www.ec.gc.ca/cov-voc/Default.asp?lang=En&n=BEE9D2C5-1

Environment and Climate Change Canada. (2016). *Volatile Organic Compound Emissions*. Retrieved from https://www.ec.gc.ca/indicateurs-indicators/default.asp?lang=en&n=64B9E95D-1

Environment and Climate Change Canada. (2016). *Volatile organic compounds that participate in atmospheric photochemical reactions*. Retrieved from http://www.ec.gc.ca/toxiques-toxics/Default.asp?lang=En&n=98E80CC6-1&xml=075320D0-CF6E-4261-890E-90725A29E3C4

Fletcher, A., Kennedy, M., Zhao, X., Bell, J., & Thomas, K. (2006). Adsorption of Organic Vapour Pollutants on Activated Carbon. *Recent Advances in Adsorption Processes for Environmental Protection and Security* (pp. 29-54). Kiev: NATO Science for Peace and Security.

Fournel, L., Mocho, P., Brown, R., & Le Cloirec, P. (2010). Modeling breakthrough curves of volatile organic compounds on activated carbon fibers. *Adsorption, 16*, 147-153.

Guenther, A. (1995). A global model of natural volatile organic compound emissions. *J. Geophy. Res., 100*(D5), 8873-8892.

Gun'ko, V., Turov, V., & Kozynchenko, O. (2008). Characteristics of adsorption phase with water/organic mixtures at a surface of activated carbons possessing intraparticle and textural porosities. *App. Surf. Sci., 25*, 3220-3231.

Gupta, V., & Verma, N. (2002). Removal of volatile organic compounds by cryogenic condensation followed by adsorption. *Chem. Eng. Sci., 57*, 2679-2696.

Hashisho, Z., Emamipour, H., Rood, M., Hay, K., Kim, B., & Thurston, D. (2008). Concomitant adsorption and desorption of organic vapor in dry and humid air streams using microwave and direct electrothermal swing adsorption. *Environ. Sci. Technol., 42*, 9317-9322.

Hashisho, Z., Rood, M., & Botich, L. (2005). Microwave-swing adsorption to capture and recover vapors from air streams with activated carbon fiber cloth. *Environ. Sci. Technol., 39*, 6851-6859.

Huggahalli, M., & Fair, J. (1996). Prediction of Equilibrium Adsorption of Water onto Activated Carbon. *Ind. Eng. Chem. Res., 35*, 2071-2074.

Hung, C., & Bai, H. (2008). Adsorption behaviors of organic vapors using mesoporous silica particles made by evaporation induced self-assembly method. *Chem. Eng. Sci., 63*, 1997-2005.

Joly, A., & Perrard, A. (2009). Linear driving force models for dynamic adsorption of volatile organic compound traces by porous adsorbent beds. *Math. Comp. Sim., 79*, 3492-3499.

Kampa, M., & Castanas, E. (2008). Human health effects of air pollution. *Environ. Pollut., 151*, 362-367.

Kawasaki, N., Kinoshita, H., Oue, T., Nakamura, T., & Tanada, S. (2004). Study on adsorption kinetic of aromatic hydrocarbons onto activated carbon in gaseous flow method. *J. Colloid Interface Sci., 275*, 40-43.

Khan, F., & Ghoshal, A. (2000). Removal of volatile organic compounds from polluted air. *J. Loss Prev. Process Ind., 13*, 527-545.

Kim, B. (2011). VOC emissions from automotive painting and their control: A review. *Environ. Eng. Res., 16*, 1-9.

Lapkin, A., Joyce, L., & Crittenden, B. (2004). Framework for evaluating the "Greenness" of chemical processes: Case studies for a novel VOC recovery technology. *Environ. Sci. Technol., 38*, 5815-5823.

Leethochawalit, M., Bustard, M., Wright, P., & Meeyoo, V. (2001). Novel vapor-phase biofiltration and catalytic combustion of volatile organic compounds. *Ind. Eng. Chem. Res., 40*(23), 5334-5341.

Leslie, G. (2000). Health risks from indoor air pollutants: Public alarm and toxicological reality. *Indoor Built Environ., 9*, 5-16.

Li, C., Xuemin, H., Fangning, F., & Fengli, J. (2010). Effect of relative humidity on adsorption capacity of organic vapors on activated carbon and prediction by the modified D-R equation. *International Conference on Digital Manufacturing & Automation* , (pp. 608-611). Changha, Hunan.

Linders, M., van den Broeke, L., Kapteijn, F., & Moulijn, J. A. (2001). Binary Adsorption Equilibrium of Organics and Water on Activated Carbon. *AIChE J., 47*, 1885-1892.

Manes, M. (1984). Estimation of the effects of humidity on the adsorption onto activated carbon of the vapors of water-immiscible organic liquids. *Fundamentals of Adsorption* (pp. 335-344). New York: Engineering Foundation.

Murillo, R., García, T., Aylón, E., Callén, M., Navarro, M., López, J., & Mastral, A. (2004). Adsorption of Phenanthrene on Activated Carbons: Breakthrough Curve Modeling. *Carbon, 42*, 2009-2017.

Nastaj, J., Witkiewicz, K., & Chybowska, M. (2016). Modeling of multicomponent and multitemperature adsorption equilibria of water vapor and organic compounds on activated carbons. *Ads. Sci. Technol., 34*, 144-175.

National Toxicology Program. (2016). *14th Report on Carcinogens*. Retrieved from https://ntp.niehs.nih.gov/pubhealth/roc/index-1.html

Okazaki, M., Tamon, H., & Toei, R. (1978). Prediction of binary adsorption equilibria of solvent and water vapor on activated carbon. *J. Chem. Eng. Japan, 11*, 209-215.

Papasavva, S., Kia, S., Claya, J., & Gunther, R. (2001). Characterization of automotive paints: An environmental impact analysis. *Prog. Org. Coat., 43*, 193-206.

Pelekani, C., & Snoeyink, V. (1999). Competitive adsorption in natural water: role of activated carbon pore size. *Water Res., 33*, 1209-1219.

Piccot, S. D., Watson, J. J., & Jones, J. W. (1992). A global inventory of volatile organic compound emissions from anthropogenic sources. *J. Geophy. Res., 97*(D9), 9897-9912.

Popescu, M., Joly, J. P., Carre, J., & Danatoiu, C. (2003). Dynamical adsorption and temperature-programmed desorption of VOCs (toluene, butyl acetate and butanol) on activated carbons. *Carbon, 41*, 739-748.

Pramar, G., & Rao, N. (2009). Emerging control technologies for volatile organic compounds. *Cri. Rev. Environ. Sci. Technol., 39*, 41-78.

Puértolas, B., López, M., Navarro, M., López, J., Murillo, R., García, T., & Mastral, A. (2010). Modelling the breakthrough curves obtained from the adsorption of propene onto microporous inorganic solids. *Ads. Sci Technol., 28*, 761-775.

Qi, N., & LeVan, M. (2005a). Adsorption equilibrium modeling for water on activated carbons. *Carbon, 43*, 2258-2263.

Qi, S., Hay, K., & Cal, M. (2000). Predicting humidity effect on adsorption capacity of activated carbon for water-immiscible organic vapors. *Adv. Environ. Res., 4*, 357-362.

Ramos, M., Bonelli, P., Cukierman, A., Ribeiro Carrott, M., & Carrott, P. (2010). Adsorption of volatile organic compounds onto activated carbon cloths derived from a novel regenerated cellulosic precursor. *J. Hazard. Mater., 177*, 175-182.

Schlüter, S., Hennig, T., Schieferstein, E., & Meller, K. (2016). Simulator for Automotive Evaporative Emissions Restraint Systems. *COMSOL Conference*. Munich: COMSOL.

Shonnard, D., & Hiew, D. (2000). Comparative environmental assessments of VOC recovery and recycle design alternatives for a gaseous waste stream. *Environ. Sci. Technol., 34*, 5222-5228.

Taqvi, S., Appel, W., & LeVan, M. (1999). Coadsorption of Organic Compounds and Water Vapor on BPL Activated Carbon. 4. Methanol, Ethanol, Propanol, Butanol, and Modeling. *Ind. Eng. Chem. Res., 38*, 240-250.

Tefera, D., Hashisho, Z., Philips, J., Anderson, J., & Nichols, M. (2014). Modeling Competitive Adsorption of Mixtures of Volatile Organic Compounds in a Fixed-Bed of Beaded Activated Carbon. *Environ. Sci. Technol., 48*, 5108-5117.

Tefera, D., Lashaki, M., Fayaz, M., Hashisho, Z., Philips, J., Anderson, J., & Nichols, M. (2013). Two-Dimensional Modeling of Volatile Organic Compounds Adsorption onto Beaded Activated Carbon. *Environ. Sci. Technol., 47*, 11700-11710.

The European Union. (2004). *Directive 2004/42/CE of the European Parliament and the Council*. Retrieved from http://eur-lex.europa.eu/LexUriServ/LexUriServ.do?uri=OJ:L:2004:143:0087:0096:EN:PDF

Thomas, W., & Crittenden, B. (1998). *Adsorption Technology and Design*. Boston: Butterworth Publishers.

Tien, C. (2013). *Adsorption Calculations and Modelling*. Butterworth_Heinemann.

United States Environmental Protection Agency. (2016). *Volatile Organic Compounds' Impact on Indoor Air Quality*. Retrieved from https://www.epa.gov/indoor-air-quality-iaq/volatile-organic-compounds-impact-indoor-air-quality#Sources

United States Environmental Protection Agency. (2017). *Technical Overview of Volatile Organic Compounds*. Retrieved from https://www.epa.gov/indoor-air-quality-iaq/technical-overview-volatile-organic-compounds#5

Weber, W., & Smith, E. (1987). Simulation and design models for adsorption processes. *Environ. Sci Technol., 21*, 1040-1050.

WHO. (1989). Indoor air quality: organic pollutants. Report on a WHO meeting. *EURO Rep Stud, 111*, 1-70.

Xu, Z., Cai, J., & Pan, B. (2013). Mathematically modeling fixed-bed adsorption in aqueous systems. *J. Zhejiang Univ. Sci. A, 16*, 147-153.

Yang, R. (1987). *Gas Separation by Adsorption Processes*. Stoneham, Massachusetts: Butterworth Publishers.

Yang, R. (2003). *Adsorbents: Fundamentals and Application*. New Jersey: John Wiley & Sons, Inc.

Ye, X., Qi, N., & LeVan, M. (2003). Prediction of adsorption equilibrium using a modified D-R equation: organic-water vapor mixtures on BPL carbon. *Carbon, 41*, 2519-2525.

CHAPTER 2 LITERATURE REVIEW

2.1 Competitive Adsorption of Water Vapor and VOCs

Competitive adsorption between water vapor and VOCs can significantly reduce the adsorption capacities of activated carbon (AC) for VOCs, particularly at RH above 60% (Keener and Zhou, 1990; Huggahalli et al., 1996; Russell and LeVan, 1997; Qi et al., 2000a; Huasheng et al., 2002; Qi et al., 2006). The potency of the negative impact by water vapor on adsorption of VOC also depends on the concentration levels of VOCs in the polluted gas streams (Manes, 1984). To further evaluate this effect, there is a need to understand the mechanism of water vapor adsorption on activated carbon.

2.1.1 Special Behaviour of Water Vapor on Activated Carbon

There is a significant difference between the adsorption of VOCs and water vapor on AC. Adsorption of VOCs is characterized by strong dispersion interactions and superposition of adsorption potential energy functions in the micropores of AC, thereby exhibiting Brunauer-Deming-Deming-Teller (BDDT) type I adsorption isotherms as per the classification of Brunauer et al. (1938) (Huggahalli et al., 1996; Taqvi et al., 1999). An adsorption isotherm describes the equilibrium relationship between an adsorbate and an adsorbent at a given temperature (Suzuki, 1990). As seen from Figure 2.1a, much of the pore volume is filled at low relative pressures of VOCs.

On the other hand, adsorption of water vapor onto the surface of AC involves primary and secondary adsorptive sites (Qi et al., 2000a). Primary adsorptive sites consist of surface functional groups such as those containing oxygen. Adsorption of water vapor on the primary adsorptive sites mainly occurs at low water vapor relative pressures or RH levels (Qi et al., 1998; 2000a). Several studies have reported the presence of oxygen-based functional groups on the surface of granular activated carbon (GAC), and BAC

(Lodewyckx et al., 1999; Lashaki et al., 2016a; 2016b). It can be implied from the reports that an increase in surface functional groups containing oxygen on AC also increases the amount of water vapor adsorbed, particularly at low RH levels (Gregg and Sing, 1982; Salame and Bandosz, 1999). These functional groups form hydrogen bonds with water vapor on the surface of AC. As water vapor relative pressure increases, adsorption occurs chiefly at the secondary adsorptive sites. These secondary adsorptive sites consist of the previously adsorbed water vapor molecules, which enhance adsorption due to the ability of water molecules to form hydrogen bonds with each other. Cluster of water molecules thus formed, are characteristic of capillary condensation at the available pore volume, and thereby exhibiting a BDDT type V (S-shaped) isotherm (Figure 2.1b) (Huggahalli et al., 1996; Taqvi et al., 1999; Qi et al., 2000a;).

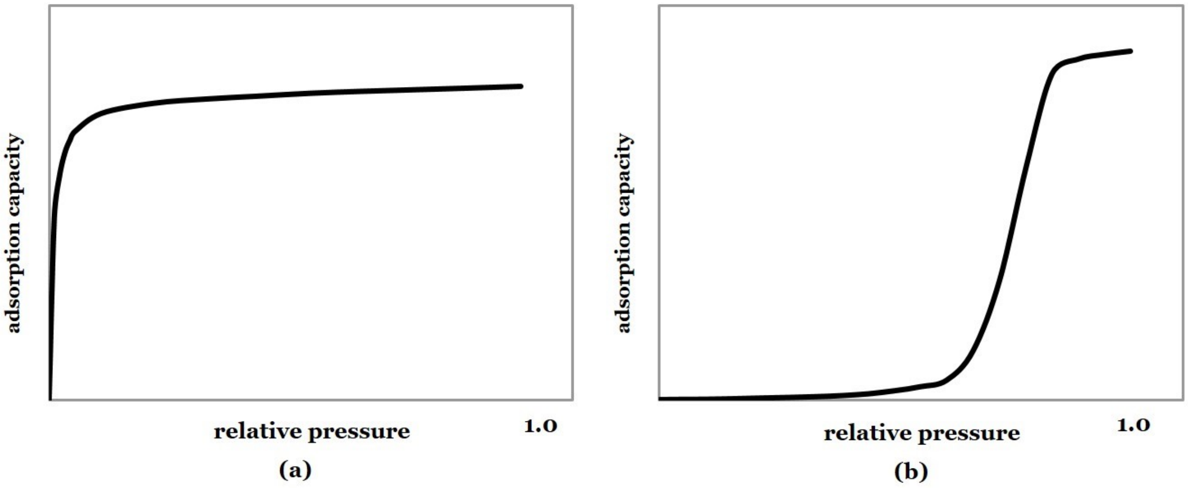

Figure 2.1. BDDT adsorption isotherms (a) Type I (b) Type V (Bansal and Goyal, 2005)

Adsorption of water vapor on microporous AC does not necessarily follow Gurvitsch rule, which states that any two adsorbates at saturation shall occupy the same volume on a given porous solid or adsorbent (Gregg and Sing, 1982). In many cases, the adsorbed liquid volume of water was found to be less than that of the other adsorbates at saturation. Such observations suggest that the adsorbed water molecules are present in a form substantially less dense than normal water or ice. This is typically due to hydrogen bonding between the water vapor molecules and the oxygen-based surface functional groups, leading to a more open structure (Gregg and Sing, 1982).

2.1.2 Impact of Relative Humidity on Adsorption Capacity for VOCs

As mentioned earlier in Chapter 1, the presence of RH has a detrimental effect on the performance of adsorbents. Adsorption capacity is often the determinant of the service life of a fixed bed adsorber for capturing VOCs (Qi et al., 2000b). An overwhelming majority of studies from literature observed similar effects, in addition to a few exceptions.

Underhill et al. (1999) tested the effect of RH on the adsorption of selected water-miscible VOCs such as acetic acid, allyl alcohol, ethoxyethanol, piperidine, and pyridine by AC at concentrations ranging from 100 mg/m^3 to 1,000 mg/m^3. They found that the presence of water vapor at saturation (RH at 100%) reduced the adsorption capacity significantly for all the selected VOCs. Similar study was conducted by Nastaj et al. (2016) for VOCs such as toluene, and n-butanol on AC at 25 – 90% RH. As expected, the negative effect on adsorption capacity was the highest at an RH of 90%. These studies quantified the adsorption capacity reduction using multicomponent adsorption equilibria. Keener et al. (1990) investigated relative humidity effect on AC adsorption using five VOCs: toluene, carbon tetrachloride, ethylbenzene, methylene chloride, and ethanol, with organic loading ranging from 300 to 900 ppm$_v$ and relative humidity varying from 54% to 92%.

They too observed up to 75% reduction in adsorption capacity for the VOCs, from their adsorption breakthrough profile studies.

Taqvi et al. (1999) reported competitive coadsorption of common alcohols such as methanol, ethanol, propanol, butanol, and water vapor on GAC at 298.15 K. Presence of water vapor enhanced the adsorption of lower alcohols such as methanol and ethanol, and inhibited the adsorption of higher alcohols such as propanol and butanol. This is mainly due to the ability of alcohol to form hydrogen bonding with water molecules, which act as additional adsorption sites at high RH levels (Taqvi et al., 1999). Similar observations were recorded by Linders et al. (2001) and Qi et al. (2006) for methanol and ethanol, especially at low concentration levels of the alcohols (1 – 100 ppm).

Li et al. (2010) and Huasheng et al. (2002) observed up to 50% reduction in AC adsorption capacity of VOCs such as benzene, toluene, acetone, and ethyl acetate at 90% RH and VOC inlet concentration ranging 500 – 8,000 mg/m^3. They concluded that the relative humidity and the polarity of the VOCs, are directly proportional to the intensity of the detrimental impact on adsorption capacity.

Few studies reported the effects of RH on adsorption of benzene with activated carbon cloths (ACC), and organic loading varying from 500 ppm$_v$ to 1,000 ppm$_v$ with RH up to 90%. The decrease in benzene adsorption capacity at 90% RH was found to be about 45% and 31% for 500 ppm$_v$ and 1,000 ppm$_v$ inlet concentration respectively (Cal, et al., 1996; Qi et al., 2000b).

Lee et al. (2005) studied the effect of relative humidity on AC adsorption of trichloroethylene (TCE) under a relative humidity range of 40 – 80% and TCE relative pressure of about 0.1. They found that the water vapor in TCE stream had negligible effect on TCE adsorption capacity up to 80% RH.

Chou et al. (1997) reported that the adsorption capacities of a GAC for two hydrophobic VOCs, hexane and cyclohexane decreased by up to 50% due to the presence of moisture in the inlet air stream at 90% RH and 307 K. They also carried out experiments at 350 K to reduce the effect of moisture, but did not observe any positive impact on adsorption capacity. This tendency makes sense as AC adsorption is an exothermic process, and adsorption efficiency typically decreases with the increase in temperature of an adsorber bed (Chou and Chiou, 1997).

Russell et al. (1997) tested the adsorption of alkanes such as ethane and propane with water vapor on GAC, and observed up to 60% reduction in adsorption capacity at 50% RH and low alkane relative pressures.

The aforementioned research emphasized how presence of water vapor greatly hampers adsorption of VOCs onto AC, despite the hydrophobicity of the carbon surface. This is mainly due to the interactions of water molecules and oxygen-based functional groups via hydrogen bonding on the surface (Do and Do, 2000).

Furthermore, as mentioned in Chapter 1, to comprehend these effects, an accurate prediction of multicomponent competitive adsorption equilibria and kinetics of water vapor and VOCs is essential. Hence, a clear and detailed understanding of both single and multicomponent isotherm models which describe equilibria concerning VOCs and water vapor is needed.

2.2 Adsorption Isotherm Models for Predicting Equilibria

Adsorption capacity of AC for any adsorbate(s) can be found from their corresponding adsorption isotherm (Foo and Hameed, 2010). There are distinct models available which can be used for single-component adsorption or multicomponent competitive adsorption. Some of the most widely used adsorption isotherm models are described in the following segments.

2.2.1 Single-Component Adsorption Isotherm Models for VOCs

2.2.1.1 Langmuir Isotherm Model

The Langmuir adsorption isotherm is a simple model describes the adsorptions of gases on solid sorbents (Langmuir, 1916). Adsorption is assumed to occur in a monolayer and on a given number of homogenous energetic sites with no lateral interactions and steric hindrance among adsorbates (Langmuir, 1916). These conditions are rarely valid and are the main weak points of this model (Jain and Snoeyink, 1973). However, the model remains of basic importance for expressing dynamic adsorption equilibrium. It follows Henry's law at low concentration levels and therefore, is thermodynamically consistent in that region (Langmuir, 1916). The Langmuir adsorption model can be represented as (Do, 1998):

$$q_e = \frac{q_m bc}{1+bc} \tag{2.1}$$

and

$$b = b_o exp\left(\frac{-\Delta H_{ad}}{RT}\right) \tag{2.2}$$

where q_e is the adsorbent equilibrium capacity, q_m the adsorbent maximum equilibrium capacity, b the temperature-dependent Langmuir affinity coefficients, c the bulk gas phase concentration, b_o the pre-exponential constant, ΔH_{ad} the heat of adsorption, R the ideal gas constant, and T the adsorption temperature.

2.2.1.2 *Freundlich Isotherm Model*

The Freundlich adsorption isotherm model is an empirical model and describes non-ideal and reversible adsorption (Freundlich, 1906). Adsorption may occur in multilayers and on heterogenous sites with different levels of affinities and heats of adsorption (Foo and Hameed, 2010). However, the model is not thermodynamically consistent and does not approach Henry's law at low concentrations. It also has no saturation limit at high concentrations (Do, 1998).

Freundlich adsorption isotherm model can be presented as (Foo and Hameed, 2010):

$$q_e = K_f C_e^{\frac{1}{n}} \tag{2.3}$$

where C_e the equilibrium concentration of adsorbate in bulk gas phase, and K_f and n are constants for a given adsorbate and adsorbent at a particular temperature. n is between 0 and 1 and indicates surface heterogeneity (Haghseresht and Lu, 1998).

2.2.1.3 *Brunauer-Emmett-Teller Isotherm Model*

Brunauer-Emmett-Teller (BET) adsorption isotherm model is a theoretical model and is applicable for heterogenous gas-solid systems (Bruanuer et al., 1938). The assumptions made for this model are the same as Langmuir theory (Do, 1998). However, the model includes multilayer adsorption, and is valid only for relative pressures ranging from 0.05 to 0.3 (Foo and Hameed, 2010).

The model can be presented as (Foo and Hameed, 2010):

$$q_e = \frac{q_S C_{BET} C_e}{(C_S - C_e)\left[1 + (C_{BET} - 1)\left(\frac{C_e}{C_S}\right)\right]} \tag{2.4}$$

where C_{BET} is the ratio of monolayer and multilayer heats of adsorption, C_e the equilibrium concentration of adsorbate in gas phase, C_s the adsorbate monolayer saturation concentration, q_s the theoretical isotherm saturation capacity, and q_e the equilibrium adsorption capacity. Typically, C_{BET} is significantly larger than unity. Therefore, the model can be simplified as (Foo and Hameed, 2010):

$$q_e = \frac{q_S}{1-\left(\frac{C_e}{C_S}\right)} \tag{2.5}$$

2.2.1.4 Toth Isotherm Model

The Toth isotherm is an empirical model which describes many systems with sub-monolayer coverage very well (Do, 1998). It is also thermodynamically consistent at low organic loadings and therefore, follows Henry's law in that region (Do, 1998).

Toth isotherm equation is given by (Nastaj et al., 2016):

$$q_e = \frac{q_m P}{(b+P^n)^{1/n}} \tag{2.6}$$

where P is the equilibrium vapor pressure of the test adsorbate.

To find the effect of temperature, the parameter b can be further derived as (Nastaj et al., 2016):

$$b = b_o exp\left(\frac{-n\Delta H_{ad}}{RT}\right) \tag{2.7}$$

The Toth isotherm model is widely used, especially for adsorption of hydrocarbons, hydrogen sulfide, alcohols, carbon oxides on AC and zeolites, because of its simplicity and correct behaviour at low and high relative pressures (Do, 1998).

2.2.1.5 *Dubinin-Radushkevich* Isotherm Model

Dubinin-Radushkevich (DR) adsorption isotherm model is based on the potential theory of adsorption developed by Polanyi (Dubinin and Radushkevich, 1947). It is fundamentally sound and highly regarded compared to other isotherm models, due to its core thermodynamic basis (Do, 1998).

The potential theory (Bansal and Goyal, 2005), is based on the concept that the adsorbed gases or vapors at the surface of a microporous adsorbent such as AC are compressed by the forces of attraction acting from the surface to a distance into the surrounding space. As the forces facilitating adsorption deteriorate with distance away from the surface, the multimolecular adsorbed film can be considered to be an intermolecular potential gradient. The forces of attraction at any point in the adsorbed film can be easily measured by the adsorption potential (ε), which is defined as the amount of work done by adsorption forces in bringing molecules from bulk gas phase to that point. It is given by (Bansal and Goyal, 2005):

$$\varepsilon = RT\,ln\frac{P_S}{P} \tag{2.8}$$

where R is the ideal gas constant, T the adsorption temperature, P_S the saturated vapor pressure of the test adsorbate at test temperature, and P the equilibrium vapor pressure of the test adsorbate.

This thermodynamic theory of formation of adsorbed film can be represented by the following relation (Do, 1998):

$$W = f(\varepsilon) \tag{2.9}$$

where W is the volume of adsorbate adsorbed. The function above is characteristic to a particular gas-solid system, and therefore is called the *characteristic curve*. Moreover, the curve is independent of temperature since the adsorption potential is mainly based on the work of temperature-independent dispersion forces. It makes the potential theory very flexible as once the characteristic curve at one temperature is established, it is possible to predict the adsorption at other temperatures for the same gas-solid system (Do, 1998).

With the basis of Polanyi potential theory and characteristic curve, Dubinin and Radushkevich suggested that for microporous sorbents such as AC the volume of adsorbed film can be expressed as a Gaussian function of adsorption potential (Bansal and Goyal, 2005). The function is given by:

$$W = W_o exp\left[-K\left(\frac{\varepsilon}{\beta}\right)^2\right] \tag{2.10}$$

where W_o is the limiting pore volume of the adsorbent, K a constant related to the adsorbent pore-size distribution, β the affinity coefficient which considers the polarizability of the adsorbate. The above equation can also be written as:

$$W = W_o exp\left[-\left(\frac{\varepsilon}{E}\right)^2\right] \tag{2.11}$$

where E is the characteristic energy which is a measure of adsorption strength between adsorbate and adsorbent. Equation (2.11) can be rearranged further as:

$$ln\, W = ln\, W_o - \frac{K}{\beta^2}(RT)^2\left(ln\frac{P_S}{P}\right)^2 \tag{2.12}$$

This equation is known as the DR equation (Bansal and Goyal, 2005). The DR isotherm is an empirical model and was initially developed for adsorption of vapors onto microporous adsorbents with heterogenous surface such as AC (Do, 1998). The model successfully predicts equilibrium adsorption capacities at intermediate and high concentrations by pore filling mechanism (Bansal and Goyal, 2005) but fails to approach Henry's law at low concentration levels (Kapoor et al., 1989).

2.2.1.6 Dubinin-Astakhov Isotherm Model

Dubinin-Astakhov (DA) isotherm model has the same basis as the DR model and is mainly applied to carbonaceous solids which have high degree of heterogeneity, due to a wider pore size distribution (Do, 1998). The model is a more general form of the DR equation, and is written as:

$$ln\,W = ln\,W_o - \frac{K}{\beta^2}(RT)^2\left(ln\frac{P_S}{P}\right)^m \tag{2.13}$$

where m is related to the pore size distribution. This equation is more flexible as it contains three parameters (W_o, $\frac{K}{\beta^2}$, m) whereas DR equation includes only two (W_o, $\frac{K}{\beta^2}$). However, like DR isotherm the DA model also fails to approach Henry's law at low concentrations and therefore, is thermodynamically inconsistent in that region (Do, 1998).

2.2.1.7 Modified Dubinin-Radushkevich Isotherm Model

As mentioned earlier, the Dubinin isotherm models are not thermodynamically consistent in the Henry's law region (limit of zero loading) even though they perform well in fitting most equilibrium data of AC adsorption during medium and high loadings (Kapoor et al., 1989). Typically, in this region a thermodynamically consistent adsorption isotherm reduces itself into a Henry's adsorption isotherm or linear adsorption isotherm with a limiting slope:

$$\lim_{P\to 0}\frac{dW}{dP}=\lim_{P\to 0}\frac{W}{P}=H \tag{2.14}$$

where H is the Henry's law constant. The DR equation (2.12) does not follow this trend. However, Kapoor et al. (1989) modified the equation to include a proper Henry's law. This modified Dubinin-Radushkevich (MDR) equation has a valid Henry's law region at low relative pressures and retains the original form and qualities of the DR equation at moderate to high relative pressures. Hence, the MDR equation can be applied over the whole relative pressure range. The equation is presented as:

$$W=\left[1-exp\left(-\alpha\frac{P}{P_S}\right)\right]W_0exp\left[-\frac{K}{\beta^2}(RT)^2\left(ln\frac{P_S}{P}\right)^2\right]+exp\left(-\alpha\frac{P}{P_S}\right)W_1\frac{P}{P_S} \tag{2.15}$$

where α, W_1, are additional fitting parameters. The above equation reduces to equation (2.14) when $P\to 0$ as $H=\frac{W_1}{P_S}$ gives the Henry's law adsorption isotherm (Kapoor et al., 1989).

The MDR model works in such a way that the second term of the equation becomes significant only at very low relative pressures and the first term remains applicable over the rest of the relative pressure range up to 1. The model contains four fitting parameters (α, W_0, $\frac{K}{\beta^2}$, W_1) compared to two in the D-R model, and therefore is more flexible (Kapoor et al., 1989). Hung and Lin (2007) too conducted similar modifications to the DR model by integrating the DR equation and the Langmuir isotherm simultaneously for the entire relative pressure range. Their model also reduced to Henry's linear isotherm at low pressures, and produced comparable results as that of Kapoor et al. (1989).

2.2.2 Single-Component Adsorption Isotherm Models for Water Vapor

As discussed earlier, adsorption of water vapor on AC follows a type V isotherm. Owing to the sigmoidal shape of type V isotherm, the functional form of type I isotherm models described above cannot be used to predict the adsorption equilibrium of water vapor (Huggahalli et al., 1996). However, there are a limited number of reliable isotherm models which have been applied successfully to describe pure water vapor adsorption equilibrium on activated carbons. They are described in the following section.

2.2.2.1 Modified Dubinin-Astakhov Isotherm Model

The DA equation has been applied reasonably well in describing adsorption equilibria for VOCs on AC (Do, 1998). However, like other Dubinin models the equation does not predict adsorption equilibria correctly at low pressures due to zero slope at zero loading. DA equation, therefore, has an inflexion point and its position depends on the value of the characteristic energy (Do, 1998). The lower the characteristic energy the higher the relative pressure value at which inflexion occurs and vice versa (Do, 1998). This zero slope and inflexion point have been utilised by some studies to describe the type V water adsorption on AC (Do, 1998; Slasli et al., 2003).

The modified DA (MDA) isotherm model for water adsorption is usually expressed as an amalgamation of two similar forms of the original DA equation: type I for adsorption on the surface functional groups, and type V for adsorption into the micropores (Stoeckli et al., 1994; Slasli et al., 2003; Kim and Agnihotri, 2008). The modified DA can be presented as (Stoeckli, 2002):

$$W = W_{o_{(I)}} exp\left[-\left(\frac{\varepsilon}{E_{(I)}}\right)^{m_{(I)}}\right] + W_{o_{(V)}} exp\left[-\left(\frac{\varepsilon}{E_{(V)}}\right)^{m_{(V)}}\right] \tag{2.16}$$

where $W_{o_{(I)}}$, $W_{o_{(V)}}$ are the limiting volumes adsorbed with corresponding characteristic energies $E_{(I)}$ and $E_{(V)}$ in type I and type V regions respectively; likewise $m_{(I)}$ and $m_{(V)}$ denote the adsorbent surface heterogeneity.

The application of DA isotherm model for water adsorption, however, is very limited since it is based on potential theory and micropore filling mechanism; and neither consider cluster formation mechanism during water adsorption, nor follow Henry's law at low loadings (Do and Do, 2000; Qi et al., 2005b; Kim and Agnihotri, 2008).

2.2.2.2 Dubinin-Serpinski Isotherm Model

The Dubinin-Serpinski (DS) equation is one of the earliest models formulated for describing water adsorption equilibrium (Dubinin and Serpinsky, 1981). Recognizing the deficiency of DA model, DS suggested a kinetic theory of water adsorption onto primary and secondary sites, and desorption. The model also has a specific allowance for a finite maximum adsorbent capacity, which was considered empirically. The DS equation is given as (Do, 1998):

$$\frac{P}{P_S} = \frac{C_\mu}{c(1-kC_\mu)(C_{\mu o}+C_\mu)} \tag{2.17}$$

where C_μ is the amount of water adsorbed at a relative pressure of $\frac{P}{P_S}$, $C_{\mu o}$ is the concentration of primary adsorption sites (typically used to categorize adsorbents with various degrees of surface oxidation), c the dimensionless ratio of the equilibrium rate constants for adsorption and desorption of water, k another fitting parameter which represents the rate of loss of the secondary sites during water adsorption because of the finiteness of the maximum adsorbed volume.

The model has had reasonable success in predicting water adsorption equilibria on AC (Dubinin and Serpinsky, 1981; Do, 1998; Sullivan et al., 2007; Kim and Agnihotri, 2008). However, it fails at low pressure region due to its hyperbolic behaviour (Do and Do, 2000). Few studies also noted that the DS model does not have a proper basis to predict the maximum water adsorption capacity, as the model gives more emphasis on the kinetic parameters rather than the adsorbent pore volume (Do and Do, 2000; Kim and Agnihotri, 2008; Do et al., 2009).

2.2.2.3 Qi-Hay-Rood Isotherm Model

The Qi-Hay-Rood (QHR) isotherm considers water adsorption on surface functional groups (primary adsorption sites) at low water vapor pressures, and cluster formation mechanism (secondary adsorption sites) at medium to high water vapor pressures (Qi et al., 1998). Its assumptions are:

- The number of secondary adsorption sites is directly proportional to the amount of water adsorbed (q_e) at a certain $\frac{P}{P_S}$.
- The number of primary adsorption sites is proportional to the remaining water adsorption capacity ($q_m - q_e$) at a given $\frac{P}{P_S}$.
- The driving force for the change in adsorption capacity with respect to the change in relative pressure is proportional to the product of ($q_m - q_e$) and (q_e).

These assumptions give the following equation:

$$\frac{d\left(\frac{q_e}{q_m}\right)}{d\left(\frac{P}{P_S}\right)} = k_p\left[1 - \left(\frac{q_e}{q_m}\right)\right]\left(\frac{q_e}{q_m}\right) \tag{2.18}$$

where k_p is a proportionality constant. Equation (2.18) generates a sigmoidal curve and upon further integration it gives:

$$q_e = \frac{q_m}{1+exp\left[k_p\left(\frac{P_{50}}{P_S}-\frac{P}{P_S}\right)\right]} \tag{2.19}$$

where P_{50} is an isotherm constant, and $P = P_{50}$ at $q_e/q_m = 0.5$.

To express the effect of adsorption temperature, q_m was assumed to be constant at all temperatures as an adsorbent structural property, and empirical modifications of the proportionality constant and the isotherm constant were applied to the above equation (Qi et al., 1998). They are given as:

$$\frac{P_{50}}{P_S} = a + bT \tag{2.20}$$

and

$$k_p = Ae^{-(E_a/RT)} \tag{2.21}$$

where a, b, E_a are QHR multitemperature constants, A a pre-exponential factor.

The multitemperature QHR isotherm model gives a better fit for describing water adsorption equilibria at various temperatures, when compared to the DS equation (Qi et al., 1998, 2000a). The model was successfully tested for water vapor adsorption onto ACC and GAC at relative vapor pressures from 0.0 to 0.95 and temperatures between 288 and 373 K (Qi et al., 1998).

2.2.2.4 *Talu-Meunier Isotherm Model*

The Talu-Meunier (TM) isotherm model is based on classical thermodynamics (Talu and Meunier, 1996). It considers water adsorption on surface functional groups at low loading, cluster formation mechanism at medium to high loadings, and caps the maximum amount adsorbed up to a finite adsorbent micropore volume. The model gives a type V isotherm and is therefore used for predicting water adsorption equilibrium. The TM equation is given by:

$$\frac{P}{P_S} = \frac{H\psi}{1+K_{eq}\psi} exp\left(\frac{\psi}{q_m}\right) \tag{2.22}$$

where K_{eq} is the equilibrium constant for the association of water molecules to form clusters on the adsorbent. Parameter ψ is further defined as:

$$\psi = \frac{-1+\sqrt{1+4K_{eq}\zeta}}{2K_{eq}} \tag{2.23}$$

where

$$\zeta = \frac{q_m q_e}{(q_m - q_e)} \tag{2.24}$$

For the effect of temperature on adsorption, Talu and Meunier (1996) suggested modifications to the Henry's law constant H and equilibrium constant K_{eq} in its original equation (2.22). They are given as:

$$H = exp\left(H_o + \frac{H_1}{T}\right) \tag{2.25}$$

and

$$K_{eq} = exp\left(K_{eq_o} + \frac{K_{eq_1}}{T}\right) \tag{2.26}$$

where H_o, H_1, K_{eq_o}, K_{eq_1}, are the multitemperature fitting parameters.

Using equation (2.22) only five temperature-independent parameters q_m, H_o, H_1, K_{eq_o}, and K_{eq_1} are required to describe water adsorption at any temperature. The multitemperature TM isotherm model gives a good fit when describing water adsorption on AC and has been tested successfully at temperatures ranging from 298.15 K to 398.15 K (Talu and Meunier, 1996; Sullivan et al., 2007).

2.2.2.5 *Qi-LeVan Isotherm Model*

Qi-LeVan (QLV) isotherm model has similar basis as the TM model except that it does not consider the cluster formation of water molecules as a chemical reaction (Talu and Meunier, 1996; Qi et al., 2005b). It is presented as (Qi et al., 2005b):

$$\frac{P}{P_S} = \frac{q_e}{\xi_o + \xi_1 q_e + \xi_2 q_e^2 + \xi_3 q_e^3 + \cdots + \xi_i q_e^i} \tag{2.27}$$

where ξ_o, ξ_1, ξ_2, ξ_3, ξ_i are the model parameters.

The multitemperature QLV isotherm for describing water adsorption equilibrium is given by (Qi et al., 2005b):

$$\frac{P}{P_S} = \left(\frac{P}{P_S}\right)_{ref} exp\left[\frac{\delta_o + \delta_1 q_e}{R}\left(\frac{1}{T} - \frac{1}{T_{ref}}\right) + \frac{\delta_2}{2R}\left(\frac{1}{T^2} - \frac{1}{T_{ref}^2}\right)\right] \tag{2.28}$$

where δ_o, δ_1, δ_2, are the temperature and loading independent fitting parameters. $\left(\frac{P}{P_S}\right)_{ref}$ is the reference relative vapor pressure at a particular temperature T_{ref}, and is derived from the original equation (2.27).

Once the reference adsorption isotherm at a given temperature is fixed, the model can be used to generate adsorption isotherms at different temperatures (Qi et al., 2005b).

The multitemperature QLV model usually needs four parameters to accurately predict water adsorption on AC and is mathematically simpler than TM model. It is thermodynamically consistent at Henry's law region, and has been successfully validated at adsorption temperatures ranging 298.15 to 398.15 K with ACs having different types of surface functional groups, and pore structures (Qi et al., 2005b).

2.2.2.6 Do and Do Isotherm Model

The Do and Do isotherm model emphasizes the water adsorption mechanism and the role of adsorbent microstructure in the process (Do and Do, 2000). It assumes that water molecules are chemisorbed onto the surface functional groups at the mesopores and at the entrance to the micropores. With the increase in water loading, the clusters of water formed grows up to the size of a pentamer (five molecules, approximate width 0.6 nm) on the functional groups. The pentamers acquire sufficient dispersive energy to move into the micropores. This process continues until the micropores are filled. At very high relative pressures of about 0.9 capillary condensation occurs, which fills up the mesopores. The Do and Do model for AC is a BET-type equation, and consists of two parts. The first part includes adsorption on surface functional groups, and the second part consists of micropore filling due to dispersive forces. The model is given by:

$$W = W_f \frac{K_f \sum_{i=1}^{N} i\left(\frac{P}{P_S}\right)^i}{1+K_f \sum_{i=1}^{N}\left(\frac{P}{P_S}\right)^i} + W_\mu \frac{K_\mu\left(\frac{P}{P_S}\right)^6}{K_\mu\left(\frac{P}{P_S}\right)^6+\left(\frac{P}{P_S}\right)} \tag{2.29}$$

where W_μ is the limiting volume adsorbed due to micropore filling during water adsorption, W_f a fitting parameter, K_f, K_μ are the unitless equilibrium rate constants for the chemisorption of water on surface functional groups and water filling of micropores respectively, N the average number of water molecules in a fully developed cluster on the surface functional groups.

Do and Do equation has been extensively used for describing water adsorption equilibrium. It fits very well with experimental data, especially for adsorption on GAC, ACC, and single-walled carbon nanotube (SWNT) (Do and Do, 2000; Sullivan et al., 2007; Kim and Agnihotri, 2008; Do et al., 2009).

2.2.3 Multicomponent Competitive Adsorption Isotherm Models

Multicomponent adsorption equilibrium is an area of increasing research interest (Wood, 2000; Foo and Hameed, 2010; Nastaj et al., 2016). Although it is a well-known fact that water vapor is ubiquitous during VOC adsorption and that it has strong effects on VOC adsorption capacity, multicomponent competitive adsorption equilibria involving VOCs and water vapor are limited and rarely reported in literature (Taqvi et al., 1999; Furmaniak et al., 2008; Nastaj et al., 2016). The following section will review and discuss some of the most widely applied multicomponent competitive adsorption isotherm models which describe equilibria for organic-organic systems and/or organic-water vapor systems.

2.2.3.1 Jain and Snoeyink's Extended Langmuir Isotherm Model

Langmuir model for competitive adsorption is one of the first models to describe multicomponent adsorption equilibrium in multi-adsorbate systems (Butler and Ockrent, 1930). It was first developed by Butler and Ockrent and includes the same assumptions as the original Langmuir isotherm model for single-components. The model for a two-component system is given by:

$$q_{e,1} = \frac{q_{m,1} b_1 c_1}{1 + b_1 c_1 + b_2 c_2} \tag{2.30}$$

$$q_{e,2} = \frac{q_{m,2} b_2 c_2}{1 + b_1 c_1 + b_2 c_2} \tag{2.31}$$

where $q_{e,1}$, $q_{e,2}$ are the equilibrium adsorbent capacities for component 1 and 2 respectively at equilibrium concentrations of component 1 (c_1) and component 2 (c_2); $q_{m,1}$, $q_{m,2}$ are the maximum equilibrium adsorbent capacities for component 1 and 2 respectively obtained from their corresponding pure single-adsorbate isotherms; b_1, b_2 are the respective Langmuir affinity coefficient of component 1 and component 2.

The above model assumes that there is competition for all the adsorption sites (Butler and Ockrent, 1930). However, this is not always the case in reality. A difference in molecular size of adsorbates can result in the smaller adsorbate having easy access to smaller pores without competition (Butler and Ockrent, 1930). Furthermore, different adsorption sites on the surface of an adsorbent contain different chemical composition and functional groups which attract a specific kind of adsorbates, leading to no competition (Butler and Ockrent, 1930).

Jain and Snoeyink (1973) extended the Langmuir competitive adsorption model to include the factors mentioned above. The extended version of the model for a binary system can be presented as:

$$q_{e,1} = \frac{(q_{m,1} - q_{m,2}) b_1 c_1}{1 + b_1 c_1} + \frac{q_{m,2} b_1 c_1}{1 + b_1 c_1 + b_2 c_2} \tag{2.32}$$

$$q_{e,2} = \frac{q_{m,2} b_2 c_2}{1 + b_1 c_1 + b_2 c_2} \tag{2.33}$$

where ($q_{m,1} > q_{m,2}$)

The first term of equation (2.32) considers the amount of component 1 adsorbed without competition, which is proportional to $(q_{m,1} - q_{m,2})$. The second part of the equation represents the amount of component 1 adsorbed when under competition with component 2. Equation (2.33) is the same as equation (2.31), and includes the amount of component 2 adsorbed when under competition with component 1. The extended Langmuir isotherm model for competitive adsorption can also be written for the i^{th} component as (Jain and Snoeyink, 1973):

$$q_{e,i} = \sum_{x=i}^{y} \frac{b_i c_i a_x}{1+\left(\sum_{j=1}^{x} b_j c_j\right)} \tag{2.34}$$

where $q_{e,i}$ is the equilibrium adsorption capacity for the i^{th} component ($i = 1\ to\ y$); $a_x = (q_{m,x} - q_{m,x+1})$ for $x = i\ to\ y - 1$, and $a_x = q_{m,y}$ for $x = y$; and b_j is the Langmuir affinity coefficient where $j = 1\ to\ x$.

and

$$b_i = b_{o,i} exp\left(\frac{-\Delta H_{ad,i}}{RT}\right) \tag{2.35}$$

where $b_{o,i}$, $\Delta H_{ad,i}$ are the pre-exponential constant and heat of adsorption of the i^{th} component respectively.

The model has been tested experimentally with reasonable success by various studies, especially for competitive adsorption on AC involving mixtures of gases and VOCs (Jain and Snoeyink, 1973; Tefera et al., 2014). It is valid only for components with similar adsorption profiles, and cannot be applied to organic mixtures containing water vapor because of the difference in adsorption mechanism and isotherm type of water and organic vapors (Huggahalli et al., 1996). The multicomponent Langmuir isotherm model contains all the shortcomings of the original single-component model, and is thermodynamically consistent only in the special case where $q_{m,1} = q_{m,2}$ (considering binary systems) (Jain and Snoeyink, 1973).

2.2.3.2 Ideal Adsorbed Solution Theory

The thermodynamically consistent ideal adsorbed solution theory (IAST) was developed by Myers and Prausnitz (Myers and Prausnitz, 1965). It is based on solution thermodynamics and Raoult's law. The main assumptions of this theory include:

- The adsorbent is thermodynamically inert, and no change in its internal energy occurs during adsorption.
- The adsorbent has a temperature-invariant surface, which is available to all the adsorbates.
- The Gibbs definition of adsorption is considered, which usually involves the volumetric technique of obtaining experimental adsorption isotherm.

During equilibrium, the chemical potential in the adsorbed phase is equal to the chemical potential in the gas phase (Myers and Prausnitz, 1965). Using this concept, the equation of equilibrium for mixed gas adsorption for the i^{th} component at a constant temperature is given as:

$$P_t y_i = P_i^o(\pi) x_i \gamma_i \quad \{i = 1,2, \dots, N\} \tag{2.36}$$

where P_t is the total pressure, y_i the mole fraction of component i in gas phase, x_i the mole fraction of component i in the adsorbed phase, γ_i the activity coefficient of component i in the adsorbed phase, and N the number of components present in the mixture. $P_i^o(\pi)$ is the pure adsorbate vapor pressure of component i at the same temperature and spreading pressure π of the mixture. If the adsorbed mixture is ideal, the activity coefficients are equal to unity. Equation (2.36) then reduces to Raoult's law. For a pure component i, integration of Gibbs adsorption isotherm at constant temperature yields the spreading pressure π_i, given by (Myers and Prausnitz, 1965):

$$\pi_i(P_i^o) = \frac{RT}{A}\int_0^{P_i^o} \frac{n_i^o(P)}{P} dP \qquad (2.37)$$

where A is the specific area of the adsorbent, n_i^o is the amount of pure component i adsorbed at the spreading pressure π_i and temperature of the mixture, that is, at P_i^o. $n_i^o(P)$ is represented through different single-component isotherms. Since the mixing process is carried out at a constant spreading pressure π, the spreading pressure is equal for all the components involved in adsorption. That is:

$$\pi_1^o = \pi_2^o = \pi_N^o \qquad (2.38)$$

Other conditions in solving IAST theory are (Myers and Prausnitz, 1965):

$$\sum_{i=1}^{N} x_i = 1 \qquad (2.39)$$

and

$$\frac{1}{n_t} = \sum_{i=1}^{N} \frac{x_i}{n_i^o} \qquad (2.40)$$

where n_t is the total amount adsorbed. Equations (2.36), (2.37), (2.38), (2.39), and (2.40) are solved simultaneously to predict multicomponent adsorption equilibria (Myers and Prausnitz, 1965).

IAST has been extensively used with good agreement to predict multicomponent competitive equilibria for mixtures of gases and VOCs, mainly due to its minimal input requirements (Myers and Prausnitz, 1965; O'Brien and Myers, 1985; Myers and Valenzuela, 1986; Benjamin, 2009; Ilic et al., 2010; Chen et al., 2011; Landa and Flockerzi, 2013; Mangano et al., 2015; Simon et al., 2016). An IAST-based model does not need any mixture parameters to estimate equilibria, as the predictions are based entirely on the pure single-component adsorption isotherms (Myers and Prausnitz, 1965). Furthermore, the success of the IAST in predicting multicomponent competitive adsorption equilibria depends solely on the quality of these pure single-component data (Richter et al., 1989). An advantage of IAST is that any kind of single-component isotherm model which fits experimental data well can be applied (Richter et al., 1989).

Several single-component adsorption isotherm models such as Langmuir, Freundlich, DR, DA have been integrated to measure the spreading pressure in IAST model (Richter et al., 1989; Linders et al., 2001). However, studies have pointed out the mathematical difficulty in solving them both numerically or analytically, especially for Polanyi-based DR and DA equations (Wood, 2000; Linders et al., 2001). Some researchers developed alternative Polanyi-type correlations to minimise the mathematical complications (Wood, 2000).

Linders et al. (2001) applied IAST model to study the effect of water vapors on water-miscible VOC adsorption on AC, and were able to get a fairly good agreement for up to 60% RH. But most studies available in literature contradict with Linders et al. (2001) regarding the application of IAST in VOC mixtures involving water vapor (Huggahalli et al., 1996; Qi et al., 2000b; Ye et al., 2003; Li et al., 2010;). This is because there is a fundamental difference in the adsorption mechanism of water and VOCs, which the IAST model does not consider (Huggahalli et al., 1996; Tien, 2013). Furthermore, no explanation was provided by Linders et al. (2001) regarding IAST’s non-applicability beyond an RH level of 60%. Several reports also highlighted the rather poor performances of IAST model when water vapor is one of the components in a mixture (Tien, 2013; Wood, 2000). The IAS theory is, therefore, recommended only for components exhibiting similar adsorption isotherm profiles.

2.2.3.3 *Real Adsorbed Solution Theory*

The real adsorbed solution theory (RAST) is basically the adsorbed solution theory developed by Myers and Prausnitz, which has been extended for non-ideal adsorbed phases and gas phases (Myers and Prausnitz, 1965).

During equilibrium between the chemical potentials of the gas phase and the adsorbed phase in non-ideal and high pressure scenarios, the equation based on RAST is represented using fugacity instead of pressure (Myers and Prausnitz, 1965). It is given as:

$$P_t y_i \phi_i = f_i^o(\pi) x_i \gamma_i \quad \{i = 1,2,\dots,N\} \tag{2.41}$$

where $\phi_i (= \frac{f_t}{P_t})$ is the fugacity coefficient of component i, and $f_i^o(\pi)$ is the pure adsorbate fugacity of component i at the same temperature and spreading pressure π of the mixture. ϕ_i is equal to unity for ideal gases, and denotes the extent of deviation of vapors from ideal behaviour. For RAST, the activity coefficients γ of the adsorbed phase are measured from binary equilibrium experimental data and their theoretical models (Gothard et al., 1976; Myers et al., 1983). Wilson and UNIQUAC (UNIversal QUAsiChemical) models are the most well-known models for activity coefficients (Yun et al., 1996).

Wilson equation for a binary mixture is given as (Yun et al., 1996):

$$ln\,\gamma_1 = -\,ln(x_1 + \Lambda_{12}x_2) + x_2\left(\frac{\Lambda_{12}}{x_1+\Lambda_{12}x_2} - \frac{\Lambda_{21}}{x_2+\Lambda_{21}x_1}\right) \tag{2.42}$$

$$ln\,\gamma_2 = -\,ln(x_2 + \Lambda_{21}x_1) - x_1\left(\frac{\Lambda_{12}}{x_1+\Lambda_{12}x_2} - \frac{\Lambda_{21}}{x_2+\Lambda_{21}x_1}\right) \tag{2.43}$$

where Λ_{12}, Λ_{21} are the binary interaction parameters between components 1 and 2.

UNIQUAC equations for a binary mixture is represented as (Yun et al., 1996):

$$ln\,\gamma_1 = ln\frac{\Phi_1}{x_1} + \frac{z}{2}q_1\,ln\frac{\theta_1}{\Phi_1} + \Phi_2\left(\iota_1 - \frac{r_1}{r_2}\iota_2\right) - q_1 ln(\theta_1 + \theta_2\tau_{21}) + \theta_2 q_1\left(\frac{\tau_{21}}{\theta_1+\theta_2\tau_{21}} - \frac{\tau_{12}}{\theta_2+\theta_1\tau_{12}}\right) \tag{2.44}$$

$$ln\,\gamma_2 = ln\frac{\Phi_2}{x_2} + \frac{z}{2}q_2\,ln\frac{\theta_2}{\Phi_2} + \Phi_2\left(\iota_2 - \frac{r_2}{r_1}\iota_1\right) - q_2 ln(\theta_2 + \theta_1\tau_{12}) + \theta_1 q_2\left(\frac{\tau_{12}}{\theta_2+\theta_1\tau_{12}} - \frac{\tau_{21}}{\theta_1+\theta_2\tau_{21}}\right) \tag{2.45}$$

and

$$\Phi_1 = \frac{x_1r_1}{x_1r_1+x_2r_2} \tag{2.46}$$

$$\Phi_2 = \frac{x_2r_2}{x_1r_1+x_2r_2} \tag{2.47}$$

$$\theta_1 = \frac{x_1q_{ms1}}{x_1q_{ms1}+x_2q_{ms2}} \tag{2.48}$$

$$\theta_2 = \frac{x_2q_{ms2}}{x_1q_{ms1}+x_2q_{ms2}} \tag{2.49}$$

$$\iota_1 = \frac{z}{2}(r_1 - q_{ms1}) - (r_1 - 1) \tag{2.50}$$

$$\iota_2 = \frac{z}{2}(r_2 - q_{ms2}) - (r_2 - 1) \tag{2.51}$$

where τ_{12}, τ_{21} are the binary interaction parameters; z the coordination number; r_1, r_2, q_{ms1}, q_{ms2} are the pure component molecular structure constants depending on molecular size and external surface area. Some activity coefficients models are also based on spreading pressure to provide more flexibility to the RAST (Talu and Zwiebel, 1987; Talu et al., 1995). The theory considers the same fundamental equations and spreading-pressure relations as those of IAST, which can be solved simultaneously with the activity coefficient models mentioned above (Myers and Prausnitz, 1965).

The RAST model is applied usually when there are significant deviations from ideality for both the adsorbed and gas phases (Talu and Zwiebel, 1986; Chen et al., 1990; Sakuth et al., 1998; Siperstein and Myers, 2001; Myers, 2005; Heinonen et al., 2012; Hefti et al., 2015;). It has similar advantages (Myers and Prausnitz, 1965) and limitations (Huggahalli et al., 1996) as those of IAST, and therefore, is recommended for multicomponent competitive adsorption equilibria involving components with similar adsorption profiles and mechanism. However, an additional limitation might be the mathematical and experimental complications of measuring activity coefficients (Wood, 2000).

2.2.3.4 Vacancy Solution Model

The vacancy solution model (VSM) was first developed by Suwanayuen and Danner (Suwanayuen and Danner, 1980). It assumes that the adsorption system consists of vacancies, and two solutions: gas phase and adsorbed phase. The composition and density of the solutions differ, with the adsorbed phase being denser than the gas phase (Suwanayuen and Danner, 1980). The vacancies are considered to be vacuum spaces which act as the solvent of the system, and have the same size as the adsorbate molecules (Suwanayuen and Danner, 1980).

At equilibrium, according to VSM, chemical potential of the vacancies is equal at the adsorbed phase and at the gas phase (Suwanayuen and Danner, 1980). The equation is presented as:

$$\pi = -\frac{RT}{\sigma} ln(\gamma x) \tag{2.52}$$

where σ is the partial molar surface area of adsorbed molecules. The activity coefficient γ is equal to unity for ideal solutions, and is measured through binary equilibrium experimental data and models for non-ideal solutions (Yun et al., 1996).

The main inputs for this model are the pure single-component isotherms to measure the mixture spreading pressure π (Suwanayuen and Danner, 1980), similar to the solution procedures for IAST and RAST (Myers and Prausnitz, 1965). Equation (2.52) can be applied to any number of components in a mixture. It has been successful to describe adsorption of many VOCs on AC (Wood, 2000). However, since the VSM model does not consider the unique behaviour of water vapor adsorption, it cannot be applied to predict the effect of RH on VOC adsorption (Huggahalli et al., 1996). Other limitations of this model include the ones mentioned for IAST and RAST.

2.2.3.5 *Method of Chou and Chiou*

Chou and Chiou (1997) developed a simple Freundlich-like model which predicts the VOC adsorption capacity in humid conditions. Its main inputs are the pure single-component adsorption isotherms for VOC and water vapor.

The model considers that the pure VOC adsorption isotherm is represented by the Langmuir model. For pure water vapor adsorption equilibrium, Freundlich isotherm is considered. Chou and Chiou (1997) assumed that some adsorption sites on AC are relatively more hydrophilic than the others and therefore adsorb more water vapor. The remaining sites and pores are covered by VOCs. The proposed model is given as:

$$\frac{q_{VOC}}{q_{VOC,RH=0}} = 1 - K_f RH^{\frac{1}{n}} \tag{2.53}$$

where q_{VOC} is the equilibrium adsorption capacity for VOC at a given RH, $q_{VOC,RH=0}$ is the equilibrium adsorption capacity for VOC at dry conditions derived from the pure single-component Langmuir isotherm at the same temperature. Other parameters in equation (2.53) are same as defined for Freundlich isotherm earlier.

The Chou and Chiou model has been used by a few studies with reasonable success, especially for predicting adsorption capacity for VOCs such as hexane, cyclohexane, benzene, toluene, methanol, acetone in humid streams on GAC (Chou and Chiou, 1997; Wood, 2000) and more recently on zeolites (Tao et al., 2004). However, its application is very limited mainly due to its failure to consider the fundamental difference in adsorption mechanism of water and VOCs, and its lack of a finite limit for adsorption capacity at saturation (Chou and Chiou, 1997; Wood, 2000).

2.2.3.6 Virial Mixture Coefficient Method

In the virial mixture coefficient (VMC) approach, multicomponent adsorption equilibria are predicted using thermodynamically consistent two-dimensional equation of states (EOS) (Taqvi and LeVan, 1997). The two-dimensional virial equation of state (2D-VEOS) is given as:

$$\frac{\pi A}{RT} = q + \frac{1}{A}\sum_i \sum_j q_i q_j B_{ij} + \frac{1}{A^2}\sum_i \sum_j \sum_k q_i q_j q_k C_{ijk} + \cdots \qquad (2.54)$$

where q_i, q_j, q_k are the concentration of component i, j, k respectively in the solid phase; B_{ij}, C_{ijk} are the virial coefficients. These coefficients account for molecular interactions between adsorbed molecules. Interactions between adsorbates and adsorbent are described by Henry's law, and are considered by pure single-component adsorption isotherms. Virial coefficients with the same subscripts such as B_{11}, C_{333} represent interactions between same components. Interactions between different components are described by VMCs such as B_{12}, C_{123}.

For a binary competitive adsorption equilibrium, 2D-VEOS is written as (Taqvi and LeVan, 1997):

$$\frac{\pi A}{RT} = q_1 + \frac{1}{A}B_{11}q_1^2 + \frac{1}{A^2}C_{111}q_1^3 + \cdots + q_2 + \frac{1}{A}B_{22}q_2^2 + \frac{1}{A^2}C_{222}q_2^3 + \cdots + \frac{2}{A}B_{12}q_1q_2 + \frac{3}{A^2}C_{112}q_1^2q_2 + \frac{3}{A^2}C_{122}q_1q_2^2 + \cdots \tag{2.55}$$

Equation (2.55) can also written as:

$$\frac{\pi A}{RT} = \left[\frac{\pi A}{RT}\right]_{pure\ 1} + \left[\frac{\pi A}{RT}\right]_{pure\ 2} + \left[\frac{\pi A}{RT}\right]_{mixture} \tag{2.56}$$

Therefore, for a binary adsorption system, it can be clearly seen that the mixture term is an adjustment to the spreading pressure contributions from the pure components.

The basis of VMC approach was postulated by Van Ness (1969), who derived a relation between spreading pressure of adsorbed components and their fugacities from Helmholtz free energy. The model when combined with equation (2.56) is given as (Appel et al., 1998):

$$ln\, f_i = ln\, f_{pure\ i} + \int_A^\infty \left(\frac{\delta\left(\left[\frac{\pi A}{RT}\right]_{mixture}\right)}{\delta q_i}\right)_{T,A,q_j} \frac{dA}{A} \tag{2.57}$$

Equation (2.57) implies that for component *i* in a multicomponent adsorption system, the adsorption equilibrium of *i* is equal to a sum of adsorption of pure component *i* and a term which considerers interactions of *i* with other adsorbates in the mixture. Assuming ideal behaviour, fugacity can be replaced by partial pressure, and the mixture term in equation (2.57) can be substituted with equation (2.55). After rearrangement and integration, the VMC-based equation can be given as (Nastaj et al., 2016):

$$ln\, P_i = ln\, P_{pure\ i} + \frac{2}{A}\sum_i \sum_j B_{ij} q_i + \frac{3}{2A^2}\sum_i \sum_j \sum_k C_{ijk} q_j q_k + \cdots \quad (2.58)$$

The pure component adsorption term in equation (2.58) can be represented either by a good fitting isotherm or by an EOS, and the VMCs are measured as approximate parameters by minimizing the objective function (Appel et al., 1998):

$$f_{min} = \sum_{i=1}^{N} \sum_{j=1}^{M} \left(ln\, P_{i_j}^{cal} - ln\, P_{i_j}^{exp}\right)^2 \quad (2.59)$$

VMC approach to multicomponent competitive adsorption equilibria is relatively a new method. It shows good agreement with several experimental data conducted by Taqvi et al. (1997,1999), Nastaj et al. (2016), Qi et al. (2005a, 2006), and Appel et al. (1998) involving organic-organic and organic-water vapor systems. However, it is mathematically more intensive and complex compared to other models.

2.2.3.7 Method of Doong and Yang

Doong and Yang developed a thermodynamically consistent model based on Polanyi potential theory to predict multicomponent adsorption equilibria involving organics and water vapor (Tien, 2013). They modified the DR equation to include a term to account for water hysteresis, and activity coefficients for the adsorbed phase. For a binary system, Doong and Yang's model can be given as (Tien, 2013):

$$W_1 = (W_o - W_2) exp\left\{-\left(\frac{RT}{\beta_1 E_o}\right)^2 \left[\left(ln \frac{\gamma_1 P_{S1}}{P_1}\right)^2 - \left(\frac{ln\, h_{o1}}{1 - \frac{P_2^O}{\gamma_2^O P_{S2}}}\right)^2\right]\right\} \quad (2.60)$$

$$W_2 = (W_o - W_1)exp\left\{-\left(\frac{RT}{\beta_2 E_o}\right)^2\left[\left(ln\frac{\gamma_2 P_{S2}}{P_2}\right)^2 - \left(\frac{ln\, h_{o2}}{1-\frac{P_1^O}{\gamma_1^O P_{S1}}}\right)^2\right]\right\} \tag{2.61}$$

where W_1, W_2 are the adsorbed volumes of component 1 (VOC) and 2 (water vapor) at relative pressures $\frac{P_1}{P_{S1}}$ and $\frac{P_2}{P_{S2}}$ with activity coefficients γ_1, γ_2 respectively; E_o is the characteristic energy which can be determined from a standard reference adsorbate; β_1, β_2 are the affinity coefficients of the characteristic curve; h_{o1}, h_{o2} the relative pressures of component 1 and 2 respectively at the beginning of the hysteresis loop; and $\frac{P_1^O}{P_{S1}}$, $\frac{P_2^O}{P_{S2}}$ the pure single-component relative pressures of component 1 and 2 respectively.

In an organic-water system, the model assumes the activity coefficient for organic vapors to be unity. Similarly, for water vapor the activity coefficient may also be assumed to be unity if relative pressure is more than 0.6. For relative pressures lower than 0.6, γ can be measured using the following empirical equation (Tien, 2013):

$$(W_2^o + \bar{W})(1 + J_1 W_2^o)\frac{P_2^O}{\gamma_2^O P_{S2}} = J_2\bar{W} \tag{2.62}$$

where $\bar{W}$, J_1, J_2 are the model fitting parameters; and W_2^o is the total adsorbed volume during pure water vapor adsorption at a certain $\frac{P_2^O}{P_{S2}}$.

From equations (2.60) and (2.61), it can be noted that it is a volume exclusion model (fixed total pore volume). The equations can also be used to estimate the adsorption of pure single component isotherms, by neglecting the volume exclusion term $(W_o - W_2)$ and replacing it with only the total limiting pore volume (W_o) (Wood, 2000).

The model equations are non-linear and coupled, and are solved by an iterative procedure (Wood, 2000). This Polanyi-based concept was successfully validated by numerous experiments for binary systems involving methanol-water vapor, acetone-water vapor, benzene-water vapor, and toluene-water vapor (Keener and Zhou, 1990; Huasheng et al., 2002; Li et al., 2010). Doong and Yang's model, however, is less flexible than multicomponent models such as VMC because it relies only on DR-based equations which do not universally describe water adsorption equilibria and mechanism. It also does not consider the interactions that may occur between VOCs and water vapor during adsorption.

2.2.3.8 Method of Okazaki, Tamon and Toei

Okazaki et al. (1978) proposed a model exclusively to predict binary competitive adsorption equilibrium between organics and water vapor on AC. They assumed that the total amount of adsorbed organic component in humid streams is attributed to the following three sources:

- Adsorption of organic vapor in non-wetted pores where no condensation of water vapor takes place, $\bar{q}_1$.
- Liquid-phase adsorption of organic compound within wetted pores where capillary condensation takes place, $\bar{q}_2$.
- Dissolution of organic vapor in the condensed water, $\bar{q}_3$.

Therefore, the total amount of organic vapor adsorbed in humid streams can be written as:

$$\bar{q}_t = \bar{q}_1 + \bar{q}_2 + \bar{q}_3 \tag{2.63}$$

and

$$\bar{q}_1 = q_g^o\left(\frac{A_d}{A}\right) \tag{2.64}$$

$$\bar{q}_2 = q_l^o\left(\frac{A_c}{A}\right) \tag{2.65}$$

$$\bar{q}_3 = \left[V_c - \left(\frac{q_w}{\rho_w}\right)\right]\rho_v - \bar{q}_2 \tag{2.66}$$

where q_g^o is the equilibrium adsorption capacity for the organic adsorbate measured from its pure single-component adsorption isotherm at the mixture relative pressure; q_l^o is the equilibrium adsorption capacity for the organic adsorbate in an aqueous solution and is obtained from its liquid phase adsorption isotherm at the mixture relative pressure; A_d, A_c account for the dry and wet surface areas of the adsorbent respectively; V_c denotes volume of the condensed phase; q_w is the amount of water vapor adsorbed; ρ_w, ρ_v are the densities of water and organic vapor in their adsorbed state respectively.

The values of V_c, A_d, A_c are determined from the desorption isotherm data of water vapor, and the Kelvin equation modified by Okazaki et al. (1978). The modified equation is given as:

$$r = \frac{2\sigma_t v_m \cos\theta}{\left(RT\, ln\frac{P_t}{P_{tS}}\right)} \tag{2.67}$$

and

$$P_{tS} = P_{wS}x_w' + P_{vS}(1 - x_w') \tag{2.68}$$

where r is the pore radius; v_m the molar volume of the liquid adsorbate; σ_t the surface tension; θ the contact angle; P_{tS} the saturated total (water and organic) vapor pressure of the condensed phase; P_{wS} and P_{vS} are the saturated vapor pressures of water vapor and organic vapor, respectively; and x'_w the mole fraction of water vapor in the condensed phase.

Once V_c, A_d, A_c are determined, the total amount of adsorbed organic vapor in humid conditions can easily be calculated from equations (2.63), (2.64), (2.65), and (2.66). The method of Okazaki et al (1978) was applied by few studies. However, the accuracy of the model's predictions was found to be inferior, in terms of accuracy, for selected VOC-water systems in comparison with the Doong and Yang model (Tien, 2013). Furthermore, the model also requires significantly higher number of input requirements such as adsorption profiles of gas phase and liquid phase organic vapors, desorption profile of water vapor, adsorbent specific surface area, adsorbent cumulative pore volume, adsorbent pore radius, and adsorbed phase composition; unlike Doong and Yang's model.

2.2.3.9 Method of Manes

Manes (1984) developed a graphical model to describe the effects of humidity on AC adsorption of water-immiscible VOCs. It is based on Polanyi's potential theory and is therefore, thermodynamically consistent. The model requires only the pure adsorption profiles of the organic vapor and water vapor as input. Initially, these profiles were represented by the adsorption characteristic curves and therefore, the model was solved graphically. However, the characteristic curves can be replaced with good fitting single-component adsorption isotherms for all the components in a mixture. These modifications make the model more compatible for computer simulation of a dynamic adsorption process (Qi et al., 2000b).

The major assumptions of this model for a binary (organic vapor and water vapor) mixture coadsorption on AC are (Manes, 1984):

- At the relative pressures of organic $\left(\frac{P_v}{P_{vS}}\right)$ and water vapor $\left(\frac{P_w}{P_{wS}}\right)$ in the mixture, if the adsorbed volume of pure organic vapor (V_v^o) is more than the adsorbed volume of pure water vapor (V_w^o), then there is no interference by water vapor on the adsorption capacity for organic vapor during multicomponent adsorption. Therefore, the adsorbed volume of organic vapor adsorbed during competitive adsorption (V_v) with water vapor can be directly given by its pure single-component adsorption isotherm.
- Similarly at $\frac{P_v}{P_{vS}}$ and $\frac{P_w}{P_{wS}}$, if V_v^o is less than V_w^o, then there is significant effect by water vapor on the organic adsorption capacity during multicomponent competitive adsorption. This phenomenon is predicted using Manes' derivation based on Polanyi's potential theory.

For the first condition ($V_v^o > V_w^o$), the model equations are written as:

$$q_w = 0 \tag{2.69}$$

$$q_v = \rho_v V_v^o \tag{2.70}$$

where q_w and q_v are the equilibrium adsorption capacities for water and organic vapor in a mixture, respectively; V_v^o is measured directly from the pure single-component organic vapor adsorption isotherm.

For the second condition ($V_v^o < V_w^o$), the equations involved are given as:

$$\frac{\varepsilon_v'}{v_v} = \frac{\varepsilon_v^o}{v_v} - \frac{\varepsilon_w^o}{v_w} - \frac{RT}{v_w} ln \frac{P_w}{P_{wS}} \tag{2.71}$$

$$\varepsilon_v' = \varepsilon_v^o - \varepsilon_w^o \left(\frac{v_v}{v_w}\right) \tag{2.72}$$

$$\varepsilon_v^o = RT\, ln \frac{P_{vS}}{P_v^o} \tag{2.73}$$

$$\varepsilon_v' = RT\, ln \frac{P_{vS}}{P_v'} \tag{2.74}$$

$$\varepsilon_w^o = RT\, ln \frac{P_{wS}}{P_w^o} \tag{2.75}$$

where ε_v^o and ε_v' are the adsorption potentials of organic vapor in its pure and mixture state, respectively; ε_w^o the adsorption potential of water vapor in its pure state; v_v and v_w are the molar volumes of organic and water vapors, respectively; and $\frac{P_v^o}{P_{vS}}$ and $\frac{P_w^o}{P_{wS}}$ the relative pressures of organic and water vapors in their pure component systems, respectively.

Equation (2.71) is the thermodynamic potential theory-based relation derived by Manes (1984); which shows that the net adsorption potential of an organic vapor in a mixture at $V_v^o < V_w^o$ is equal to its adsorption potential in pure state, diminished by the adsorption potential of an equal volume of pure water vapor, and corrected for water vapor pressure less than saturation. It reduces to equation (2.72) at $\frac{P_w}{P_{wS}}$ equal to unity, that is, at an RH of 100%.

For multicomponent organic mixtures with water vapor, the condition of Grant and Manes (1966) may be considered:

$$\frac{1}{V_1} log\, x_1 \left(\frac{P_S}{P}\right)_1 = \frac{1}{V_2} log\, x_2 \left(\frac{P_S}{P}\right)_2 = \frac{1}{V_3} log\, x_3 \left(\frac{P_S}{P}\right)_3 = \cdots \tag{2.76}$$

where V_1, V_2, V_3, are the total adsorbed volume of component 1, 2, 3 respectively; at mole fractions x_1, x_2, x_3; and relative pressures $\left(\frac{\mathrm{P}}{\mathrm{P_S}}\right)_1$, $\left(\frac{\mathrm{P}}{\mathrm{P_S}}\right)_2$, $\left(\frac{\mathrm{P}}{\mathrm{P_S}}\right)_3$ of component 1, 2, 3 respectively.

The competitive adsorption between organic and water adsorbates onto an AC can generally be predicted by Manes' method either through an iterative procedure numerically (Qi et al., 2000b) or graphically (Manes, 1984) to satisfy equation (2.71). It provides good predictions and was successfully verified experimentally for selected water-immiscible VOC-water systems on AC (Manes, 1984; Cal, et al., 1996). The model is thermodynamically consistent, flexible, easy to use, and its results are far superior to that of the method of Okazaki et al. (Tien, 2013). However, the Manes model does not take into account the solubility of VOCs in water and vice versa during competitive adsorption (Manes, 1984).

2.3 Summary and Conclusions

This chapter provided an overview of the existing studies on the impact of relative humidity on adsorption of VOCs and other gases onto activated carbon. It also included a critical literature review of the single- and multicomponent adsorption isotherms involving VOCs and water vapor to understand the mechanism of water vapor adsorption on activated carbon, especially during competitive adsorption, and to support the development of a dynamic and predictive multicomponent competitive adsorption model.

For the VOCs, Polanyi's potential-theory-based models such as the DR, DA, and MDR isotherm equations seem to be the most versatile and proven single-component adsorption models and are recommended for predicting adsorption capacities. The original equations of DR and the more generic DA are thermodynamically consistent at medium and high concentrations, except at low loadings. This issue was addressed by other researchers (Kapoor et al., 1989; Hung and Lin, 2007), who modified the Dubinin-equations to make them thermodynamically consistent in all the regions. Other isotherm equations such as Langmuir, Freundlich, and Toth are useful for fitting experimental isotherm data but have little value in predicting adsorption capacities due to the lack of strong fundamental basis.

For single-component water vapor adsorption, QHR, TM, QLV, and Do and Do isotherm models are recommended for predicting adsorption capacities. All of them consider the fundamental mechanism related to water adsorption on AC, i.e., adsorption on surface functional groups (primary adsorption sites) at low loadings, and cluster formation mechanism (secondary adsorption sites) at medium to high loadings. The models have been successfully verified and tested on several types of AC at different adsorption temperatures. The Dubinin-based models for water adsorption such as MDA, DS have limited use as they do not consider cluster formation mechanism.

For prediction of competitive adsorption equilibria involving organic-organic systems, the IAST, RAST, VSM, and VMC models are suggested, mainly because they are based on solution thermodynamics and are therefore thermodynamically consistent throughout the entire region. All of them are mathematically straightforward to solve, except for VMC.

For organic-water vapor systems, VMC, method of Doong and Yang, and method of Manes are recommended. All of these are thermodynamically consistent and account for water vapor adsorption mechanism exclusively during competitive adsorption. Most of these multicomponent adsorption models are solved through iterations and are therefore mathematically intensive. They have been extensively tested and were found to be more accurate than other organic-water vapor competitive adsorption isotherm models such as the method of Okazaki et al., the method of Chou and Chou, and the IAST. The models are also flexible enough for computer simulations and numerical solutions.

The majority of the widely applied multicomponent competitive adsorption models such as IAST, RAST, VSM, VMC, method of Manes, method of Okazaki et al. either require single-component adsorption isotherms directly as inputs, or use them as some form of an extension. In addition, some multicomponent models involving organic-water vapor systems such as the method of Doong and Yang are meant only for binary systems unlike others. Taking this into account, the chapter intends to serve as a guide for selecting suitable adsorption isotherm models for predicting multicomponent adsorption equilibria for organic-organic and/or water vapor-organic systems, which can then be taken as an input to solve the mass, momentum, and energy transfer equations across the adsorber. Table 2-1. summarises all the different models mentioned here with their advantages and disadvantages.

Table 2-1. Advantages and disadvantages of the commonly used adsorption isotherms

isotherm	advantage(s)	disadvantage(s)	reference(s)
single-component adsorption isotherm models for VOC			
Langmuir	• thermodynamically consistent at low loadings • easy to use	• main model assumptions are rarely valid • lack of strong fundamental basis	Langmuir, 1916; Jain and Snoeyink, 1973
Freundlich	• easy to use for fitting experimental data	• no Henry's law limit at low concentrations • no saturation limit at high concentrations	Do, 1998
Brunauer-Emmett-Teller (BET)	• includes multilayer adsorption • easy to use	• lack of strong fundamental basis • valid only for relative pressure from 0.05 to 0.3	Do, 1998; Foo and Hameed, 2010
Toth	• includes Henry's law limit and finite saturation limit • easy to use	• poor accuracy at medium relative pressures	Do, 1998
Dubinin-Radushkevich (DR)	• strong thermodynamic basis	• thermodynamically inconsistent at low loadings	Bansal and Goyal, 2005; Do, 1998

isotherm	advantage(s)	disadvantage(s)	reference(s)
	• accurate predictions at medium and high concentrations		
Dubinin-Astakhov (DA)	• strong thermodynamic basis • more flexible than DR • accurate predictions at medium and high concentrations	• thermodynamically inconsistent at low loadings	Do, 1998
modified Dubinin-Radushkevich (MDR)	• thermodynamically consistent at low loadings • accurate predictions across the entire region	• model fitting parameters do not have any physical meaning	Kapoor et al., 1989; Hung and Lin, 2007
single-component adsorption isotherm models for water vapor			
Modified Dubinin-Astakhov (MDA)	• mathematically straightforward and easy to solve	• no Henry's law limit at low concentrations • does not consider cluster formation mechanism during water adsorption	Do and Do, 2000; Qi, et al., 2005b; Kim and Agnihotri, 2008
Dubinin-Serpinski (DS)	• considers kinetic theory of water adsorption	• hyperbolic behaviour at low pressures • no proper basis to predict the maximum water adsorption capacity	Do, 1998; Do and Do, 2000; Kim and Agnihotri, 2008; Do et al., 2009
Qi-Hay-Rood (QHR)	• considers water adsorption at both primary and secondary adsorption sites • good accuracy	• does not have a thermodynamic basis	Qi et al., 1998
Talu-Meunier (TM)	• based on classical thermodynamics • considers water adsorption at both primary and secondary adsorption sites • good accuracy	• model fitting parameters do not have any physical meaning	Talu and Meunier, 1996; Nastaj et al., 2016
Qi-LeVan (QLV)	• based on classical thermodynamics • considers water adsorption at both primary and secondary adsorption sites	• model fitting parameters do not have any physical meaning	Talu and Meunier, 1996; Qi et al., 2005b

isotherm	advantage(s)	disadvantage(s)	reference(s)
	• good accuracy • mathematically simpler than TM		
Do and Do	• considers water adsorption mechanism and the role of adsorbent structure in the process • extensively tested with good accuracy	• does not have a thermodynamic basis	Do and Do, 2000; Do et al., 2009
multicomponent competitive adsorption isotherm models			
Jain and Snoeyink's extended Langmuir	• easy to solve • can be extended to more than two components • reasonable accuracy	• main model assumptions are rarely valid • lack of strong fundamental basis • thermodynamically consistent only during special cases • valid only for components with similar adsorption profiles	Jain and Snoeyink, 1973; Huggahalli et al., 1996; Tefera et al., 2014
ideal adsorbed solution theory (IAST)	• strong thermodynamic basis • very flexible • minimal input requirements • extensively tested with good accuracy	• not valid for non-ideal solutions and mixtures involving water vapor	Myers and Prausnitz, 1965; Huggahalli et al., 1996; Tien, 2013
real adsorbed solution theory (RAST)	• strong thermodynamic basis • very flexible • can be applied to non-ideal solutions • extensively tested with good accuracy	• not valid for mixtures involving water vapor • mathematical and experimental complications of measuring activity coefficients	Myers and Prausnitz, 1965; Huggahalli et al., 1996; Wood, 2000; Myers, 2005
vacancy solution model (VSM)	• thermodynamic basis • flexible • can be applied to non-ideal solutions • extensively tested with good accuracy	• not valid for mixtures involving water vapor • mathematical and experimental complications of measuring activity coefficients	Suwanayuen and Danner, 1980; Huggahalli et al., 1996; Wood, 2000
Chou and Chiou	• valid for mixtures involving water vapor • easy to solve	• limited application • cannot be extended beyond binary systems	Chou and Chiou, 1997; Wood, 2000

isotherm	advantage(s)	disadvantage(s)	reference(s)
		• does not consider the difference in adsorption mechanism of water vapor and VOCs • no finite limitation in adsorption capacity at saturation • does not consider the interactions between VOCs and water vapor during adsorption • not valid for mixtures without water vapor	
virial mixture coefficient (VMC)	• strong thermodynamic basis • valid for any kind of mixtures • good accuracy	• mathematically more intensive than other models	Taqvi et al., 1997, 1999; Nastaj et al., 2016
Doong and Yang	• valid for mixtures involving water vapor • thermodynamically consistent • accounts for water hysteresis • extensively tested with good accuracy	• does not consider the difference in adsorption mechanism of water vapor and VOCs • cannot be extended beyond binary systems • not valid for mixtures without water vapor • requires iterative solution method • does not consider the interactions between VOCs and water vapor during adsorption	Wood, 2000; Huasheng et al., 2002; Tien, 2013
Okazaki et al.	• valid for mixtures involving water vapor	• high number of input parameters • lower accuracy compared to Doong and Yang model • cannot be extended beyond binary systems • not valid for mixtures without water vapor	Okazaki et al., 1978; Tien, 2013

isotherm	advantage(s)	disadvantage(s)	reference(s)
Manes	• thermodynamically consistent • valid for mixtures involving water vapor • very flexible • minimal input requirements • can be extended beyond binary mixtures • good accuracy	• not valid for mixtures without water vapor • does not take into account the solubility of VOCs in water during competitive adsorption • requires iterative solution method	Manes, 1984; Qi et al., 2000b; Tien, 2013

2.4 References

Appel, W., LeVan, M., & Finn, J. (1998). Nonideal adsorption equilibria described by pure component isotherms and virial mixture coefficients. *Ind. Eng. Chem. Res., 37*, 4774-4782.

Bansal, R., & Goyal, M. (2005). *Activated Carbon Adsorption*. Taylor & Francis Group.

Benjamin, M. (2009). New Conceptualization and Solution Approach for the Ideal Adsorbed Solution Theory (IAST). *Environ. Sci. Technol., 43*, 2530-2536.

Bruanuer, S., Emmett, P., & Teller, E. (1938). Adsorption of gases in multimolecular layers. *J. Am. Chem. Soc, 60*, 309-319.

Butler, J., & Ockrent, C. (1930). Studies in Electrocapillarity. Part III. *J. Phys. Chem., 34*, 2841-2859.

Cal, M., Rood, M., & Larson, S. (1996). Removal of VOCs from humidified gas streams using activated carbon cloth. *Gas Sep. Purif., 10*, 117-121.

Chen, J., Loo, L., & Wang, K. (2011). An Ideal Absorbed Solution Theory (IAST) Study of Adsorption Equilibria of Binary Mixtures of Methane and Ethane on a Templated Carbon. *J. Chem. Eng. Data, 56*, 1209-1212.

Chen, Y., Ritter, J., & Yang, R. (1990). Nonideal Adsorption from Multicomponent Gas Mixtures at Elevated Pressures on a 5A Molecular Sieve. *Chem. Eng. Sci., 45*, 2877-2894.

Chou, M., & Chiou, J. (1997). Modeling effects of moisture on adsorption capacity of activated carbon for VOCs. *J. Environ. Eng., 123*, 437-443.

Do, D. (1998). *Adsorption Analysis: Equilibria and Kinetics*. London: Imperial College Press.

Do, D., & Do, H. (2000). A model for water adsorption in activated carbon. *Carbon, 38*, 767-773.

Do, D., Junpirom, S., & Do, H. (2009). A new adsorption–desorption model for water adsorption in activated carbon. *Carbon, 47*, 1466-1473.

Dubinin, M., & Radushkevich, L. (1947). The equation of the characteristic curve of the activated charcoal. *Proc. Acad. Sci. USSR Phys. Chem. Sec., 55*, 331-337.

Dubinin, M., & Serpinsky, V. (1981). Isotherm equation for water vapor adsorption by microporous carbonaceous adsorbents. *Carbon, 19*, 402-403.

Foo, K., & Hameed, B. (2010). Insights into the modeling of adsorption isotherm systems. *Chem. Eng. J., 156*, 2-10.

Freundlich, H. (1906). Over the adsorption in solution. *J. Phys. Chem., 57*, 385-471.

Furmaniak, S., Gauden, P., Terzyk, A., & Rychlicki, G. (2008). Water adsorption on carbons — Critical review of the most popular analytical approaches. *Adv. Colloid Interface Sci., 137*, 82-143.

Gothard, F., Clobanu, M., Breban, D., & Bucur, C. (1976). Predicting the Parameters in the Wilson Equations for Activity Coefficients in Binary Hydrocarbon Systems. *Ind. Eng. Chem. Process Des. Dev., 15*, 333-337.

Grant, R., & Manes, M. (1966). Adsorption of Binary Hydrocarbon Gas Mixtures on Activated Carbon. *Ind. Eng. Chem. Fund., 5*, 490-498.

Gregg, S., & Sing, K. (1982). *Adsorption, Surface Area and Porosity*. New York: Academic Press.

Haghseresht, F., & Lu, G. (1998). Adsorption characteristics of phenolic compounds onto coal-reject-derived adsorbents. *Energy Fuels, 12*, 1100-1107.

Hefti, M., Marx, D., Joss, L., & Mazzotti, M. (2015). Adsorption equilibrium of binary mixtures of carbon dioxide and nitrogen on zeolites ZSM-5 and 13X. *Microporous Mesoporous Mater., 215*, 215-228.

Heinonen, J., Landa, H., Sainio, T., & Seidel-Morgenstern, A. (2012). Use of Adsorbed Solution theory to model competitive and co-operative sorption on elastic ion exchange resins. *Sep. Purif. Technol., 95*, 235-247.

Huasheng, G., Dahui, W., Yunchun, Y., & Tian'en, T. (2002). Binary Adsorption Equilibrium of Benzene-Water Vapor Mixtures on Activated Carbon. *Chinese J. Chem. Eng., 10*, 367-370.

Huggahalli, M., & Fair, J. (1996). Prediction of Equilibrium Adsorption of Water onto Activated Carbon. *Ind. Eng. Chem. Res., 35*, 2071-2074.

Hung, H., & Lin, T. (2007). Prediction of the Adsorption Capacity for Volatile Organic Compounds onto Activated Carbons by the Dubinin–Radushkevich–Langmuir Model. *J. Air & Waste Manage. Assoc., 57*, 497-506.

Ilic, M., Flockerzi, D., & Seidel-Morgenstern, A. (2010). A thermodynamically consistent explicit competitive adsorption isotherm model based on second-order single component behaviour. *J. Chromatogr. A, 1217*, 2132-2137.

Jain, J., & Snoeyink, V. (1973). Adsorption from bisolute systems on active carbon. *J. Water Pollut. Control Fed., 45*, 2463-2479.

Kapoor, A., Ritter, J., & Yang, R. (1989). On the Dubinin-Radushkevich Equation for Adsorption in Microporous Solids in the Henry's Law Region. *Langmuir, 5*, 1118-1121.

Keener, T., & Zhou, D. (1990). Prediction of Activated Carbon Adsorption Performance Under High Relative Humidity Conditions. *Environ. Progr., 9*, 40-46.

Kim, P., & Agnihotri, S. (2008). Application of water–activated carbon isotherm models to water adsorption isotherms of single-walled carbon nanotubes. *J. Colloid Interface Sci., 325*, 64-73.

Landa, H., & Flockerzi, D. (2013). A Method for Efficiently Solving the IAST Equations with an Application to Adsorber Dynamics. *AIChE J., 59*, 1263-1277.

Langmuir, I. (1916). The constitution and fundamental properties of solids and liquids. *J. Am. Chem. Soc., 38*, 2221-2295.

Lashaki, M., Atkinson, J., Hashisho, Z., Phillips, J., Anderson, J., & Nichols, M. (2016a). The role of beaded activated carbon's surface oxygen groups on irreversible adsorption of organic vapors. *J. Hazard. Mater., 317*, 284-294.

Lashaki, M., Atkinson, J., Hashisho, Z., Phillips, J., Anderson, J., Nichols, M., & Misovski, T. (2016b). Effect of desorption purge gas oxygen impurity on irreversible adsorption of organic vapors. *Carbon, 99*, 310-317.

Lee, J., Choi, D., Kwak, D., & Jung, H. (2005). Adsorption Dynamics of Water Vapor on Activated Carbon. *Adsorption, 11*, 437-441.

Li, C., Xuemin, H., Fangning, F., & Fengli, J. (2010). Effect of relative humidity on adsorption capacity of organic vapors on activated carbon and prediction by the modified D-R equation. *International Conference on Digital Manufacturing & Automation* , (pp. 608-611). Changha, Hunan.

Linders, M., van den Broeke, L., Kapteijn, F., & Moulijn, J. A. (2001). Binary Adsorption Equilibrium of Organics and Water on Activated Carbon. *AIChE J., 47*, 1885-1892.

Lodewyckx, P., & Vansant, E. (1999). Water Isotherms of Activated Carbons with Small Amounts of Surface Oxygen. *Carbon, 37*, 1647-1649.

Manes, M. (1984). Estimation of the effects of humidity on the adsorption onto activated carbon of the vapors of water-immiscible organic liquids. *Fundamentals of Adsorption* (pp. 335-344). New York: Engineering Foundation.

Mangano, E., Friedrich, D., & Brandani, S. (2015). Robust Algorithms for the Solution of the Ideal Adsorbed Solution Theory Equations. *AIChE J., 61*, 981-991.

Myers, A. (1983). Activity Coefficients of Mixtures Adsorbed on Heterogeneous Surfaces. *AIChE J., 29*, 691-693.

Myers, A. (2005). Prediction of Adsorption of Nonideal Mixtures in Nanoporous Materials. *Adsorption, 11*, 37-42.

Myers, A., & Prausnitz, J. (1965). Thermodynamics of Mixed-Gas Adsorption. *AIChE J., 11*, 121-126.

Myers, A., & Valenzuela, D. (1986). Computer Algorithm and Graphical Method for Calculating Adsorption Equilibria of Gas Mixtures. *J. Chem. Eng. Jap., 19*, 392-395.

Nastaj, J., Witkiewicz, K., & Chybowska, M. (2016). Modeling of multicomponent and multitemperature adsorption equilibria of water vapor and organic compounds on activated carbons. *Ads. Sci. Technol., 34*, 144-175.

O'Brien, J., & Myers, A. (1985). Rapid Calculations of Multicomponent Adsorption Equilibria from Pure Isotherm Data. *Ind. Eng. Chem. Process Des. Dev., 24*, 1188-1191.

Okazaki, M., Tamon, H., & Toei, R. (1978). Prediction of binary adsorption equilibria of solvent and water vapor on activated carbon. *J. Chem. Eng. Japan, 11*, 209-215.

Qi, N., & LeVan, M. (2005a). Coadsorption of Organic Compounds and Water Vapor on BPL Activated Carbon. 5. Methyl Ethyl Ketone, Methyl Isobutyl Ketone, Toluene, and Modeling. *Ind. Eng. Chem. Res., 44*, 3733-3741.

Qi, N., & LeVan, M. (2005b). Adsorption equilibrium modeling for water on activated carbons. *Carbon, 43*, 2258-2263.

Qi, N., Appel, W., & LeVan, M. (2006). Adsorption Dynamics of Organic Compounds and Water Vapor in Activated Carbon Beds. *Ind. Eng. Chem. Res., 45*, 2303-2314.

Qi, S., Hay, K., & Cal, M. (2000b). Predicting humidity effect on adsorption capacity of activated carbon for water-immiscible organic vapors. *Adv. Environ. Res., 4*, 357-362.

Qi, S., Hay, K., & Rood, M. (1998). Isotherm Equation for Water Vapor Adsorption onto Activated Carbon. *J. Environ. Eng., 124*, 1130-1134.

Qi, S., Hay, K., Rood, M., & Cal, M. (2000a). Equilibrium and Heat of Adsorption for Water Vapor and Activated Carbon. *J. Environ. Eng., 126*, 267-271.

Richter, E., Schutz, W., & Myers, A. (1989). Effect of Adsorption Equation on Prediction of Multicomponent Adsorption Equilibria by the Ideal Adsorbed Solution Theory. *Chem. Eng. Sci., 44*, 1609-1616.

Russell, B., & LeVan, M. (1997). Coadsorption of Organic Compounds and Water Vapor on BPL Activated Carbon. 3. Ethane, Propane, and Mixing Rules. *Ind. Eng. Chem. Res., 36*, 2380-2389.

Sakuth, M., Meyer, J., & Gmehling, J. (1998). Measurement and prediction of binary adsorption equilibria of vapors on dealuminated Y-zeolites (DAY). *Chem. Eng. Process, 37*, 267-277.

Salame, I., & Bandosz, T. (1999). Experimental Study of Water Adsorption on Activated Carbons. *Langmuir, 15*, 587-593.

Simon, C., Smit, B., & Haranczyk, M. (2016). pyIAST: Ideal adsorbed solution theory (IAST) Python package. *Comput. Phys. Commun., 200*, 364-380.

Siperstein, F., & Myers, A. (2001). Mixed-Gas Adsorption. *AIChE J., 47*, 1141-1159.

Slasli, A., Jorge, M., Stoeckli, F., & Seaton, N. (2003). Water adsorption by activated carbons in relation to their microporous structure. *Carbon, 41*, 479-486.

Stoeckli, F. (2002). Water adsorption in activated carbons of various degrees of oxidation described by the Dubinin equation. *Carbon, 40*, 969-971.

Stoeckli, F., Jakubov, T., & Lavanchy, A. (1994). Water Adsorption in Active Carbons described by the Dubinin-Astakhov Equation. *J. Chem. Soc. Faraday. Trans., 90*, 783-786.

Sullivan, P., Stone, B., Hashisho, Z., & Rood, M. (2007). Water adsorption with hysteresis effect onto microporous activated carbon fabrics. *Adsorption, 13*, 173-189.

Suwanayuen, S., & Danner, R. (1980). A gas adsorption isotherm equation based on vacancy solution theory. *AIChE J., 26*, 68-76.

Suzuki, M. (1990). *Adsorption Engineering*. Amsterdam: Elsevier Science Publishing Company, Inc.

Talu, O., & Meunier, F. (1996). Adsorption of Associating Molecules in Micropores and Application to Water on Carbon. *AIChE J., 42*, 809-819.

Talu, O., & Zwiebel, I. (1986). Multicomponent Adsorption Equilibria of Nonideal Mixtures. *AIChE J., 32*, 1263-1276.

Talu, O., & Zwiebel, I. (1987). Spreading Pressure Dependent Equation for Adsorbate Phase Acitivity Coefficients. *React. Polym., 5*, 81-91.

Talu, O., Li, J., & Myers, A. (1995). Activity Coefficients of Adsorbed Mixtures. *Adsorption, 1*, 103-112.

Tao, W., Yang, T., Chang, Y., Chang, L., & Chung, T. (2004). Effect of Moisture on the Adsorption of Volatile Organic Compounds by Zeolite 13X. *J. Environ. Eng., 130*, 1210-1216.

Taqvi, S., & LeVan, M. (1997). Virial Description of Two-Component Adsorption on Homogeneous and Heterogeneous Surfaces. *Ind. Eng. Chem. Res., 36*, 2197-2206.

Taqvi, S., Appel, W., & LeVan, M. (1999). Coadsorption of Organic Compounds and Water Vapor on BPL Activated Carbon. 4. Methanol, Ethanol, Propanol, Butanol, and Modeling. *Ind. Eng. Chem. Res., 38*, 240-250.

Tefera, D., Hashisho, Z., Philips, J., Anderson, J., & Nichols, M. (2014). Modeling Competitive Adsorption of Mixtures of Volatile Organic Compounds in a Fixed-Bed of Beaded Activated Carbon. *Environ. Sci. Technol., 48*, 5108-5117.

Tefera, D., Lashaki, M., Fayaz, M., Hashisho, Z., Philips, J., Anderson, J., & Nichols, M. (2013). Two-Dimensional Modeling of Volatile Organic Compounds Adsorption onto Beaded Activated Carbon. *Environ. Sci. Technol., 47*, 11700-11710.

Tien, C. (2013). *Adsorption Calculations and Modelling*. Butterworth_Heinemann.

Underhill, D., & Kawar, K. (1999). Effect of Relative Humidity on the Adsorption of Selected Water-Miscible Organic Vapors by Activated Carbon. *AIHA J., 60*, 730-736.

Van Ness, H. (1969). Adsorption of gases on solids: Review of the role of thermodynamics. *Ind. Eng. Chem. Fundam., 8*, 464-473.

Wood, G. (2000). *Review of Models for Adsorption of Single Vapors, Mixtures of Vapors, and Vapors at High Humidities on Activated Carbon for Applications including Predicting Service Lives of Organic Vapor Respirator Cartridges*. Washington, D.C.: Los Alamos National Laboratory.

Ye, X., Qi, N., & LeVan, M. (2003). Prediction of adsorption equilibrium using a modified D-R equation: organic-water vapor mixtures on BPL carbon. *Carbon, 41*, 2519-2525.

Yun, J., Park, H., & Moon, H. (1996). Multicomponent Adsorption Calculations Based on Adsorbed Solution Theory. *Korean J. Chem. Eng., 13*, 246-254.

Chapter 3 MATERIALS AND METHODS

The chapter provides a detailed description of the materials and methods used for the thesis research. It is divided into three sections. The first section describes the setup used for experimental validation. The second section explains the basis and parameters of the model including the VOC-water vapor multicomponent adsorption isotherm, the governing equations, and the initial and boundary conditions. The third section provides details on the statistical approach used to verify the developed model.

3.1 Experimental Setup and Method

Figure 3-1 portrays the bench-scale adsorption unit used for the experimental study of competitive adsorption between the VOC and water vapor onto a fixed bed of BAC. The measured data were then used to verify the model at the same operating conditions and parameters.

The experimental setup consisted of an adsorption tube containing the BAC adsorbent bed, a VOC-water vapor mixture generation system, a gas detection system, a heating system with variac, and a data acquisition and control (DAC) system. The adsorption tube was a cylindrical stainless-steel tube measuring 15.24 cm in length and 1.575 cm inner diameter. It was loaded with 13.3 g of dry virgin BAC such that the BAC bed length (L) was 11.5 cm. The BAC had a BET area of 1390 m^2/g, micropore volume of 0.51 cm^3/g, and total pore volume of 0.57 cm^3/g. A 1.5-cm-thick glass wool was used as a support for the fixed BAC bed at the bottom and top of the adsorption tube.

The VOC-water vapor mixture generation system consisted of two impingers, diffuser stones, mass flow controllers, and a syringe pump. The flow rate of dry air was controlled with a 0-20 standard liters per minute (SLPM) mass flow controller (Alicat Scientific). Dry air stream was humidified using two water-filled impingers (1 L) with diffuser stones, connected in parallel. A parallel configuration of impingers provided a stable supply of required relative humidity levels. A syringe pump (KD Scientific, KDS-220) was then used to inject the VOC into the humidified air stream, which is then introduced to the fixed-bed adsorption tube.

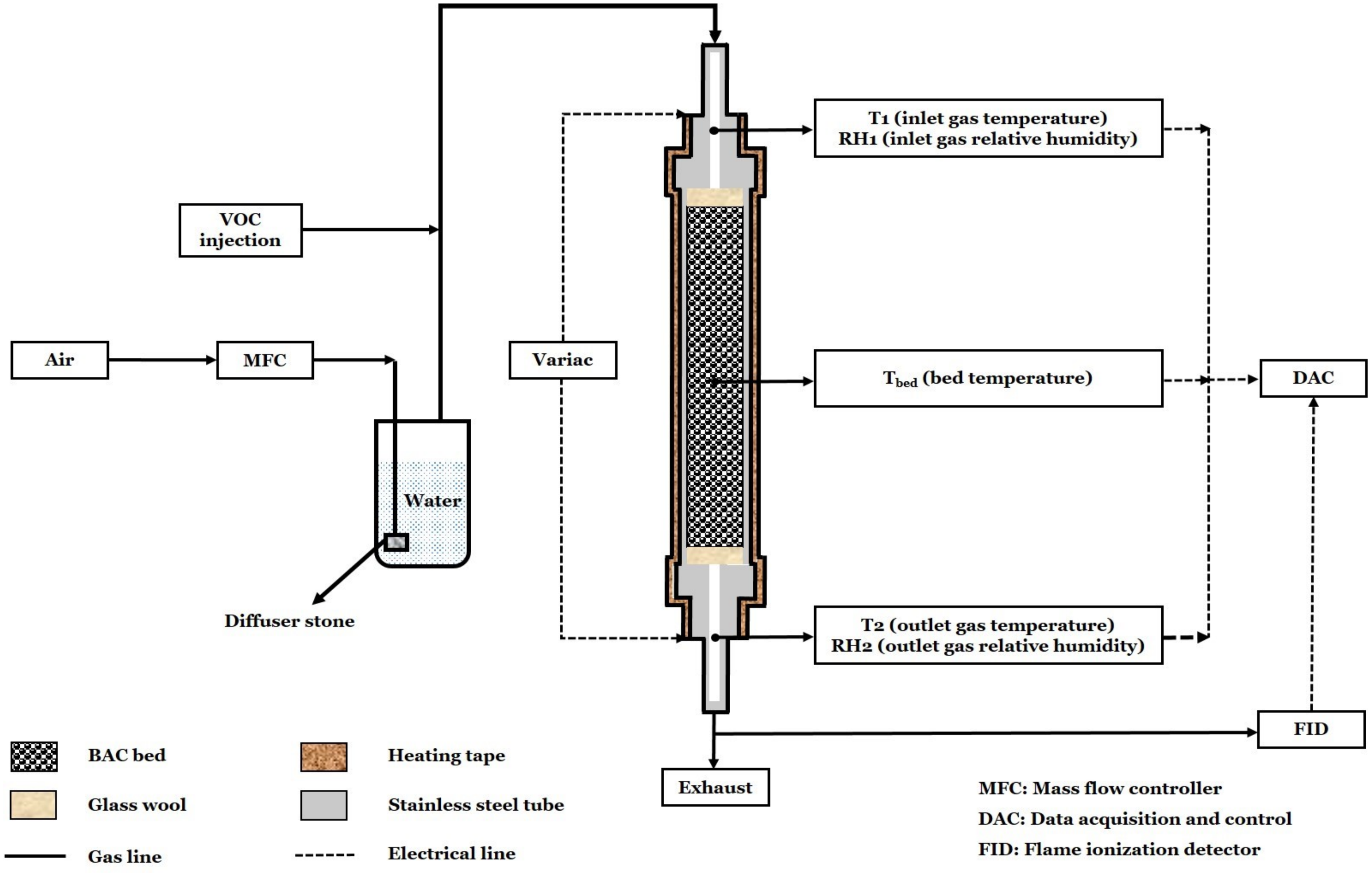

Figure 3-1. Bench-scale experimental setup for competitive adsorption between VOC and water vapor.

The gas detection system consisted of a flame ionization detector (FID) (Baseline Mocon, Series 9000) to measure the adsorbent bed effluent VOC concentration, and RH sensors (Vaisala HMT330) to measure the gas relative humidity. Two-point calibration of the FID was conducted with fresh air for zero and a steady state concentration of the dry adsorbate stream from the VOC-water vapor mixture generation system for span. Before the start of each adsorption test, the generated adsorbate gas stream was monitored using the FID and RH sensor, and was used as a reference for monitoring effluent stream. After a steady concentration stream is achieved, the gas stream was directed into the inlet of the adsorber tube to start the adsorption. A slip stream from the effluent was directed to the FID for effluent concentration measurement. Adsorption was continued until the BAC was fully saturated, as indicted by stable effluent concentrations, equal to the influent concentrations, measured by the FID.

The heating system consisted of a heating tape (Omega) wrapped around the adsorption tube, which was connected to a variable transformer (Staco Energy Products Co.). The heating tape is a fiberglass-covered electrical resistive wire to convert electrical energy to heat energy. The heating tape was used to provide constant energy to the fixed bed of BAC throughout the adsorption process. The tested bed temperatures for this work were 298.15 K (25 ^{o}C) and 305.15 K (32 ^{o}C). As adsorption progresses, the bed temperature variations were measured by a 0.9 mm type K thermocouple (Omega), inserted at the center of the tube. Resistant temperature detectors integrated with the RH meter probes (Vaisala HMT 330) measured gas temperature at the inlet and outlet of the adsorption tube.

The DAC system consisted of LabVIEW software package (National Instruments) and a data logger (National Instruments, CompactDAQ) with analog input and output modules. For this experimental setup, the data logger was interfaced with the FID, RH sensors, and thermocouples to record the signals from these sensors.

More information about the experimental setup and method can be found elsewhere (Lashaki et al., 2012a; Wang et al., 2012).

3.2 Model Development

3.2.1 Physical Model

The simulated bench-scale adsorber consisted of a cylindrical stainless steel tube with a 0.787-cm inner radius (R), containing 11.5-cm-long fixed bed of BAC particles (mean diameter = 0.75 mm) as shown in Figure 3-1. During dry conditions, a 10-SLPM dry air stream containing 1000 ppmv of VOC entered from the top of the fixed-bed adsorption tube at a superficial velocity (u_s) of 0.856 m/s and exited from the bottom of the tube. During wet conditions, the air stream with a flow rate of 10 SLPM was humidified up to 55 to 95% RH and then mixed with the VOC to generate a concentration of 1,000 ppmv before being fed into the fixed bed adsorber.

Major assumptions implemented for the proposed model development include negligible variation of flow properties in the angular direction of the cylindrical tube; negligible adsorption of the carrier gas (air); ideal gas behaviour; and symmetric flow conditions. These assumptions simplified the model geometry representing the adsorber into a 2D axisymmetric geometry (Figure 3-2), which also reduces the overall computation cost.

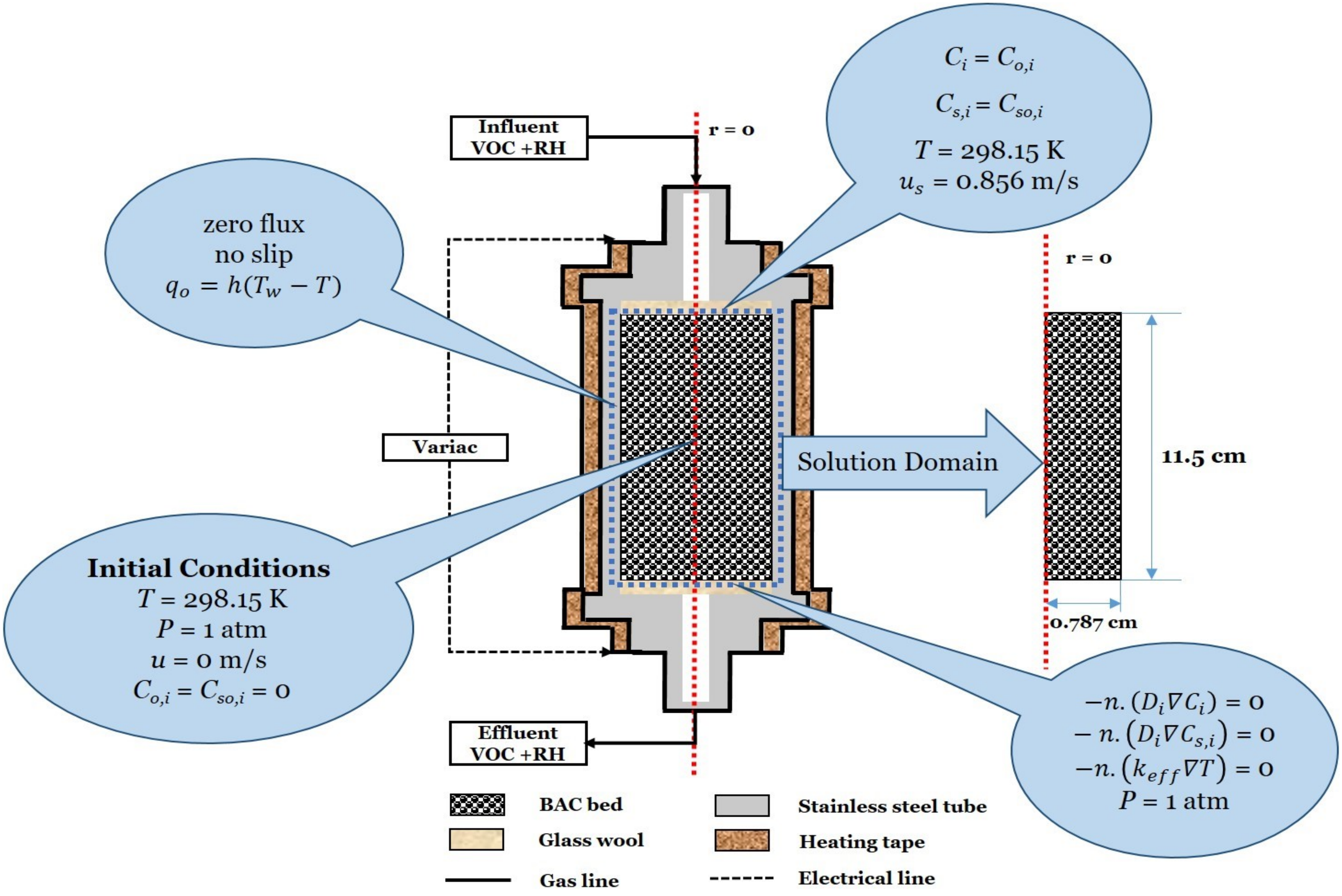

Figure 3-2. Simplification of the simulated adsorption unit into an 2D axisymmetric geometry.

Table 3-1. Model variables and parameters

symbol	description	value/formula	units	reference(s)
main variables				
C_i	gas-phase concentration		kg/m^3	eq. (3.26)
$C_{s,i}$	adsorbed-phase concentration		kg/m^3	eq. (3.31)
$C_{se,i}$	equilibrium adsorbed-phase concentration	$\rho_b(q_v \ or \ q_{mv})$; $\rho_b(q_{\mathrm{w}} \ or \ q_{m\mathrm{w}})$	kg/m^3	eq. (3.32) & (3.33)
F	body force	$g * \rho_f$	N/m^3	(Nield and Bejan, 2006)
P	gas pressure		kPa	eq. (3.19)
r	radial distance		m	N/A
t	adsorption time		s	N/A
T	fixed-bed temperature		K	eq. (3.1)
u	gas velocity vector		m/s	eq. (3.41)
$\|u\|$	resultant gas velocity		m/s	eq. (3.43)
z	axial distance		m	N/A
input variables				
a	QHR multitemperature constant	Table 4.2	1	eq. (3.3)
A	pre-exponential factor	Table 4.2	1	eq. (3.4)
b	QHR multitemperature constant	Table 4.2	1/K	eq. (3.3)
$B_{p,i}$	pore Biot number	Table 4.4; $(k_{ex,i}d_p)/(2D_{eff,i})$	1	(Sontheimer et al., 1988)
$C_{o,i}$	inlet gas concentration of the i^{th} component	1000 (VOC)	ppmv	boundary condition
		0, 55 or 95 (relative humidity)	%	
		0, 18000 or 31000 (relative humidity)	ppmv	
$C_{so,i}$	adsorbed phase concentration of the i^{th} component in equilibrium with its inlet gas phase concentration	$\rho_b(q_v \ or \ q_{mv})$; $\rho_b(q_{\mathrm{w}} \ or \ q_{m\mathrm{w}})$	kg/m^3	boundary condition
C_{eff}	effective volumetric heat capacity		J/(m^3.K)	(Tefera et al., 2013)
C_F	empirical correction factor for Forchheimer's drag coefficient calculation	$0.55\left(1 - 5.5\left(d_p/D_b\right)\right)$	1	(Nield and Bejan, 2006)
$C_{p,f}$	heat capacity of air		J/(kg.K)	COMSOL material database

symbol	description	value/formula	units	reference(s)
$C_{p,p}$	heat capacity of BAC	706.7	J/(kg.K)	(Tefera et al., 2013)
D_b	tube inner diameter	0.01575	m	measured
d_p	average BAC particle diameter	7.5 * 10^{-4}	m	(Lashaki et al., 2012a)
$D_{ax,i}$	axial dispersion coefficient		m^2/s	eq. (3.29)
$D_{AB,i}$	molecular diffusivity		m^2/s	eq. (3.30)
$D_{eff,i}$	effective diffusion coefficient		m^2/s	eq. (3.38)
D_i	symmetric mass dispersion tensor		m^2/s	eq. (3.27)
$D_{p,i}$	pore diffusion coefficient	Table 4.4	m^2/s	eq. (3.40)
$D_{r,i}$	radial dispersion coefficient		m^2/s	eq. (3.28)
$D_{s,i}$	surface diffusion coefficient	Table 4.4	m^2/s	eq. (3.39)
D_{so}	surface diffusion constant	1.1 * 10^{-8}	m^2/s	(Suzuki, 1990)
E_a	QHR multitemperature constant	Table 4.2	J/mol	eq. (3.4)
g	acceleration of gravity	9.81	m^2/s	
h	adsorber wall heat transfer coefficient	$(2.4/d_p)k_p + 0.054(k_f/d_p)\left(1 - (d_p/D_b)\right)Re_pPr^{1/3}$	W/(m^2.K)	(Bey and Eigenberger, 2001)
$\Delta H_{vap,i}$	adsorbate heat of vaporization	Table 4.3	kJ/mol	eq. (3.47)
$\Delta H_{ad,i}$	heat of adsorption		kJ/mol	eq. (3.47)
$\Delta H_{sol,i}$	heat of dissolution	17.42 (acetone-water system)	kJ/mol	(Kister and Waldman, 1958)
		210.35 (2-propanol-water system)	kJ/mol	(Lama and Lu, 1965; (Fujisawa et al., 2002))
IP_i	ionization potential	Table 4.3	eV	eq. (3.47); (Haynes, 2017)
J	shear stress		N/m^2	eq. (3.42)
K	MDR fitting parameter		mol^2/J^2	eq. (3.1)
k_{ax}	axial thermal conductivity		W/(m.K)	eq. (3.52)
k_b	stagnant bed thermal conductivity		W/(m.K)	eq. (3.53)
k_{eff}	effective thermal conductivity tensor		W/(m.K)	eq. (3.50)
$k_{ex,i}$	external mass transfer coefficient	Table 4.4	m/s	eq. (3.36)

symbol	description	value/formula	units	reference(s)
k_f	air thermal conductivity		W/(m.K)	COMSOL material database
$k_{in,i}$	internal mass transfer coefficient		1/s	eq. (3.37)
$k_{ov,i}$	overall mass transfer coefficient		1/s	eq. (3.35)
k_p	BAC particle thermal conductivity	0.17	W/(m.K)	(Kuwagaki et al., 2003)
k_r	radial thermal conductivity		W/(m.K)	eq. (3.51)
k_{QHR}	QHR fitting parameter		1	eq. (3.4)
L	tube bed length	0.115	m	measured
$M_{A,i}$	molecular weight of adsorbate	Table 4.3	g/mol	(Haynes, 2017); eq. (3.30)
M_B	molecular weight of air	29	g/mol	(Haynes, 2017)
m_{BAC}	mass of BAC in tube	13.3	g	measured
Pe_o	molecular Peclet number for heat transfer	$\left(u_s \rho_f C_{p,f} d_p\right)/k_f$	1	(Kwapinski, 2009)
Pr	Prandtl number	$\left(\mu_f C_{p,f}\right)/k_f$	1	(Bey and Eigenberger, 2001)
P_v^o	VOC vapor pressure in a pure component system		kPa	eq. (3.1)
P_{vS}	saturated VOC vapor pressure	Table 4.3	kPa	(Haynes, 2017); eq. (3.1)
P_v'	VOC vapor pressure in a mixture		kPa	eq. (3.5)
P_w^o	water vapor pressure in a pure component system		kPa	eq. (3.2)
P_{wS}	saturated water vapor pressure	Table 4.3	kPa	(Haynes, 2017)
P_w'	water vapor pressure in a mixture		kPa	eq. (3.6)
P_{50}	QHR fitting parameter		kPa	eq. (3.2)
q_{mv}	equilibrium adsorption capacity for water-miscible VOC in a mixture		kg/kg	eq. (3.24)
Q	gas flow rate	10	SLPM	measured
q_w	equilibrium adsorption capacity for water vapor in a mixture		kg/kg	eq. (3.7) & (3.18)
q_v	equilibrium adsorption capacity for VOC in a mixture		kg/kg	eq. (3.8) & (3.17)

symbol	description	value/formula	units	reference(s)
q_{mw}	equilibrium adsorption capacity for water vapor in a mixture containing water-miscible VOC		kg/kg	eq. (3.25)
Re_p	particle Reynolds number	$\left(\rho_f u_s d_p\right)/\left(\mu_f\left(1-\varepsilon_p\right)\right)$	1	(Nemec and Levec, 2005)
r_{pore}	average BAC pore radius	1.1	nm	(Tefera et al., 2014)
R_g	ideal gas constant	8.314	J/(mol.K)	
S	momentum sink		N/m^3	eq. (3.45)
Sc_i	Schmidt number	$\mu_f/\left(\rho_f D_{AB,i}\right)$	1	(Dantas et al., 2011)
$S_{m,i}$	mass sink of the gas phase		kg/(m^3.s)	eq. (3.31)
$S_{h,i}$	heat source		J/(m^3.s)	eq. (3.46)
$T_{b,i}$	adsorbate boiling point	Table 4.3	K	(Haynes, 2017); eq. (3.39)
T_w	adsorber wall temperature	298.15	K	boundary condition
u_s	superficial velocity	0.856	m/s	boundary condition
V_{pore}	BAC pore volume	0.57	cm^3/g	(Tefera et al., 2013)
$V^o_{v,max}$	adsorbed volume of pure VOC at pure component relative pressure $\left(\frac{P^o_v}{P_{vS}}\right)$		cm^3/g	eq. (3.1)
$V_{v,o}$	limiting adsorption volume for VOC in a pure component system	Table 4.1	cm^3/g	eq. (3.1)
V_1	MDR fitting parameter	Table 4.1	cm^3/g	eq. (3.1)
$V^o_{w,max}$	adsorbed volume of pure water vapor at pure component relative pressure $\left(\frac{P^o_w}{P_{wS}}\right)$		cm^3/g	eq. (3.2)
$V_{w,o}$	limiting adsorption volume for water vapor in a pure component system	Table 4.2	cm^3/g	eq. (3.2)
$V_{v,max}$	adsorbed volume of pure VOC at its mixture relative pressure $\left(\frac{P'_v}{P_{wS}}\right)$		cm^3/g	eq. (3.5)
$V_{w,max}$	adsorbed volume of pure water vapor at its mixture relative pressure $\left(\frac{P'_w}{P_{wS}}\right)$		cm^3/g	eq. (3.6)
v_v	molar volume of VOC adsorbed	$M_{A,1}/\rho_v$	cm^3/mol	
v_w	molar volume of water vapor adsorbed	$M_{A,2}/\rho_w$	cm^3/mol	

symbol	description	value/formula	units	reference(s)
w_{mic}	average micropore width of BAC	1.02	nm	(Tefera et al., 2013)
x_v	mole fraction of VOC in adsorbed phase		1	eq. (3.19)
x_w	mole fraction of water vapor in adsorbed phase		1	eq. (3.20)
y_v	mole fraction of VOC in gas phase		1	eq. (3.19)
y_w	mole fraction of water vapor in gas phase		1	eq. (3.20)
α_i	polarizability	Table 4.3	cm^3 x 10^{-24}	(Haynes, 2017); eq. (3.47)
α	MDR fitting parameter	Table 4.1	1	eq. (3.1)
α_0	empirical correction factor for mass diffusion terms	20	1	(Dantas et al., 2011)
β	affinity coefficient		1	eq. (3.1)
β_f	Forchheimer's drag coefficient	$\rho_f\left(C_F/\sqrt{\kappa}\right)$	kg/m^4	(Nield and Bejan, 2006)
γ_v	activity coefficient of VOC in adsorbed phase		1	eq. (3.19)
γ_w	activity coefficient of water vapor in adsorbed phase		1	eq. (3.20)
ε_b	bulk bed porosity	$0.379 + \left(0.078/\left(\left(D_b/d_p\right) - 1.8\right)\right)$	1	(Nield and Bejan, 2006)
ε_p	particle porosity	$V_{pore}\rho_p$	1	(Tefera et al., 2013)
ε_r	bed porosity as a function of radial distance from the center	$\varepsilon_b\left(1 + ((1 - \varepsilon_b)/\varepsilon_b) * exp((-6 * (R - r))/d_p\right)$	1	(Nield and Bejan, 2006)
ε_v'	adsorption potential of VOC in a mixture		J/mol	eq. (3.12)
ε_v^o	adsorption potential of VOC in a pure component system		J/mol	eq. (3.12)
ε_w^o	adsorption potential of water vapor in a pure component system		J/mol	eq. (3.12)
κ	bed permeability	$\left(\varepsilon_r{}^3 d_p{}^2\right)/(150(1 - \varepsilon_r)^2)$	m^2	(Nield and Bejan, 2006)
μ_f	air viscosity	temperature dependent	Pa.s	COMSOL material database
ρ_b	bulk bed density	595	kg/m^3	measured
ρ_w	density of adsorbed water vapor	0.92	g/ cm^3	(Alcaniz-Monge et al., 2002)

symbol	description	value/formula	units	reference(s)
$\rho_v(T)$	density of adsorbed VOC at any temperature		g/cm^3	(Haynes, 2017)
$\rho_v(T_{ref})$	density of adsorbed VOC at a reference temperature		g/cm^3	(Haynes, 2017)
ρ_f	air density	temperature dependent	kg/m^3	COMSOL material database
ρ_p	BAC particle density	$\rho_b/(1-\varepsilon_b)$	kg/m^3	(Tefera et al., 2013)
σ_i	surface tension		mN/m	(Haynes, 2017); eq. (3.47)
τ_p	BAC particle tortuosity	$1/{\varepsilon_p}^2$	1	(Guo, 2012)
$\upsilon_{A,i}$	atomic diffusion volume of adsorbate	Table 4.3	1	(Haynes, 2017); eq. (3.30)
υ_B	atomic diffusion volume of air	20.1	1	(Logan, 1997)
φ_i	surface to pore diffusion flux ratio	Table 4.4; $(\rho_b D_{s,i} V^o_{v,max}\rho_v)/(D_{eff,i}C_{o,i})$	1	(Do and Rice, 1987)
		Table 4.4; $(\rho_b D_{s,i} V^o_{w,max}\rho_w)/(D_{eff,i}C_{o,i})$	1	
indices				
i	component 1 (VOC); component 2 (water vapor)			
N/A	not applicable			

3.2.2 VOC-Water Vapor Multicomponent Adsorption Isotherm Formulation

As mentioned in previous chapters, adsorption equilibria are fundamental to establishing a model to accurately simulate a dynamic multicomponent competitive adsorption process.

In this research work, applicability of several popular multicomponent adsorption equilibria models such as IAST, RAST, vacancy solution model, method of Chou and Chiou, method of Manes, virial mixture coefficient theory, and method of Okazaki were investigated; especially in the areas of theoretical basis of water and VOC competitive adsorption, flexibility, and compatibility with computer simulation. Out of these models, the Manes method was selected to represent the competitive adsorption equilibria between water vapor and a VOC on activated carbon. The method was previously verified experimentally by a few studies for selected water-immiscible VOC-water systems on AC (Manes, 1984; Cal et al., 1996; Qi et al., 2000b). The main reasons for this selection include:

- Manes method is thermodynamically-consistent as it is based on Polanyi's adsorption potential theory (Manes, 1984).
- The main input requirements are pure single-component adsorption isotherm models of the VOC and water vapor (Manes, 1984), making it highly flexible and compatible with computer simulation compared to other multicomponent adsorption isotherm models.
- Unlike other models the Manes method has no requirements for vapor-liquid equilibrium data, and complex models for adsorbed-phase activity coefficients, which are dependent on experimental data (Myers and Prausnitz, 1965; Suwanayuen and Danner, 1980; Manes, 1984).
- The method explicitly considers the difference in fundamental adsorption mechanism of water vapor and VOC during competitive adsorption; which is the main shortcoming of several popular models such as IAST, RAST, and VSM (Myers and Prausnitz, 1965; Suwanayuen and Danner, 1980; Manes, 1984).

Further details on all the aforementioned multicomponent adsorption isotherm models including Manes method are given in Chapter 2. Definitions of model parameters and variables are presented in Table 3-1.

3.2.2.1 Input Parameters for Manes Method

3.2.2.1.1 Pure Single-Component VOC Adsorption Isotherm

A modified Dubinin-Radushkevich (MDR) isotherm was chosen to fit the VOC experimental isotherms and predict the adsorption equilibrium of the pure VOC on BAC at different VOC concentrations. The MDR isotherm easily aligns with the Manes method as it also based on potential theory (Manes, 1984; Kapoor, et al., 1989). It is a modified version of Dubinin-Radushkevich (DR) equation, and has a valid Henry's law term at low loadings (Kapoor et al., 1989). Therefore, it is thermodynamically consistent throughout the entire relative pressure range. The MDR model has been very successful in predicting equilibrium adsorption capacities for VOCs in microporous adsorbents such as AC (Kapoor et al., 1989; Hung and Lin, 2007). Its equation is given as (Kapoor et al., 1989):

$$V_{v,max}^{o} = \left[1 - exp\left(-\alpha \frac{P_v^o}{P_{vS}}\right)\right] V_{v,o} exp\left[-\frac{K}{\beta^2}\left(R_g T\right)^2 \left(ln \frac{P_{vS}}{P_v^o}\right)^2\right] + exp\left(-\alpha \frac{P_v^o}{P_{vS}}\right) V_1 \frac{P_v^o}{P_{vS}} \tag{3.1}$$

Once the above equation is fitted at a given adsorption temperature, the same equation can be used for multiple adsorption temperatures by applying a minor modification to $V_{v,o}$, given as $V_{v,o}\left[\frac{\rho_v(T)}{\rho_v(T_{ref})}\right]$ (Do, 1998).

More information on MDR and other single-component adsorption isotherm models for VOCs can be found in Chapter 2.

3.2.2.1.2 Pure Single-Component Water Vapor Adsorption Isotherm

Adsorption equilibrium of pure water vapor onto BAC was modeled using the Qi-Hay-Rood (QHR) isotherm. It considers the unique behaviour of water vapor adsorption on BAC; mainly adsorption through surface functional groups at low loadings, and cluster formation mechanism at medium to high loadings (Qi et al., 1998). These processes are attributed to the hydrogen bonding among the water molecules and oxygen-based surface functional groups (Qi et al., 2000a). More information on QHR and other pure water vapor adsorption isotherm models can be found in Chapter 2.

The multi-temperature sigmoidal QHR equation can be given as (Qi, et al., 1998):

$$V^{o}_{w,max} = \frac{V_{w,o}}{1+exp\left[k_{QHR}\left(\frac{P_{50}}{P_{wS}} - \frac{P^{o}_{w}}{P_{wS}}\right)\right]} \quad (3\ 2)$$

$$\frac{P_{50}}{P_{wS}} = a + bT \quad (3\ 3)$$

and

$$k_{QHR} = Ae^{-(E_a/R_gT)} \quad (3.4)$$

where $\mathrm{P_{wS}} = \mathrm{P_{50}}$ at $\frac{\mathrm{V^{o}_{w,max}}}{\mathrm{V_{w,o}}} = 0.5$.

The same fitting parameters ($V_{w,o}, a, b, A, E_a$) can be used for modeling adsorption equilibrium at different temperatures (Qi et al., 2000a). QHR model gave a very good fit for predicting pure water vapor adsorption equilibrium at various temperatures on microporous adsorbents (Qi et al., 1998; 2000a).

3.2.2.2 Solving Manes Method

During its initial development, Manes method was typically solved graphically (Manes, 1984). This is because pure component adsorption equilibrium profiles of water vapor and VOCs were represented by their characteristic curves. But, with the introduction of good-fitting single-component adsorption isotherm models to replace the characteristic curves, numerical solution technique became possible, as shown by Qi et al., (2000b). Even with the numerical solution techniques, the Manes method has only been solved for a single set of concentrations of components (VOC and water vapor) involved in competitive adsorption, at a time (Qi et al., 2000b).

In this study, the Manes method was solved for the entire range of concentrations up to saturation levels for water vapor and VOC in a single run. This was implemented using MATLAB's (MathWorks) programming language tools. The computation time was usually around 5 to 10 seconds using MATLAB R2016a on a computer with Intel Core i7 processor. Complete MATLAB code for the Manes method is available in Appendix A. The results from the code are further represented using interpolation functions in COMSOL Multiphysics software for modeling adsorption transport phenomena.

The Manes method revolves around two conditions:

The first condition is when the adsorbed volume of pure VOC is larger than the adsorbed volume of pure water vapor at their respective mixture relative vapor pressures ($V_{v,max} > V_{w,max}$). According to Manes (1984), there is no negative impact by water vapor on the adsorption capacities for VOCs during this scenario. The equations are:

$$V_{v,max} = \left[1 - exp\left(-\alpha \frac{P_v'}{P_{vS}}\right)\right] V_{v,o} exp\left[-\frac{K}{\beta^2}\left(R_g T\right)^2 \left(ln \frac{P_{vS}}{P_v'}\right)^2\right] + exp\left(-\alpha \frac{P_v'}{P_{vS}}\right) V_1 \frac{P_v'}{P_{vS}} \tag{3.5}$$

$$V_{w,max} = \frac{V_{w,o}}{1 + exp\left[k_{QHR}\left(\frac{P_{50}}{P_{wS}} - \frac{P_w'}{P_{wS}}\right)\right]} \tag{3.6}$$

$$q_w = 0 \tag{3.7}$$

$$q_v = \rho_v V_{v,max} \tag{3.8}$$

The second condition is when the adsorbed volume of pure water vapor is larger than the adsorbed volume of pure VOC at their respective mixture relative vapor pressures ($V_{w,max} < V_{v,max}$), and during which competitive adsorption between water vapor and

VOC occurs (Manes, 1984). Adsorption of VOC during this scenario results in displacing an equal volume of pure condensed water (equation (3.9)). $V_{v,max}$ and $V_{w,max}$ are calculated using equations (3.5) and (3.6). When $V_{v,max} < V_{w,max}$, VOC adsorption capacity decreases due to its lower adsorption potential compared to water vapor's.

$$V_{v,max}^{o} = V_{w,max}^{o} \tag{3.9}$$

Using equation (3.9) with (3.2) gives:

$$V_{v,max}^{o} = \frac{V_{w,o}}{1+exp\left[k_{QHR}\left(\frac{P_{50}}{P_{wS}} - \frac{P_{w}^{o}}{P_{wS}}\right)\right]}$$

(3.10)

Arranging equation (3.10):

$$\frac{P_{w}^{o}}{P_{wS}} = \frac{P_{50}}{P_{wS}} - \frac{1}{k_{QHR}} ln\left[\frac{V_{w,o}}{(V_{v,max}^{o})} - 1\right] \tag{3.11}$$

The other important equations involved in this condition are (Manes, 1984):

$$\frac{\varepsilon_{v}'}{v_{v}} = \frac{\varepsilon_{v}^{o}}{v_{v}} - \frac{\varepsilon_{w}^{o}}{v_{w}} - \frac{R_{g}T}{v_{w}} ln\frac{P_{w}'}{P_{wS}} \tag{3.12}$$

$$\varepsilon_{v}' = \varepsilon_{v}^{o} - \varepsilon_{w}^{o}\left(\frac{v_{v}}{v_{w}}\right) \tag{3.13}$$

$$\varepsilon_{v}' = R_{g}T\, ln\frac{P_{vS}}{P_{v}'} \tag{3.14}$$

$$\varepsilon_{v}^{o} = R_{g}T\, ln\frac{P_{vS}}{P_{v}^{o}} \tag{3.15}$$

$$\varepsilon_{w}^{o} = R_{g}T\, ln\frac{P_{wS}}{P_{w}^{o}} \tag{3.16}$$

$$q_{v} = \rho_{v}V_{v,max}^{o} \tag{3.17}$$

$$q_{w} = \rho_{w}\left(V_{w,max} - V_{v,max}^{o}\right) \tag{3.18}$$

Equation (3.12) is the adsorption-potential-theory-based relation derived by Manes (1984), which shows that the net adsorption potential of VOC in a mixture is equal to its adsorption potential in pure state, reduced by the adsorption potential of an equal volume of pure water vapor, and corrected for water vapor pressure less than saturation. Equation (3.12) reduces to equation (3.13) when RH is 100%. The solution of this model requires an iterative procedure in such a way that the guesses satisfy equation (3.12) (Figure 3-3). The criterion considered here was up to eight decimal places; to minimize errors, and that no significant change in results occurs with further increase in decimal places.

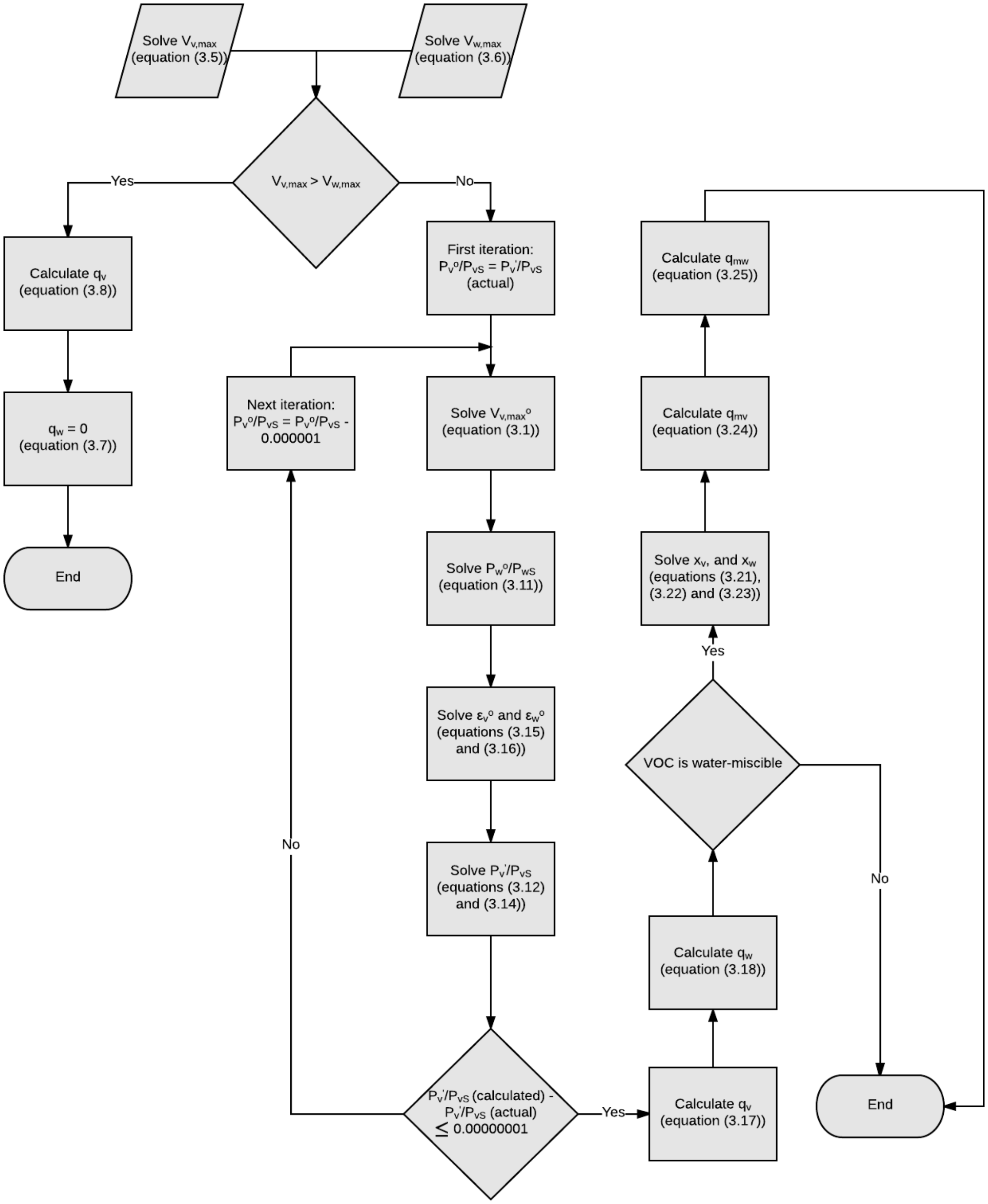

Figure 3-3. Flowchart describing the procedure to numerically solve Manes-method and its extension for water-miscible VOCs.

Manes method is exclusively for water-immiscible VOCs due to its direct dependency on potential theory (Manes, 1984). However, in this research work it has also been applied for water-miscible VOCs by introducing a Raoult's-law-like relation:

$$Py_v = \gamma_v x_v P_{vS} \tag{3.19}$$

$$Py_w = \gamma_w x_w P_{wS} \tag{3.20}$$

$$x_v + x_w = 1 \tag{3.21}$$

Similar relation was also used by Okazaki et al. (1978) for their multicomponent adsorption model. Here, the purpose of the relation is to calculate the composition of Manes-method-calculated water adsorbed phase during competitive adsorption; considering complete dissolution of the VOC into that phase. The composition is then used to predict the effect of RH on VOC adsorption capacity. Manes-method-calculated VOC adsorbed phase was not considered here because it is extremely underestimated for water-miscible VOCs and therefore, can be neglected. The activity coefficients of the components in the mixture in equations (3.19) and (3.20) are assumed to be ideal and therefore, are equal to unity. The equations then reduce to:

$$Py_v = x_v P_{vS} \tag{3.22}$$

$$Py_w = x_w P_{wS} \tag{3.23}$$

Adsorption capacities for water-miscible VOC and water vapor during competitive adsorption can be calculated by:

$$q_{mv} = \rho_v V_{v,max}^{o} + x_v q_w \tag{3.24}$$

$$q_{mw} = x_w q_w \tag{3.25}$$

Equations (3.24) and (3.25) are only applicable when $V_{v,max} < V_{w,max}$.

3.2.3 Transport Phenomena Formulation

An accurate prediction of multicomponent adsorption isotherm serves as a good basis to describe the dynamics of a fixed-bed adsorber with competitive adsorption between water vapor and VOC (Yang, 1987). The adsorption transfer kinetics considered here is discussed below.

3.2.3.1 Governing Transport Phenomena

The transport phenomena model used here is an extension of the model developed by Tefera et al. (2013, 2014) for single and multicomponent VOC adsorption. The transfer kinetics to be simulated are: adsorbate mass balance in the gas phase and adsorbed phase as well as the heat and momentum balance across the fixed bed adsorber. These transport phenomena are described by partial differential equations (PDEs), ordinary differential equations, and algebraic equations; as given in the following subsections.

3.2.3.1.1 Gas-Phase Mass Balance

Adsorbate mass transfer in the gas phase of a fixed-bed adsorber is governed by dispersion and convection. The equation describing this behaviour is given as (Yang, 1987):

$$-\nabla(D_i * \nabla C_i) + (u * \nabla C_i) + \frac{\partial C_i}{\partial t} + \left(\frac{1-\varepsilon_p}{\varepsilon_p}\right) * S_{m,i} = 0 \tag{3.26}$$

where D_i is the symmetric mass dispersion tensor:

$$D_i = \begin{vmatrix} D_{r,i} & 0 \\ 0 & D_{ax,i} \end{vmatrix} \tag{3.27}$$

The radial ($D_{r,i}$) and axial ($D_{ax,i}$) dispersion coefficients are described in equations (3.28) and (3.29) respectively (Dantas et al., 2011; Cohen and Metzner, 1981).

$$D_{r,i} = \left(\alpha_0 + \frac{Sc_i Re_p}{8}\right)\frac{D_{AB,i}}{\varepsilon_b} \tag{3.28}$$

$$D_{ax,i} = \left(\alpha_0 + \frac{Sc_i Re_p}{2}\right)\frac{D_{AB,i}}{\varepsilon_b} \tag{3.29}$$

where $D_{AB,i}$ is the molecular diffusivity of the i^{th} component described as (Logan, 1997):

$$D_{AB,i} = \frac{0.0101325*\left(10^{-3}T^{1.75}\sqrt{\frac{M_{A,i}+M_B}{M_{A,i}M_B}}\right)}{P\left({(\sum v)_{A,i}}^{0.33}-{(\sum v)_B}^{0.33}\right)^2} \tag{3.30}$$

The mass sink $\left(S_{m,i}\right)$ of the gas phase is represented by the linear driving force (LDF) model given as (Sircar and Hufton, 2000):

$$S_{m,i} = k_{ov,i}(C_{se,i} - C_{s,i}) \tag{3.31}$$

The LDF has similar accuracy when compared to other complex diffusion models in modeling mass transfer kinetics in an adsorbent particle. The complex diffusion models rely on individual particle mass transfer and therefore are time-consuming and computationally costlier, unlike the LDF model (Sircar and Hufton, 2000).

$C_{se,i}$, the equilibrium adsorbed-phase concentration, is obtained from the multicomponent competitive adsorption isotherm (equations (3.32) and (3.33)).

$$C_{se,1} = \rho_b(q_v \; or \; q_{mv}) \tag{3.32}$$

$$C_{se,2} = \rho_b(q_w \; or \; q_{mw}) \tag{3.33}$$

Here, the LDF-based gas-phase mass sink acts as the source for the adsorbed phase (Sircar and Hufton, 2000).

3.2.3.1.2 Adsorbed-Phase Mass Balance

The diffusive adsorbate transport in the adsorbed phase is characterized using the LDF model as mentioned above, and is given as (Yang, 1987; Sircar and Hufton, 2000):

$$\frac{\partial C_{s,i}}{\partial t} = k_{ov,i}\left(C_{se,i} - C_{s,i}\right) = S_{m,i} \tag{3.34}$$

The LDF overall mass transfer coefficient $\left(k_{ov,i}\right)$ here considers both the internal $(1/k_{in,i})$ and external $\left(1/k_{ex,i}\right)$ mass transfer resistances described as (Dantas, et al., 2011; Jarvie, et al., 2005):

$$\frac{1}{k_{ov,i}} = \frac{d_p}{k_{ex,i}} + \frac{1}{k_{in,i}} \tag{3.35}$$

where

$$k_{ex,i} = \frac{[1+1.5(1-\varepsilon_b)]D_{AB,i}}{d_p}\left(2 + 0.644Re_p^{1/2}Sc_i^{1/3}\right) \tag{3.36}$$

$$k_{in,i} = \frac{60\varepsilon_p C_{o,i} D_{eff,i}}{\tau_p C_{so,i} {d_p}^2} \tag{3.37}$$

The internal mass transfer coefficient here is controlled by macropore molecular diffusion system (Dantas, et al., 2011). Applicability of the external mass transfer resistance depends on the pore Biot number $\left(B_{p,i}\right)$. If $B_{p,i}$ is larger than unity, then the effect of external mass transfer resistance is negligible and the overall mass transfer is governed by internal or intraparticle diffusion (Shaverdi, 2012).

The effective diffusion coefficient $\left(D_{eff,i}\right)$ comprises surface $\left(D_{s,i}\right)$ and pore $\left(D_{p,i}\right)$ diffusion; and is written as (Suzuki, 1990; Hui et al., 2003; Chahbani and Tondeur, 2000):

$$D_{eff,i} = D_{p,i} + \frac{\partial C_{s,i}}{\partial C_i} D_{s,i} \tag{3.38}$$

$$D_{s,i} = D_{so} exp\left(\frac{-5.38T_{b,i}}{T}\right) \tag{3.39}$$

$$D_{p,i} = D_{AB,i} \tag{3.40}$$

Surface diffusion can be neglected from the effective diffusion resistance if the surface to pore diffusion flux ratio $\left(\varphi_i\right)$ is found to be less than unity; otherwise pore diffusion can be neglected (Do and Rice, 1987). Here, pore diffusion consists of molecular diffusion.

3.2.3.1.3 Momentum Balance

The momentum balance equation considered here accounts for Darcy and Brinkman viscous terms, Navier-Stokes' convective term, and Forchheimer's inertial term (Nield and Bejan, 2006). This model has been previously applied with good success (Tefera, et al., 2013, 2014), and is given by:

$$\frac{\rho_f}{\varepsilon_r}\left(\left(\frac{\partial u}{\partial t}\right) + (u * \nabla)\frac{u}{\varepsilon_r}\right) = -\nabla P + \nabla J - S + F \tag{3.41}$$

The shear stress (J) in terms of gas viscosity (μ_f) is written as:

$$J = (\mu_f \frac{1}{\varepsilon_r}\left((\nabla u + (\nabla u)') - \left(\frac{2}{3} * (\nabla u)\right)\right) \tag{3.42}$$

Momentum dissipation of the gas flow across the fixed-bed adsorber is represented by Darcy's friction loss factor, Forchheimer's inertial term, and a sink term due to the adsorption of VOC and/or water vapor (equation (3.43)).

$$S = \left(\frac{\mu_f}{\kappa} + \beta_f|u| + \frac{1}{\varepsilon_r}\left(\sum_{i=1}^{2}\frac{\partial C_{s,i}}{\partial t}\right)\right)u \tag{3.43}$$

The continuity equation given below accounts for the compressibility of the gas flow in the fixed-bed adsorber and the sink due to VOC and/or water vapor adsorption.

$$\frac{\partial(\varepsilon_r\rho_f)}{\partial t} + \nabla * (\rho_f u) = \sum_{i=1}^{2}\frac{\partial C_{s,i}}{\partial t} \tag{3.44}$$

3.2.3.1.4 Energy Balance

The main assumptions for formulating energy balance equation across the fixed-bed adsorber are: local thermal equilibrium between the solid adsorbent and the gas; and negligible pressure work and viscous heat dissipation. The convection-diffusion-based heat transfer equation was previously validated for single and multicomponent adsorption systems (Tefera, et al., 2013, 2014).

$$C_{eff}\frac{\partial T}{\partial t} + C_{p,f}\rho_f u * \nabla T - \nabla(k_{eff}\nabla T) = \sum_{i=1}^{2} S_{h,i} \tag{3.45}$$

The domain heat source is the heat of adsorption of the i^{th} component (equation (3.46)).

$$S_{h,i} = (-\Delta H_{ad,i})\frac{dC_{s,i}}{dt} \tag{3.46}$$

where the heat of adsorption $(\Delta H_{ad,i})$ is dependent on the properties of the adsorbate and the solid adsorbent (Giraudet, et al., 2006):

$$-\Delta H_{ad,i} = 103.2 + 1.16\alpha_i + 0.76\Delta H_{vap,i} - 3.87(IP_i) - 0.7\sigma_i - 26.1w_{mic} \quad (3.47)$$

In mixtures involving polar adsorbates and water vapor, heat of dissolution $(\Delta H_{sol,i})$ was also considered additionally (equation (3.48)).

$$S_{h,i} = \left(-\Delta H_{ad,i} - \Delta H_{sol,i}\right)\frac{dC_{s,i}}{dt} \quad (3.48)$$

The effective volumetric heat capacity (C_{eff}) of the solid-gas system is calculated from:

$$C_{eff} = (1-\varepsilon_p)\rho_p C_{p,p} + \varepsilon_p \rho_f C_{p,f} \quad (3.49)$$

The effective thermal conductivity tensor (k_{eff}) is given as:

$$k_{eff} = \begin{vmatrix} k_r & 0 \\ 0 & k_{ax} \end{vmatrix} \quad (3.50)$$

k_r and k_{ax} are the radial and axial effective thermal conductivities (Suzuki, 1990) of the fixed-bed adsorber respectively (equations (3.51) and (3.52)).

$$k_r = k_b + \frac{1}{8}Pe_o k_f \quad (3.51)$$

$$k_{ax} = k_b + \frac{1}{2}Pe_o k_f \quad (3.52)$$

where k_b is the stagnant bed thermal conductivity, that is, the thermal conductivity of the fixed-bed with stagnant gas (Suzuki, 1990).

$$k_b = (1-\varepsilon_p)k_p + \varepsilon_p k_f \quad (3.53)$$

3.2.3.2 Variable and Parameters Definition

Table 3-1 exclusively describes and defines the model parameters and variables.

3.2.3.3 Initial and Boundary Conditions

The initial and boundary conditions applied to the 2D mathematical model here are described in Table 3-2 and graphically in Figure 3-2. For mass transfer, a constant concentration boundary condition and a flux boundary condition are set at the inlet and the outlet of the fixed-bed adsorption tube, respectively. For momentum balance; a normal inflow velocity boundary condition at the inlet, an atmospheric pressure at the outlet, and a no slip boundary condition was applied to the wall of the adsorption tube. For heat transfer; a constant temperature boundary condition, a flux boundary condition, and a convective heat flux were specified at the inlet, outlet, and wall of the fixed-bed adsorber respectively.

Table 3-2. Initial and boundary conditions

physics	inlet ($Z = L$)	outlet ($Z = 0$)	adsorber wall ($r = R$)	initial condition ($t = 0$)
mass transfer	$C_i = C_{o,i}$ $C_{s,i} = C_{so,i}$	boundary flux, $-n * (D_i \nabla C_i) = 0$, $-n * (D_i \nabla C_{s,i}) = 0$	zero flux	$C_{o,i} = 0$ $C_{so,i} = 0$
momentum transfer	normal velocity ($u_s = 0.856\ m/s$)	$P = 101.325\ kPa$	no slip	$u = 0$ m/s $P = 101.325\ kPa$
heat transfer	$T = 298.15\ K$	$-n * (k_{eff} \nabla T) = 0$	$q_o = h * (T_w - T)$	$T = 298.15\ K$

3.2.3.4 Solution Method

The mass, momentum, and heat transfer across the fixed-bed adsorber were coupled, and simultaneously solved using COMSOL Multiphysics software (Version 4.3a). This simulation was also coupled with interpolation-function-based MATLAB-coded Manes method as mentioned earlier. In COMSOL Multiphysics, the governing equations were solved numerically using the finite element method. The software's coefficient form

PDE interfaces, built-in momentum and energy interfaces were used respectively to represent the mass, momentum, and heat transfer equations. A second-order element was used for concentration, pressure and temperature; and a third-order element for velocity to improve model convergence and stability (Oliemans, 2000; Hutton, 2001; Oberkampf and Trucano, 2002). Convergence of the model was validated by using systematic mesh refinement to its geometry until grid-independent results were obtained. The meshing of the 2D model's geometry was finally optimized to 4,488 mesh elements, which showed a relative deviation of only 0.7% from the solution obtained through fine meshing (25,964 mesh elements).

3.3 Model Validation Method

To validate the model, adsorption capacities, breakthrough concentrations, and bed temperatures were measured and compared with the model output. The deviations between the modeled and experimental values were represented using two error metrics. The nonzero data points from the experiment and model were compared through the mean relative absolute error (MRAE) (Lashaki et al., 2012b).

$$MRAE = \frac{1}{N}\sum_{1}^{N}\left(\frac{|experimental\ value - modeled\ value|}{experimental\ value} * 100\%\right) \tag{3.54}$$

where N is the number of data points.

The normalized root-mean-square error (NRMSE) was also used to evaluate the overall error between the experimental and modeled values (Tefera, et al., 2013).

$$NRMSE = \frac{\sqrt{\frac{1}{N}\sum_{1}^{N}(experimental\ value - modeled\ value)^2}}{influent\ stream\ value} * 100\% \tag{3.55}$$

For measuring deviations in bed temperature results using MRAE and NRMSE, the temperature data points were expressed in degree Celsius instead of Kelvin to avoid low relative error bias.

To determine the single-component MDR isotherm model parameters of the selected VOCs (toluene, 2-propanol, acetone, n-butanol), their corresponding experimental isotherms were obtained from a previous study (Lashaki et al., 2012b) and the isotherm model was fitted to the experimental values. For 1,2,4- trimethylbenzene, the experimental adsorption isotherm was obtained by conducting a mass balance on a fixed-bed adsorber with 1g of BAC that was subjected to concentrations ranging from 60 to 2600 ppmv of 1,2,4- trimethylbenzene in a 10-SLPM air stream at 25 °C. The MDR isotherm model was then similarly fitted to the measured data. The adsorber setup mentioned above is similar to the one described at the beginning of this chapter.

For pure water vapor, its adsorption isotherm was obtained gravimetrically using a sorption analyzer (TA Instruments, model VTI-SA) at 25 °C and nitrogen as a carrier gas. The system logged the equilibrium weight of the BAC sample (3 to 5 mg) in response to a step change in the concentration of the water vapor in the carrier gas. The equilibrium was assumed to be reached when the weight change is less than 0.001 % in 5 minutes. The QHR model parameters were then determined and fitted to the measured data.

The fitting of the isotherm models was conducted through the least squares method in MATLAB.

$$LSM = \sum_{1}^{N}(experimental\ value - modeled\ value)^2 \tag{3.56}$$

where equation (3.56) (Vahabi, et al., 2011) runs until it reaches an optimized minimum with a relative change in residuals of about 4.09 * 10^{-8}.

The root-mean-square error (RMSE) was also used to evaluate the overall error of the isotherm models (Willmott and Matsuura, 2005).

$$RMSE = \sqrt{\frac{1}{N}\sum_{1}^{N}(experimental\ value - modeled\ value)^2} \qquad (3.57)$$

3.4 References

Alcaniz-Monge, J., Linares-Solano, A., & Rand, B. (2002). Mechanism of Adsorption of Water in Carbon Micropores As Revealed by a Study of Activated Carbon Fibers. *J. Phys. Chem. B, 106*, 3209-3216.

Bey, O., & Eigenberger, G. (2001). Gas flow and heat transfer through catalyst filled tubes. *Int. J. Therm. Sci., 40*, 152-164.

Cal, M., Rood, M., & Larson, S. (1996). Removal of VOCs from humidified gas streams using activated carbon cloth. *Gas Sep. Purif., 10*, 117-121.

Chahbani, M., & Tondeur, D. (2000). Mass transfer kinetics in pressure swing adsorption. *Sep. Purif. Technol., 20*, 185-196.

Cohen, Y., & Metzner, A. B. (1981). Wall effects in laminar flow of fluids through packed beds. *AIChE J., 27*, 705-715.

Dantas, T., Luna, F., Silva Jr., I., Torres, A., de Azevedo, D., Rodrigues, A., & Moreira, R. (2011). Modeling of the fixed-bed adsorption of carbon dioxide and a carbon dioxide-nitrogen mixture on zeolite 13X. *Braz. J. Chem. Eng., 28*, 533-544.

Do, D. (1998). *Adsorption Analysis: Equilibria and Kinetics*. London: Imperial College Press.

Do, D., & Rice, R. (1987). On the relative importance of pore and surface diffusion in non-equilibrium adsorption rate processes. *Chem. Eng. Sci., 42*, 2269-2284.

Fujisawa, M., Maeda, M., Takagi, S., & Kimura, T. (2002). Enthalpies of dilution of mono-, di- and poly-alcohols in dilute aqueous solutions at 298.15 K. *J. Therm. Anal. Calorim., 69*, 841-848.

Giraudet, S., Pre´, P., Tezel, H., & Le Cloirec, P. (2006). Estimation of adsorption energies using the physical characteristics of activated carbons and the molecular properties of volatile organic compounds. *Carbon, 44*, 2413-2421.

Guo, P. (2012). Dependency of tortuosity and permeability of porous media on directional distribution of pore voids. *Transp. Porous Media, 95*, 285-303.

Haynes, W. (2017). *CRC Handbook of Chemistry and Physics* (97th ed.). Boca Raton, Florida: CRC Press/Taylor & Francis.

Hui, C., Chen, B., & McKay, G. (2003). Pore-surface diffusion model for batch adsorption processes. *Langmuir, 19*, 4188-4196.

Hung, H., & Lin, T. (2007). Prediction of the Adsorption Capacity for Volatile Organic Compounds onto Activated Carbons by the Dubinin–Radushkevich–Langmuir Model. *J. Air & Waste Manage. Assoc., 57*, 497-506.

Hutton, A. G. (2001). Quality and trust in industrial computational fluid dynamics. *Houille Blanche, 3-4*, 25-28.

Jarvie, M. E., Hand, D. W., Bhuvendralingam, S., Crittenden, J. C., & Hokanson, D. R. (2005). Simulating the performance of fixed-bed granular activated carbon adsorbers: Removal of synthetic organic chemicals in the presence of background organic matter. *Water Res., 39*, 2407-2421.

Kapoor, A., Ritter, J., & Yang, R. (1989). On the Dubinin-Radushkevich Equation for Adsorption in Microporous Solids in the Henry's Law Region. *Langmuir, 5*, 1118-1121.

Kister, A., & Waldman, D. (1958). Heat of mixing of acetone with water and with methanol. *J. Phys. Chem., 62*, 245-246.

Kuwagaki, H., Meguro, T., Tatami, J., Komeya, K., & Tamura, K. (2003). An improvement of thermal conduction of activated carbon by adding graphite. *J. Mater. Sci., 38*, 3279-3284.

Kwapinski, W. (2009). Combined wall and thermal effects during nonisothermal packed bed adsorption. *Chem. Eng. J., 152*, 271-276.

Lama, R., & Lu, B.-Y. (1965). Excess Thermodynamic Properties of Aqueous Alcohol Solutions. *J. Chem. Eng. Data, 10*, 216-219.

Lashaki, M., Fayaz, M., Niknaddaf, S., & Hashisho, Z. (2012b). Effect of the adsorbate kinetic diameter on the accuracy of the Dubinin-Radushkevich equation for modeling adsorption of organic vapors on activated carbon. *J. Hazard. Mater., 241-242*, 154-163.

Lashaki, M., Fayaz, M., Wang, H., Hashisho, Z., Philips, J., Anderson, J., & Nichols, M. (2012a). Effect of Adsorption and Regeneration Temperature on Irreversible Adsorption of Organic Vapors on Beaded Activated Carbon. *Environ. Sci. Technol., 46*, 4083-4090.

Logan, D. (1997). Estimating physical properties for control equipment design. *Environ. Prog., 16*, 237-242.

Manes, M. (1984). Estimation of the effects of humidity on the adsorption onto activated carbon of the vapors of water-immiscible organic liquids. *Fundamentals of Adsorption* (pp. 335-344). New York: Engineering Foundation.

Myers, A., & Prausnitz, J. (1965). Thermodynamics of Mixed-Gas Adsorption. *AIChE J., 11*, 121-126.

Nemec, D., & Levec, J. (2005). Flowthrough packed bed reactors: 2. Two-phase concurrent downflow. *Chem. Eng. Sci., 60*, 6958-6970.

Nield, D., & Bejan, A. (2006). *Convection in Porous Media*. New York: Springer.

Oberkampf, W., & Trucano, T. (2002). Verification and validation in computational fluid dynamics. *Prog. Aerospace Sci., 38*, 209-272.

Okazaki, M., Tamon, H., & Toei, R. (1978). Prediction of binary adsorption equilibria of solvent and water vapor on activated carbon. *J. Chem. Eng. Japan, 11*, 209-215.

Oliemans, R. (2000). ERCOFTAC's role in promoting computational fluid dynamics. *Houille Blanche, 7-8*, 43-46.

Qi, S., Hay, K., & Cal, M. (2000b). Predicting humidity effect on adsorption capacity of activated carbon for water-immiscible organic vapors. *Adv. Environ. Res., 4*, 357-362.

Qi, S., Hay, K., & Rood, M. (1998). Isotherm Equation for Water Vapor Adsorption onto Activated Carbon. *J. Environ. Eng., 124*, 1130-1134.

Qi, S., Hay, K., Rood, M., & Cal, M. (2000a). Equilibrium and Heat of Adsorption for Water Vapor and Activated Carbon. *J. Environ. Eng., 126*, 267-271.

Shaverdi, G. (2012). *Developing a Model for Mass Transfer in Adsorption Packed-bed Filters* . Montreal: Concordia University.

Shi, Y., Lee, Y., & Kim, A. (2012). Knudsen Diffusion Through Cylindrical Tubes of Varying Radii: Theory and Monte Carlo Simulations. *Transp. Porous Media, 93*, 517-541.

Sircar, S., & Hufton, J. R. (2000). Why does the linear driving force model for adsorption kinetics work? *Adsorption, 6*, 137-147.

Sontheimer, H., Crittenden, J., & Summers, S. (1988). *Activated carbon for water treatment* (2nd ed.). Karlsruhe: DVGW-Forschungsstelle, Engler-Bunte-Institut, Universität Karlsruhe.

Suwanayuen, S., & Danner, R. (1980). A gas adsorption isotherm equation based on vacancy solution theory. *AIChE J., 26*, 68-76.

Suzuki, M. (1990). *Adsorption Engineering*. Amsterdam: Elsevier Science Publishing Company, Inc.

Tefera, D., Hashisho, Z., Philips, J., Anderson, J., & Nichols, M. (2014). Modeling Competitive Adsorption of Mixtures of Volatile Organic Compounds in a Fixed-Bed of Beaded Activated Carbon. *Environ. Sci. Technol., 48*, 5108-5117.

Tefera, D., Lashaki, M., Fayaz, M., Hashisho, Z., Philips, J., Anderson, J., & Nichols, M. (2013). Two-Dimensional Modeling of Volatile Organic Compounds Adsorption onto Beaded Activated Carbon. *Environ. Sci. Technol., 47*, 11700-11710.

Vahabi, M., Mehdizadeh, E., Kabganian, M., & Barazandeh, F. (2011). Experimental identification of IPMC actuator parameters through incorporation of linear and nonlinear least squares methods. *Sens. Actuators A Phys., 168*, 140-148.

Wang, H., Lashaki, M., Fayaz, M., Hashisho, Z., Phillips, J., Anderson, J., & Nichols, M. (2012). Adsorption and Desorption of Mixtures of Organic Vapors on Beaded Activated Carbon. *Environ. Sci. Technol., 46*, 8341-8350.

Willmott, C., & Matsuura, K. (2005). Advantages of the mean absolute error (MAE) over the root mean square error (RMSE) in assessing average model performance. *Clim. Res., 30*, 79-82.

Yang, R. (1987). *Gas Separation by Adsorption Processes*. Stoneham, Massachusetts: Butterworth Publishers.

Chapter 4 RESULTS AND DISCUSSION

4.1 Validation of Pure Single-Component Isotherms

The VOCs for this study were selected based on their water solubility and polarity: toluene, n-butanol, 1,2,4-trimethylbenze (TMB) are water-immiscible and non-polar organic adsorbates while acetone and 2-propanol are water-miscible and polar organics. n-Butanol, even though is an alcohol, is a non-polar adsorbate because of its long chain, which significantly reduces its water miscibility (0.43% w/w). Adsorption of VOCs on microporous AC is characterized by strong dispersive interactions and therefore exhibit BDDT type I adsorption isotherm as per the classification of Brunauer et al. (1938) (Huggahalli et al., 1996; Taqvi et al., 1999). All the five VOCs fitted very well with the MDR isotherm throughout the entire concentration range, with an overall r^2 value of 0.998 and RMSE of 0.004 (Figure 4-1). The higher values of the fitting parameter $\rho_v V_{v,o}$ for the non-polar VOCs clearly dictate that the non-polar VOCs have a higher affinity towards BAC adsorption than the polar ones (Table 4-1), as will be discussed in the coming sections.

Table 4-1. Multitemperature fitting parameters of MDR isotherms for adsorption of pure VOCs on BAC at 298.15 K

adsorbate	$V_{v,o}$ **(cm³/g)**	ρ_v **at 298.15 K (g/cm³)**	$\rho_v V_{v,o}$ **(kg/kg)**	$\beta/\sqrt{K}$ **(J/mol)**	V_1 **(cm³/g)**	$\rho_v V_1$ **(kg/kg)**	α **(–)**
2-propanol	0.494	0.785	0.388	21549	3.03	2.38	155.41
acetone	0.515	0.791	0.407	24428	2.56	2.03	189.64
toluene	0.484	0.865	0.419	30447	6.12	5.29	425.56
n-butanol	0.52	0.81	0.421	23311	0.71	0.58	485.64
1,2,4-TMB	0.516	0.872	0.450	32285	2.38	2.08	130.15

Adsorption of water vapor on AC is governed by hydrogen bonding and typically involves primary (surface functional groups) and secondary (previously adsorbed water vapor molecules) adsorption sites at low and high pressures respectively. Clusters of water molecules formed at high pressures are characteristic of capillary condensation, and therefore water vapor adsorption exhibits a BDDT type V isotherm (Huggahalli et al., 1996). For pure water vapor adsorption isotherm, QHR isotherm fitting parameters achieved good agreement with experimental values; with 0.999 R-squared value and RMSE of 0.007. The isotherm generates the desired type V (S-shaped) curve demonstrating the unique adsorption mechanism of water on AC (Figure 4-2).

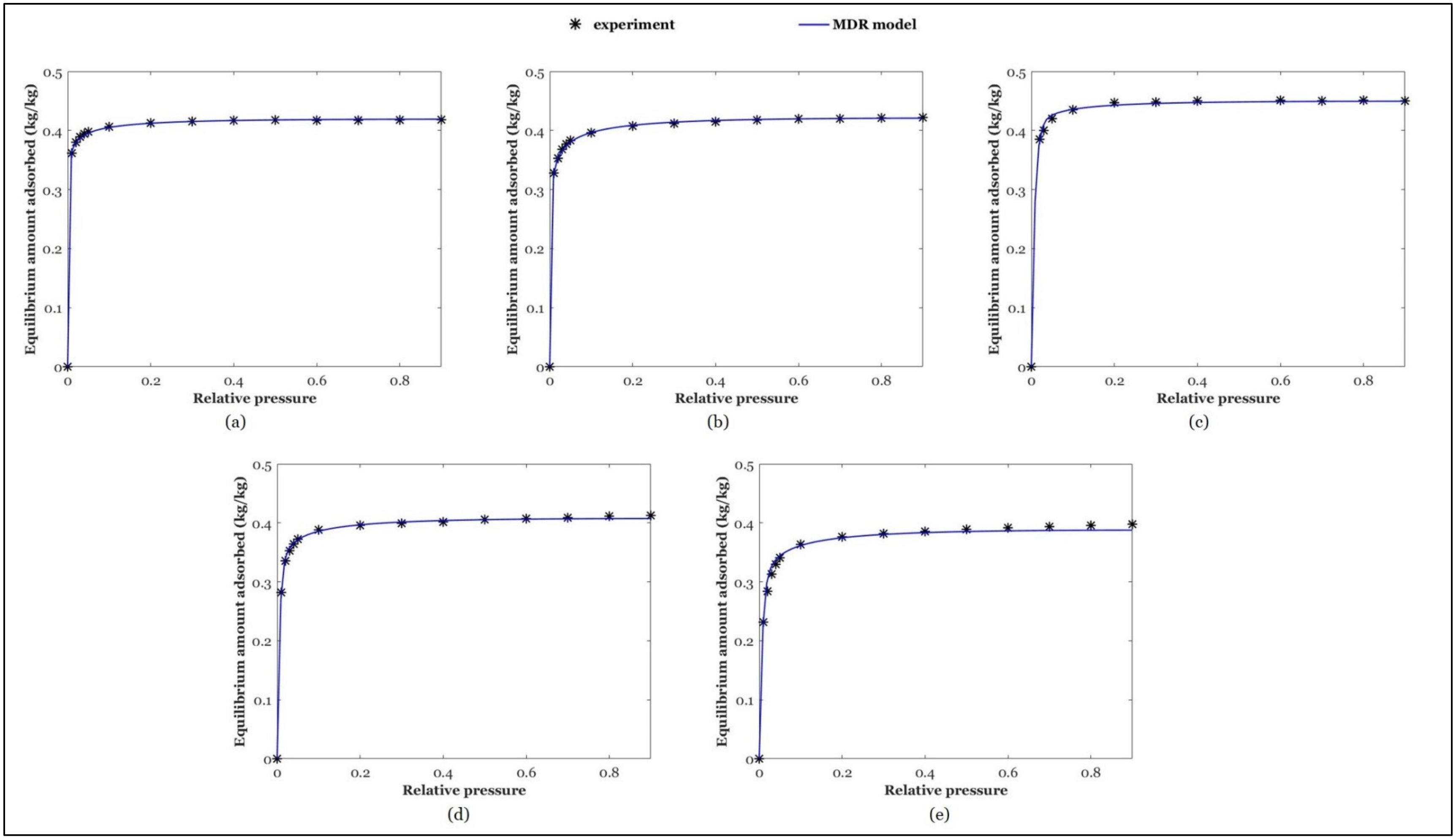

Figure 4-1. Experimental and fitted MDR isotherms for (a) toluene, (b) n-butanol, (c) 1,2,4- TMB, (d) acetone, (e) 2-propanol adsorption onto BAC at 298.15 K.

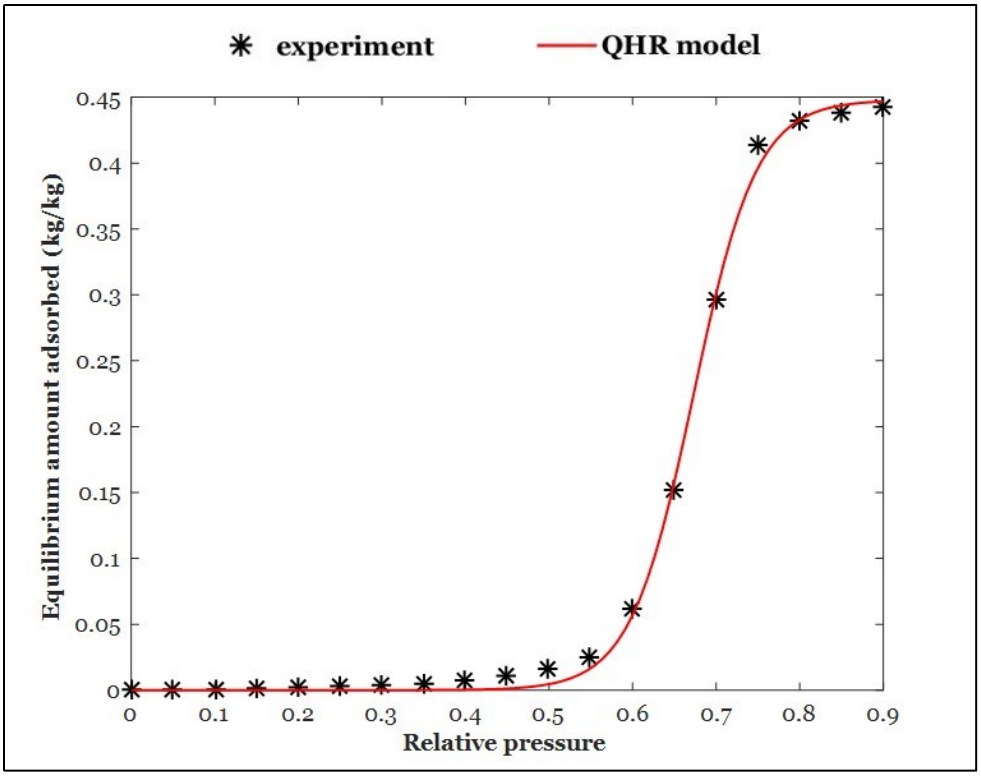

Figure 4-2. Experimental and fitted QHR isotherm for water adsorption onto BAC at 298.15 K.

The accuracy of single-component adsorption isotherms is very critical and affects the reliability of the Manes method. Since the fittings of both these isotherm models (MDR and QHR) were encouraging, they were used as inputs for Manes' multicomponent competitive adsorption isotherm model between organics and water vapor.

The multitemperature fitting parameters of the QHR isotherm are given in Table 4-2.

Table 4-2. Multitemperature fitting parameters of QHR isotherm for adsorption of pure water vapor on BAC at 298.15 K

adsorbate	$V_{w,o}$ (cm3/g)	$\rho_w V_{w,o}$ (kg/kg)	A (–)	E_a (J/mol)	a (–)	b (1/K)
water	0.487	0.448	26.06	0.053	0.0979	0.0019

4.2 Validation of VOC-Water Vapor Multicomponent Competitive Adsorption Isotherm

Figure 4-3a compares the experimental and modeled equilibrium adsorption capacities for the selected VOCs during their competitive adsorption with water vapor at 298.15 K. As noted from the figure, Manes method and its extension for water-miscible organics describe the VOC-water vapor equilibria well and satisfactorily. The method predicted the adsorption capacity for VOCs during competitive adsorption with water vapor with an overall MRAE of 1.9% for non-polar VOCs and 5.2% for polar VOCs. Among the selected VOCs, the polar VOCs 2-propanol and acetone experienced the highest reduction in their adsorption capacity of 17.5% and 14.1% respectively at about 95% RH. This was followed by the non-polar adsorbates; with VOC adsorption capacity reduction being 6.4%, 5.8%, and 0.2% for n-butanol, toluene, and 1,2,4-TMB respectively. The trend follows the affinity of the adsorbate towards BAC adsorption; with non-polar VOCs such as 1,2,4-TMB having the highest affinity among the selected adsorbates understandably encounters no impact by relative humidity. The opposite can be said for the water-miscible/polar VOCs, acetone and 2-propanol. In their case, high water-miscibility in addition to low adsorption affinity, play a role in the significant decrease in their adsorption capacities. This is mainly due to the formation of hydrogen bonding between water and acetone/2-propanol molecules during competitive adsorption (Okazaki et al., 1978). At 55% RH, no impact on adsorption capacity was observed for all the concerned VOCs chiefly due to water vapor's low affinity towards BAC adsorption at that concentration. This behavior was correctly predicted by the model as it generated similar results at 0% and 55% RH. The model predictions were encouraging; and therefore, were further applied to simulate the adsorption kinetics.

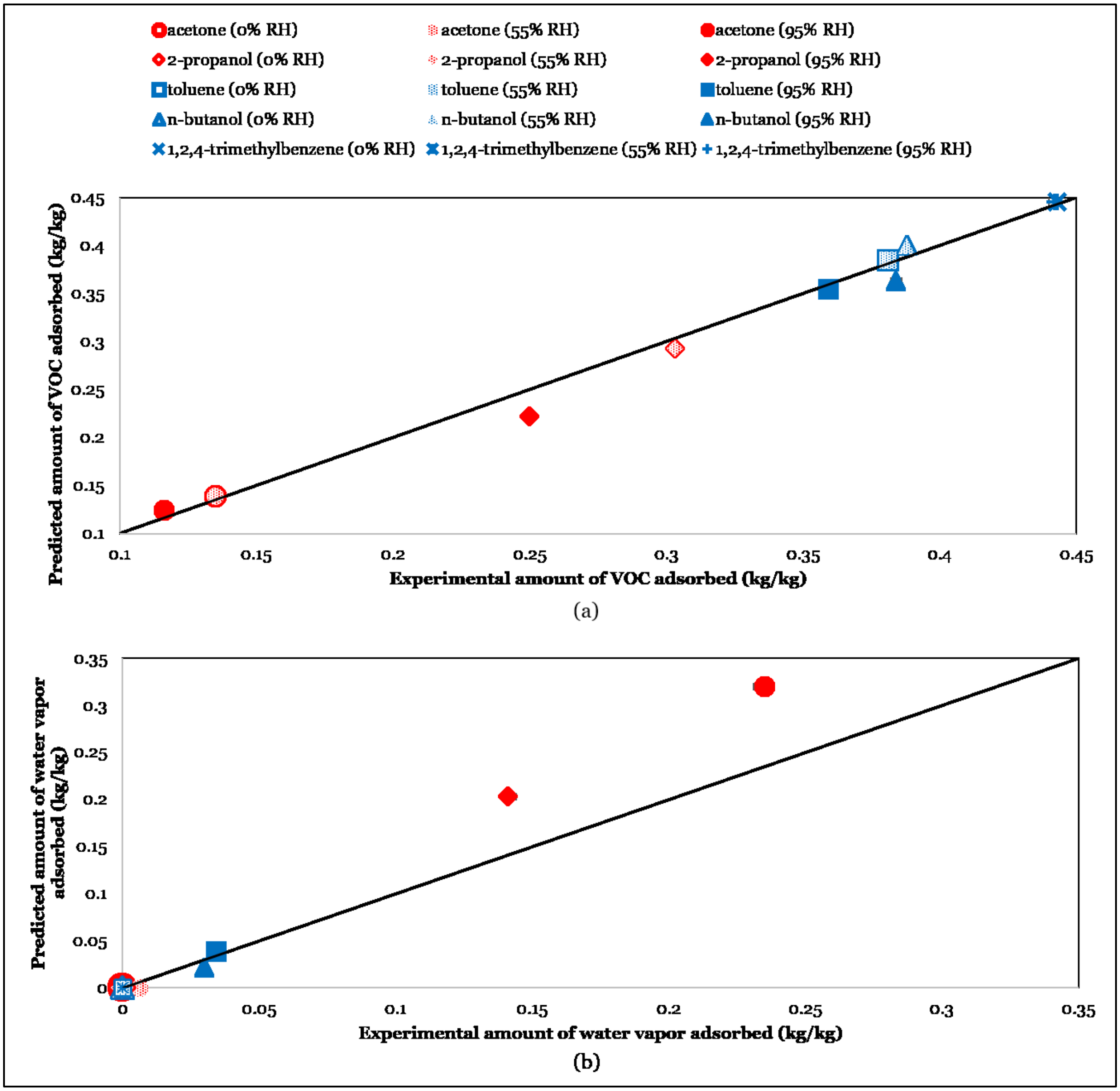

Figure 4-3. Polar versus non-polar VOC: comparison of experimental and modeled equilibrium adsorption capacities of (a) VOC and (b) water vapor during their competitive adsorption on BAC at 298.15 K.

Figure 4-3b compares the experimental and modelled water uptake during competitive adsorption between VOC and water vapor at 298.15 K. As expected, no significant water adsorption occurred at 55% RH for all the selected VOCs. However, for acetone there was 4% water uptake at 55% RH, which was mostly due to its hydrogen bonding with water molecules (Okazaki et al., 1978). The extension of Manes method for water-miscible adsorbates is considered only when RH is upwards 75%; and therefore, the 4% water uptake at 55% RH was not predicted by the model. At about 95% RH, the model projected the water uptake during competitive adsorption with an overall MRAE of 14.9% for non-polar VOCs and 40.1% for polar VOCs. With respect to non-polar VOCs, the error could be attributed to the smaller amounts of water adsorbed which would lead to large relative absolute error. For polar VOCs, non-ideality in the adsorbed phase could be a contributor to the error; since it is not considered by the model and therefore, leading to over- or under-estimation of the amount of water vapor uptake. In addition, numerical error in modelling and experimental error in measuring adsorption capacity could also be factors for both polar and non-polar VOCs. Acetone had the highest water vapor uptake of 67%, followed by 2-propanol (36.1%), toluene (8.7%), n-butanol (7.6%), and 1,2,4-TMB (0%). This trend in water vapor adsorption can be explained by adsorption potential. At their given inlet concentrations, pure adsorption potential (ε_v^o) was the highest for acetone, and lowest for 1,2,4-TMB among the selected VOCs (Table 4-3). Since at 95% RH, the pure adsorption potential for water vapor (ε_w^o) was significantly lower than the VOCs' (Table 4-3); during competitive adsorption, the extent of water adsorbed onto BAC was governed by their respective adsorption potentials. In this case, if the pure adsorption potential of water vapor is very low compared to the adsorption potential of VOC in the water-VOC mixture, the affinity of water vapor towards BAC would be higher and therefore higher amount of water is adsorbed; and vice versa. Additionally, for polar

VOCs, hydrogen bonding with water molecules may also play a part in promoting water adsorption during competitive adsorption (Okazaki et al., 1978).

Figure 4-4 and Figure 4-5 demonstrate 2D multicomponent competitive adsorption equilibria between the selected VOCs and water vapor for the entire concentration range of water vapor and up to 0.1 relative pressure for the VOCs. As can be seen in Figure 4-4, the impact of water vapor occurs at 75% RH levels (or 0.75 relative water vapor pressure) and beyond, depending upon the VOC concentration, which decreases VOC adsorption capacity and increases water uptake on BAC. Similar behavior was also predicted for polar VOCs except that at RH levels between 75% and 90% and VOC relative vapor pressure within 0.02 and 0.1, about 1% increase in VOC adsorption capacity was observed (Figure 4-5). This is primarily due to the dissolution of polar VOCs in water during competitive adsorption among them, which in turn is accounted for by the Raoult's-law-like extension to Manes method. Such exceptions are consistent with previous adsorption studies conducted on polar organic and water vapors (Taqvi et al., 1999; Linders et al., 2001; Qi et al., 2006).

Table 4-3. Physical properties of the selected adsorbates (Haynes, 2017)

adsorbate	**formula**	$M_{A,i}$ **(g/mol)**	$T_{b,i}$ **(K)**	P_{vS} **at 298.15 K (kPa)**	$\frac{P'_v}{P_{vS}}$ **at** $C_{o,i}$ **(kPa)**	ε_v^o **at** $C_{o,i}$ **(kJ/mol)**	$\left(\sum v\right)_{A,i}$ **(−)**	$\Delta H_{vap,i}$ **(kJ/mol)**	α_i **(10^{-24} cm^3)**	IP_i **(eV)**	σ_i **(mN/m)**	**water solubility (% w/w)**
2-propanol	C_3H_8O	60.10	355.36	5.87	0.0173	10.1	70.82	45.4	7.29	10.10	20.9	100
acetone	C_3H_6O	58.08	329.23	30.80	0.0033	14.2	66.86	31.0	6.40	9.69	22.7	100
toluene	C_7H_8	92.14	383.75	3.79	0.0267	9.0	111.14	38.0	12.12	8.82	27.2	0.051
n-butanol	$C_4H_{10}O$	74.12	390.75	0.86	0.1179	5.3	91.28	52.3	8.88	10.04	24.1	0.43
1,2,4-TMB	C_9H_{12}	120.19	442.55	0.30	0.3379	2.7	152.06	47.9	15.70	8.27	29.2	0.006
				P_{wS} **at 298.15 K (kPa)**	$\frac{P'_w}{P_{wS}}$ **at** $C_{o,i}$ **(kPa)**	ε_w^o **at** $C_{o,i}$ **(kJ/mol)**						
water	H_2O	18.02	373.12	3.17	0.95	0.1	12.70	40.6	1.45	12.59	72.1	100

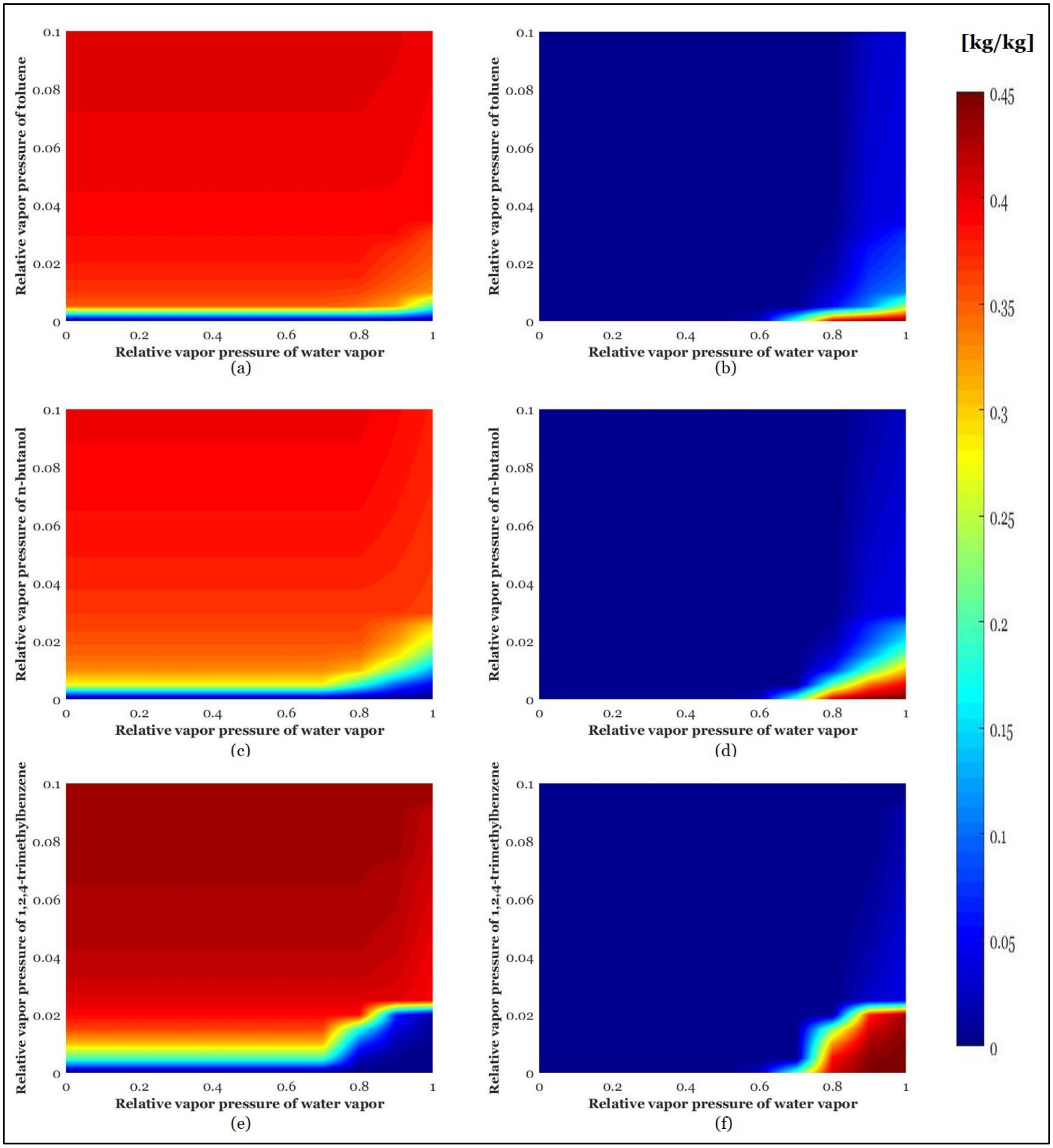

(a) (b)

(c) (d)

(e) (f)

Figure 4-4. 2D competitive adsorption isotherm for water vapor and non-polar VOC at 298.15 K on BAC: Amount of (a) toluene, (b) water vapor adsorbed in toluene-water vapor system; (c) n-butanol, (d) water vapor adsorbed in n-butanol-water vapor system; (e) 1,2,4-TMB, (f) water vapor adsorbed in 1,2,4-TMB-water vapor system.

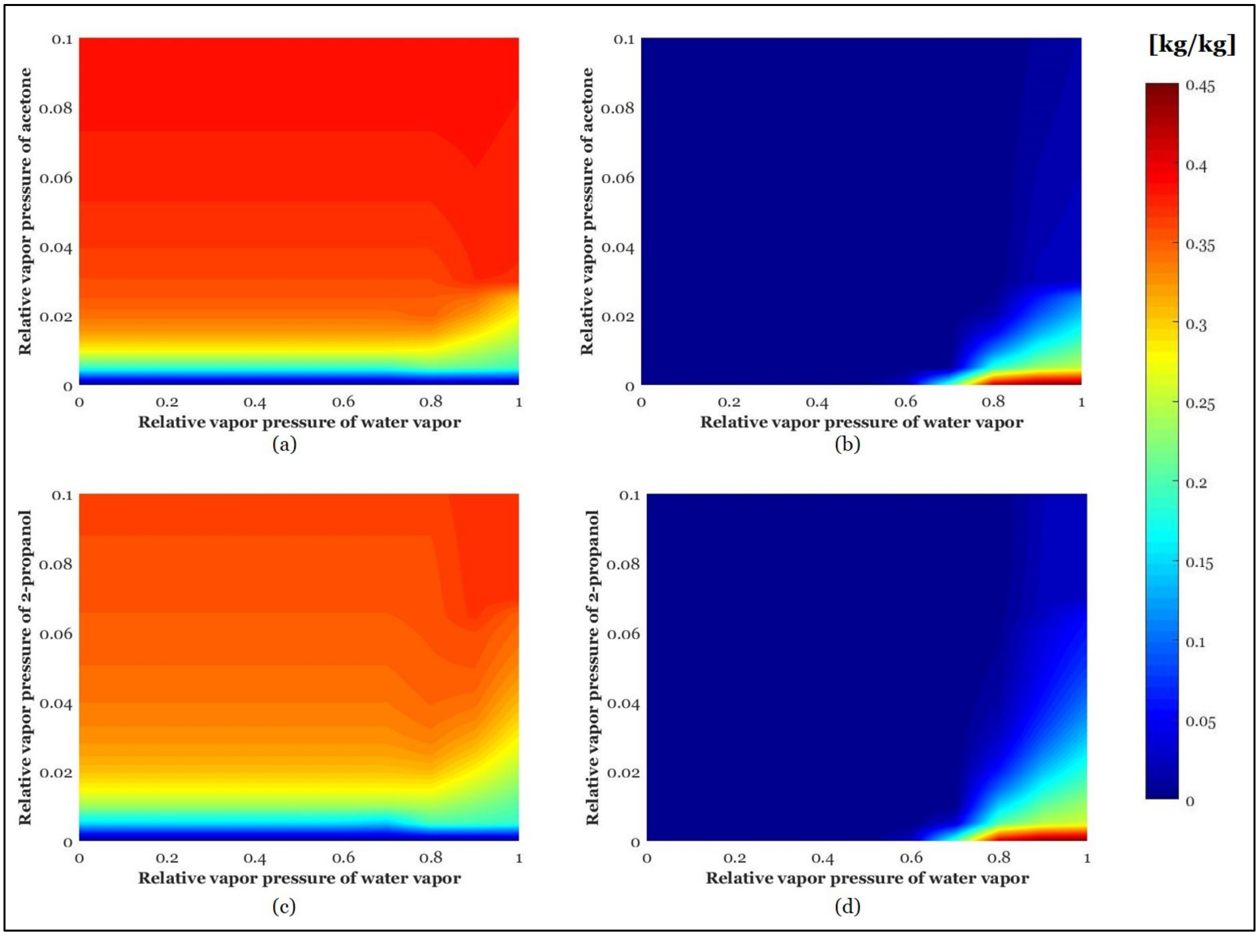

Figure 4-5. 2D competitive adsorption isotherm for water vapor and polar VOC at 298.15 K on BAC: Amount of (a) acetone, (b) water vapor adsorbed in acetone-water vapor system; (c) 2-propanol, (d) water vapor adsorbed in 2-propanol-water vapor system.

4.3 Validation of Adsorption Breakthrough Profiles

Figure 4-6 shows the adsorption breakthrough profiles at 0%, 55%, and 95% RH levels and 298.15 K of the selected VOCs. The pore Biot number $(B_{p,i})$ to be larger than unity, and therefore the overall mass transfer was governed by intraparticle diffusion (Shaverdi, 2012) (Table 4-4). Within the intraparticle diffusion, surface diffusion mechanism was neglected because the surface to pore diffusion flux ratio (φ_i) was found to be less than unity (Do and Rice, 1987) (Table 4-4). Pore diffusion, comprising of molecular diffusion, was thus considered to be the effective diffusion mechanism to calculate the overall mass transfer resistance.

Table 4-4. Surface diffusion, pore diffusion, and external mass transfer coefficient of the selected adsorbates at 298.15 K

adsorbate	$D_{s,i}$ (m²/s)	$D_{p,i}$ (m²/s)	φ_i (–)	$k_{ex,i}$ (m/s)	$B_{p,i}$ (–)
2-propanol	1.81E-11	1.06E-05	0.12	0.26	9.24
acetone	2.89E-11	1.09E-05	0.09	0.27	9.17
toluene	1.08E-11	8.26E-06	0.08	0.22	9.86
n-butanol	9.53E-12	9.22E-06	0.08	0.24	9.58
1,2,4-TMB	3.74E-12	7.02E-06	0.03	0.19	10.31
water	1.31E-11	2.56E-05	0.01	0.50	7.37

The model predicted the breakthrough curves with an overall MRAE of 15.4% and NRMSE of 7.4%. The MRAE analysis was conducted only for the nonzero data points. Numerical error, model assumptions (negligible variation of flow properties in the angular direction of the tube, negligible adsorption of the carrier gas (air), ideal gas behaviour, and symmetric flow conditions), and/or experimental error in concentration measurements could be the likely contributors to the deviations between the modeled and experimental breakthrough profiles. All the selected VOCs except 1,2,4-TMB experienced displacement in their adsorption breakthrough curves due to competition from water vapor at RH levels of about 95% (Figure 4-6). No displacement occurred at 0% and 55% RH due to the significantly lower adsorption affinity of water vapor compared to VOCs at their given inlet concentration (1000 ppm). As expected, at 95% RH polar VOCs such as 2-propanol and acetone encountered the highest reduction in the bed service time (also known as 5% breakthrough time, that is the time when the outlet adsorbate concentration is 5% of the inlet) of 16.9% and 10.7% respectively. This was followed by the non-polar VOCs in the order: n-butanol (9.6%), toluene (7.8%), and 1,2,4-TMB (0.0%). The trend in adsorption breakthrough time reduction is consistent with the decrease in VOC adsorption capacity at 95% RH. This proves the coherency of the multicomponent adsorption isotherm and transport phenomena equations in the model. The high susceptibility of polar VOCs to the impact of RH during competitive adsorption with VOCs was also reported in other studies where adsorption capacity for polar VOCs such as acetone experienced reduction of up to 50% compared to about 40% for non-polar VOCs such as benzene, toluene at 90% RH and 303 K on GAC and inlet concentrations ranging from 500 – 8000 mg/m^3 (Huasheng et al., 2002; Li et al., 2010). The breakthough curve results here for dry conditions are consistent with previous studies on single-component adsorption on BAC for VOCs such as acetone, toluene, 1,2,4-TMB at 298.15 K (Tefera et al., 2013).

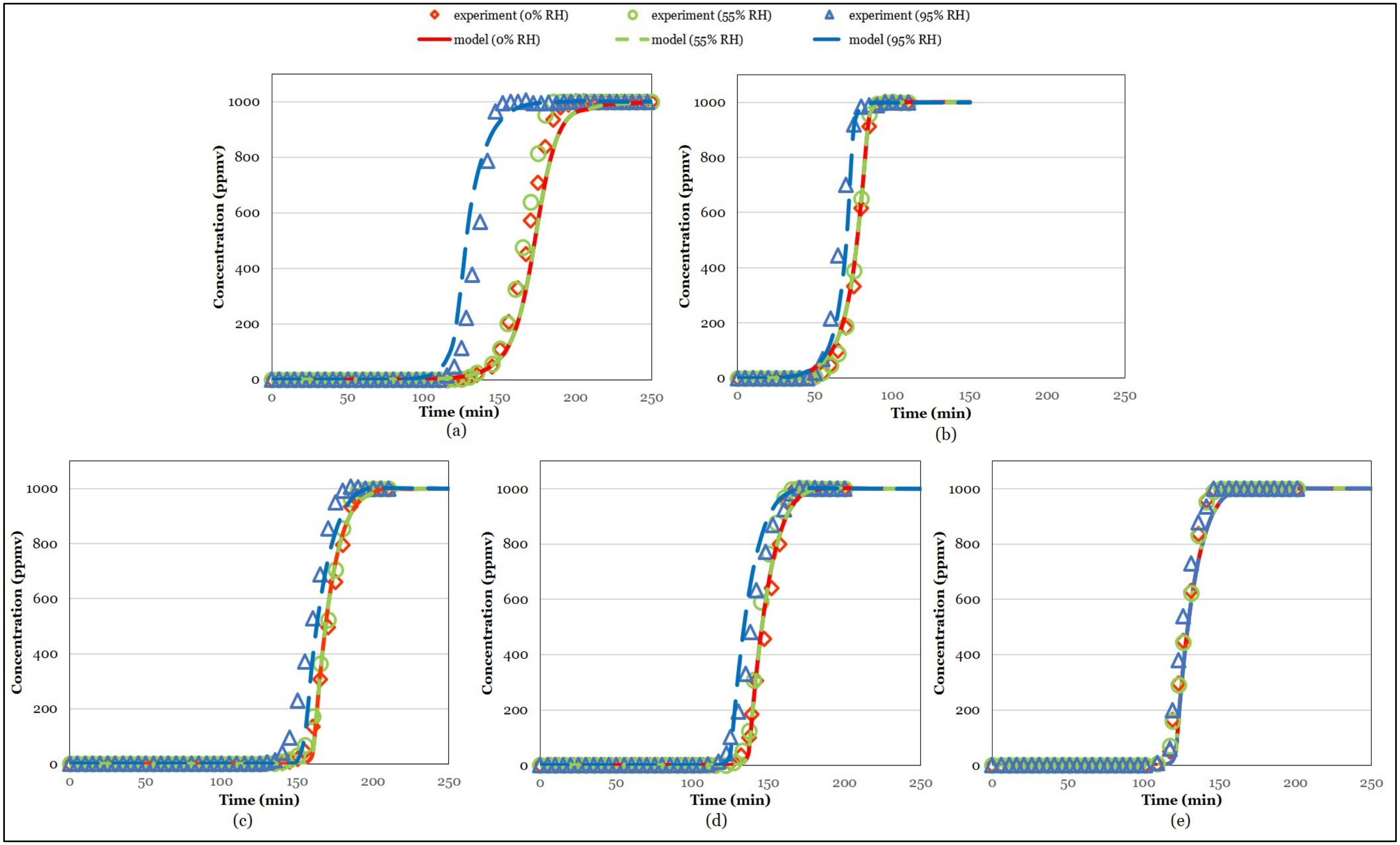

Figure 4-6. Comparison of experimental and modeled breakthrough curves during competitive adsorption of water vapor with (a) 2-propanol, (b) acetone, (c) n-butanol, (d) toluene, and (e) 1,2,4-TMB on BAC at 298.15 K.

4.4 Absorbed-Phase Concentration Distribution

Figure 4-7 shows the development of two-dimensional adsorbed-phase concentration distribution of 2-propanol during its competitive adsorption with water vapor at 298.15 K, and its comparison with dry conditions at 0%RH. As observed earlier with the validations of adsorption capacity and breakthrough profile predictions, the model here too generates the same results at 0% and 55% RH. 30 min after the start of adsorption, it can be seen that the movement of mass transfer zone (MTZ) at higher RH levels is faster than at lower RH or dry conditions; with the MTZ at 95% RH at about 35 mm from the adsorber inlet compared to 25 mm for 0%/55% RH. In addition, 17.5% reduction in equilibrium adsorption capacity at 30 min and 95% RH can also be noted from the figure; as predicted by the extended Manes method. Such behavior at high humidity is due to competition between 2-propanol and water molecules for the limited adsorption sites in the BAC fixed-bed adsorber; which results in displacement of the VOC's MTZ and reduction in its adsorption capacity. In general, it can be said that the extent of reduction in breakthrough time is governed by the affinity, adsorption potential, and polarity of the concerned VOC and water vapors at their given inlet concentrations during competitive adsorption. The difference between the MTZs at 0%/55% and 95% RH continued to be within 10 to 20 mm (9 to 17% of the entire bed length) throughout the adsorption period until saturation; which in turn leads to an early bed-saturation at 160 min for 95% RH compared to 200 min for 0%/55% RH. The movement of MTZ in 2-propanol's adsorbed-phase concentration distribution is consistent with its adsorption breakthrough profile measured at the centre of the adsorber outlet (Figure 4-6). Furthermore, the mass transfer resistance of 2-propanol did not experience any significant impact during high humidity conditions; especially because of very low diffusion resistance of the competing water vapor molecules, owing to their much smaller size when compared to 2-propanol's (Table 4-4). The same can be said for all the selected VOCs.

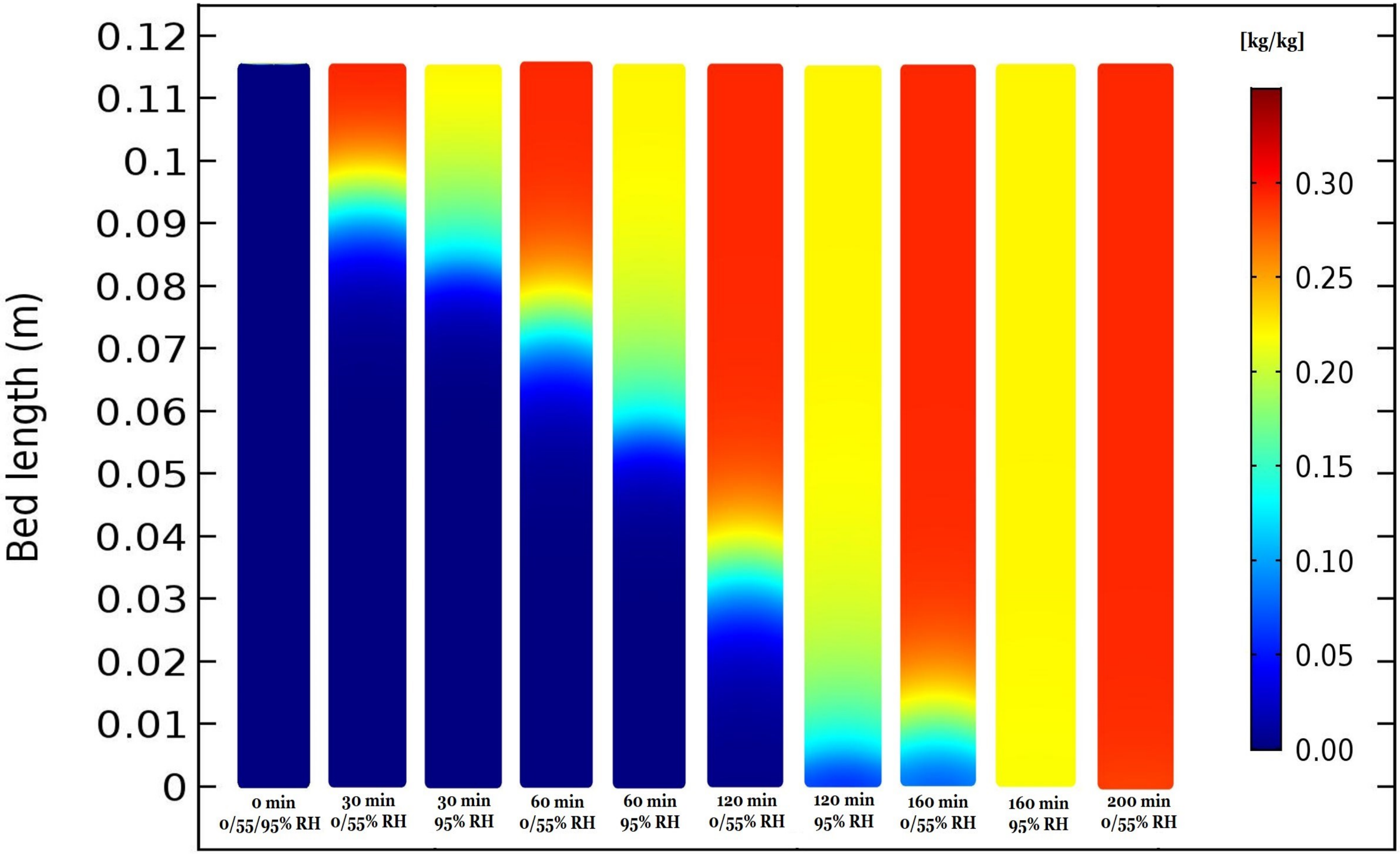

Figure 4-7. 2D adsorbed-phase concentration distribution of 2-propanol during competitive adsorption with water vapor on BAC at 298.15 K.

Also, the variation of the adsorbed phase concentration in the radiation direction reveals that the bed becomes was saturated near the wall earlier than at its centre due to wall channeling. This observation is consistent with previous 2D adsorption modeling studies (Tefera et al., 2013, 2014; Coker et al., 2015; Schlüter et al., 2016). A one-dimensional simulation would have mostly generated an earlier breakthrough in the same scenario.

4.5 Absorber Bed Temperature Distribution

Figure 4-8 demonstrates the experimental and modeled adsorber bed temperature profiles at the center of the bed (r = 0.0 cm, z = 7.5 cm) during competitive adsorption between different VOC-water vapor systems. The model predictions were good with an MRAE and NRMSE of 2.6% and 3.4% for the polar VOCs, and 1.9% and 2.5% for the non-polar VOCs, respectively. While experimental error in measuring bed temperatures could be a factor, the most likely contributor to the error could be the model's assumption of ideal adsorbed-phase for polar VOCs. Except 1,2,4-TMB, all the selected VOC-water vapor systems experienced an increase in average bed temperature of up to 1 to 2 K during competitive adsorption at 95% RH when compared to 0%/55% RH. Adsorption being an exothermic process, the temperature rise can be attributed to the adsorbate(s) loading, heat of adsorption, and heat of dissolution (for polar adsorbates in a gas mixture). The polar VOCs, which depicted a more severe impact of RH, had the highest average bed-temperature increase of up to 2 K during competitive adsorption with water vapor. For non-polar VOCs, it was about 1 K.

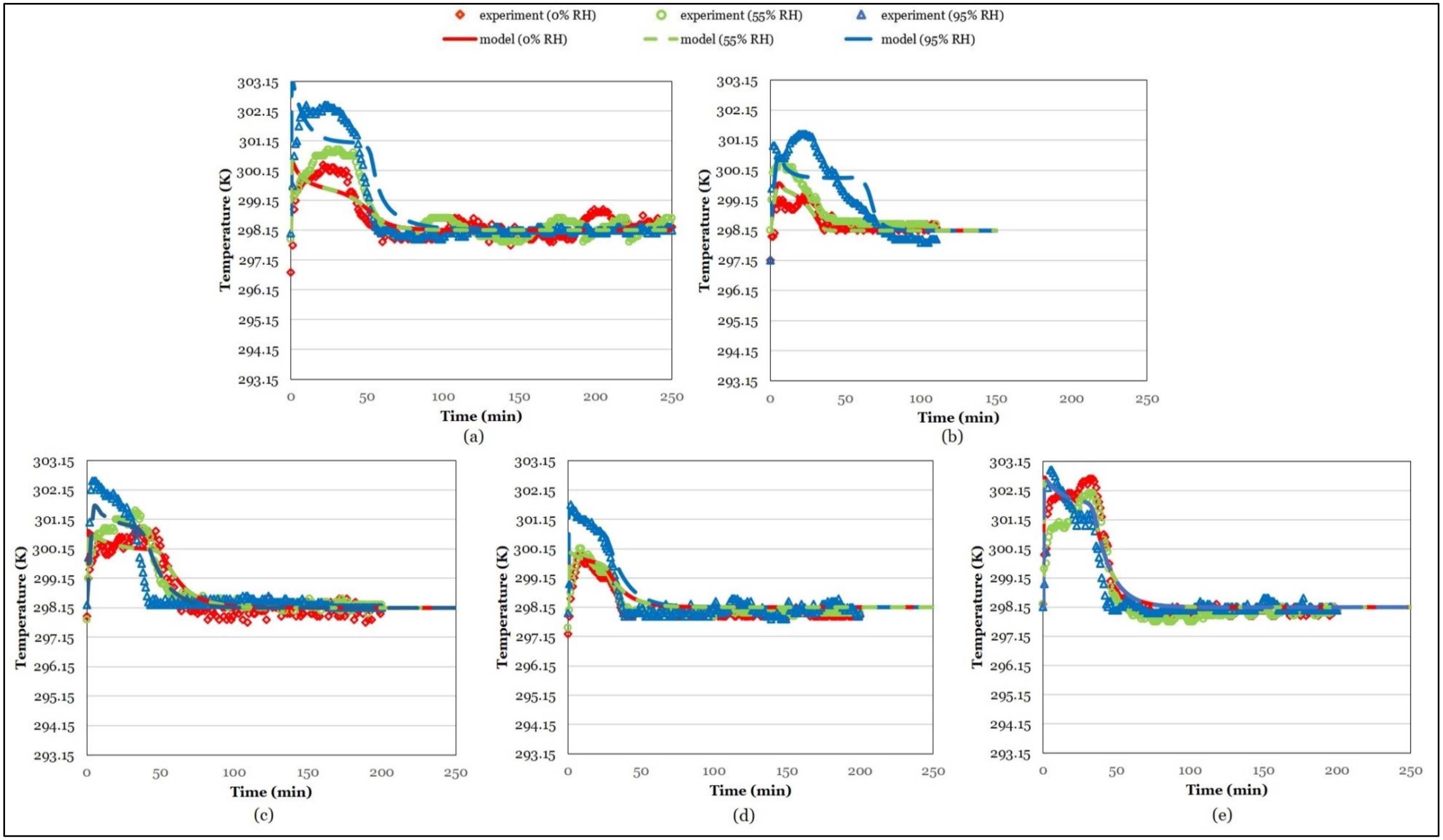

Figure 4-8. Comparison of experimental and modeled BAC-bed temperature profiles at the centre of the reactor (*r* = 0.0 cm, *z* = 7.5 cm) during competition adsorption of water vapor with (a) 2-propanol, (b) acetone, (c) n-butanol, (d) toluene, (e) 1,2,4-TMB.

Following bed temperature validations, a 2D adsorber bed temperature distribution was generated which shows the evolution and comparison of heat transfer zones (HTZ) with and without competitive adsorption between 2-propanol and water vapor (Figure 4-9). Higher temperature, as predicted earlier, was observed in the 2D temperature plot at 95% RH. This lead to a difference in HTZ at 0%/55% RH and 95% RH of up to 30 mm (26% of the entire bed length) throughout the adsorption period. Consequently, the fixed-bed at 0%/55% RH reached thermal equilibrium with the adsorption temperature at least 40 min earlier at 200 min than the fixed-bed at 95% RH. The 2D temperature distribution plot corresponds well with the 2D adsorbed-phase concentration plot (Figure 4-7); albeit the HTZ had a higher velocity than the MTZ, creating a difference of at least 10 mm at all times and conditions during adsorption. It should also be noted that the temperature during adsorption varied across the bed, and was higher at the center than at the periphery because of convective heat transfer at the tube wall. In dry conditions, similar observations in adsorber bed temperature and HTZ across the adsorber bed were made in previous modeling and experimental works on AC adsorption of VOCs such as benzene, toluene, acetone, ethanol, pentane (Marivoet et al., 1974; Kwapinski, 2009; Tefera et al., 2013; Schlüter et al., 2016), which strengthens the reliability of the model for simulating heat transfer kinetics during competitive adsorption between VOC and water vapor.

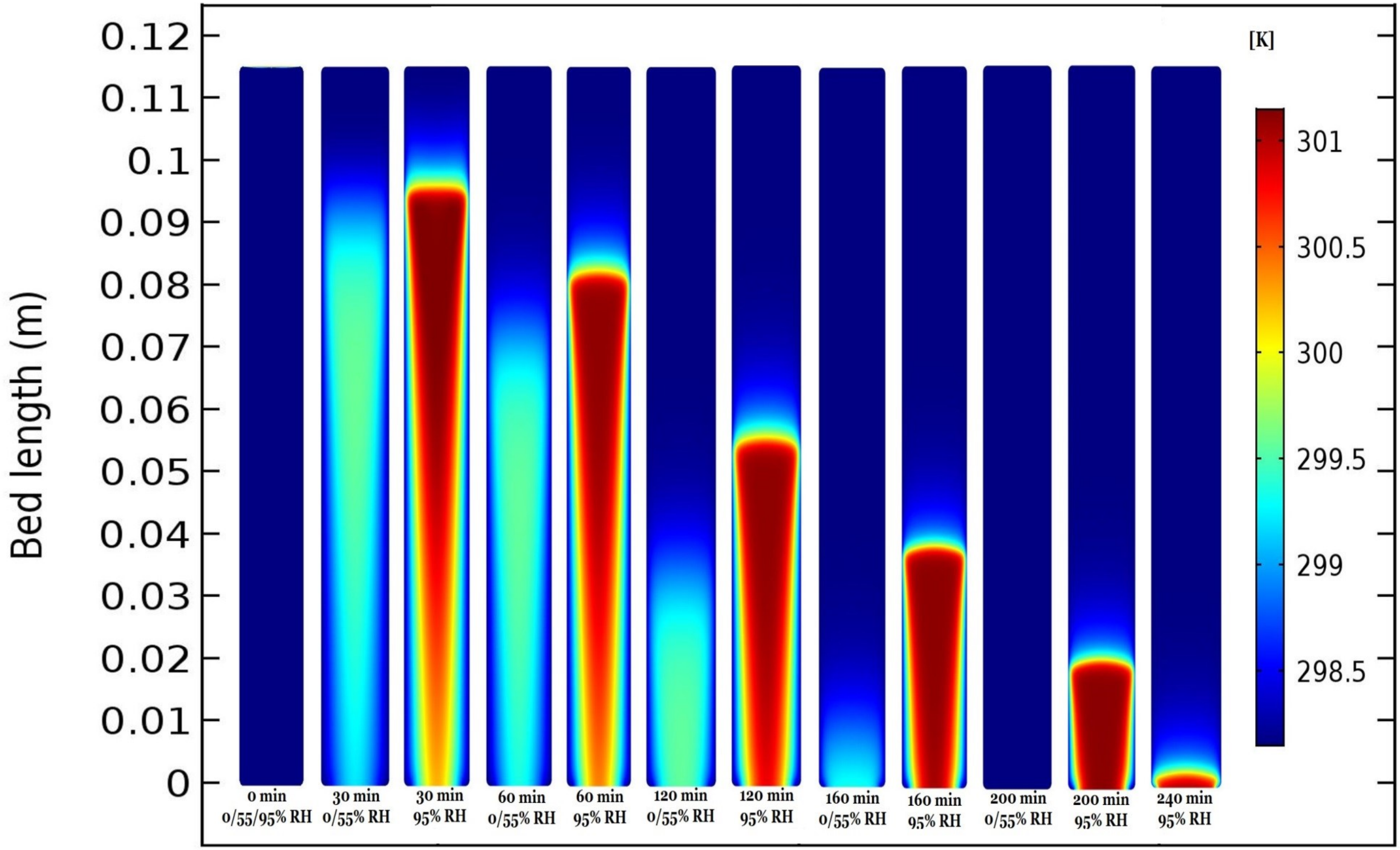

Figure 4-9. 2D adsorber bed temperature distribution during competitive adsorption of 2-propanol with water vapor at 298.15 K.

4.5 Sensitivity Analysis

Humidity in contaminated gas streams varies with operating conditions and is highly sensitive to temperature. The extent of impact of RH on VOC adsorption capacity is also critically depended on the inlet VOC concentration levels. Therefore, a proper sensitivity analysis focussing on these factors is a necessity.

4.5.1 Effect of Adsorption Temperature

Figure 4-10 shows the experimental and modeled adsorption breakthrough profiles of 2-propanol at 298.15 K and 305.15 K at RH levels of 0%, 55%, and 95%. Increasing the temperature from 298.15 K to 305.15 K completely negated the impact of RH on the bed service time and VOC adsorption capacity, which were reduced by 16.9% and 17.5% respectively at 298.15 K and 95% RH. No deterioration in the 5% breakthrough time and the VOC adsorption capacity was found at 305.15 K and the selected RH levels. However, the VOC adsorption capacity decreased by 11% at 305.15 K compared to 298.15K, 0%/55% RH. Therefore, optimization of bed temperature is a very critical requirement to maintain a balance between the effect of temperature on RH and adsorption, and its effect on the bed service time and adsorption capacity. This is where the utility and stability of the model is crucial. The model predicted the adsorption behavior of 2-propanol at 305.15 K (0%, 55%, 95% RH) with an overall MRAE of 12.4% and 7.1% for the breakthrough profiles and adsorption capacity respectively, which shows that it is sensitive to changes in operational conditions. The model's utility in optimizing bed temperature for minimizing impact of RH would lead to an increase in adsorber service lifetime; hence, a decrease in overall fixed-bed adsorber operational costs.

Optimization of other process parameters such as superficial velocity, and particle size using similar transfer kinetics equations were studied elsewhere (Tefera et al., 2013).

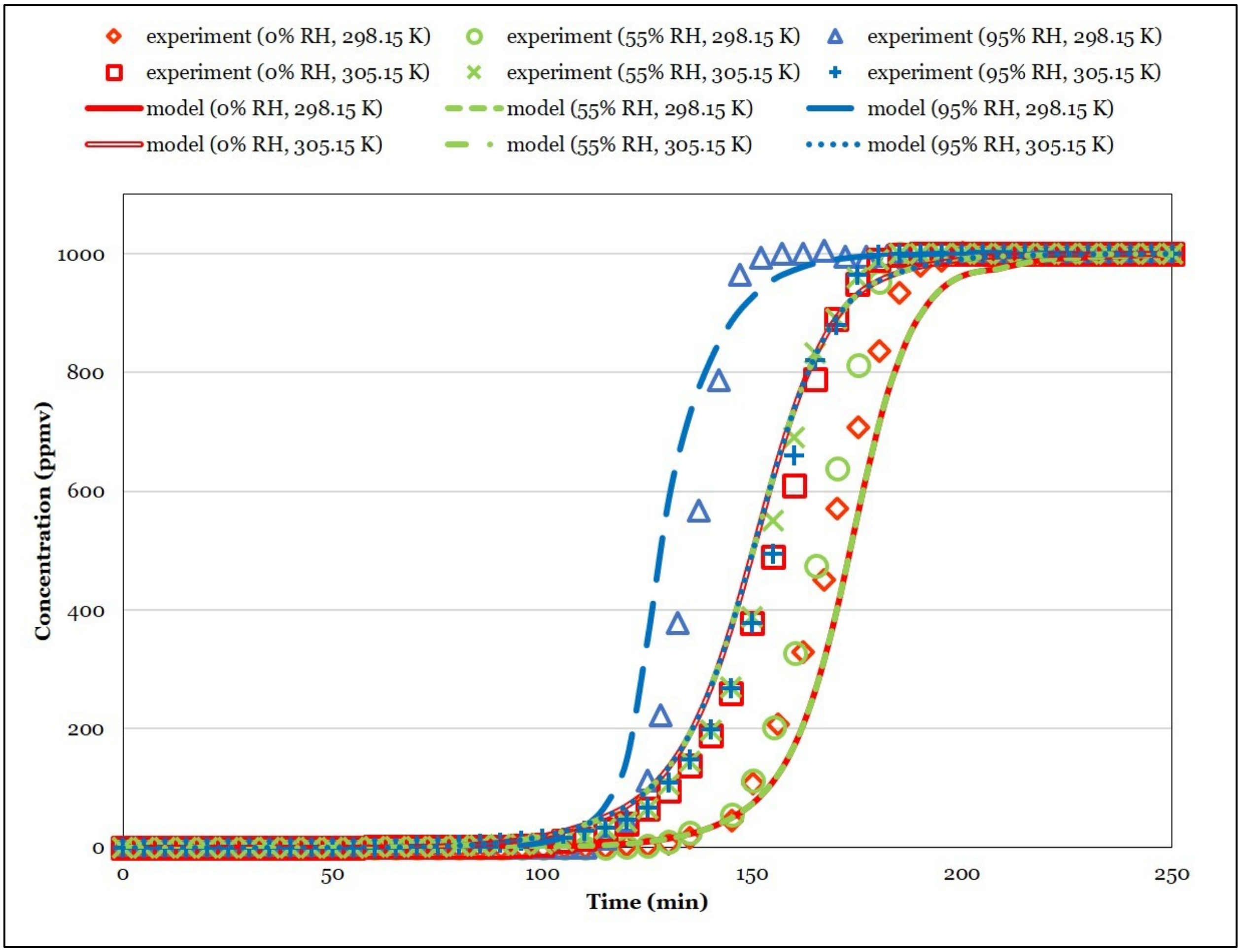

Figure 4-10. Comparison of experimental and modeled breakthrough curves during competition adsorption of water vapor with 2-propanol on BAC at 298.15 K and 305.15 K.

4.5.2 Effect of Inlet Gas Concentration

Figure 4-11 illustrate the experimental and modeled breakthrough profiles and adsorption capacities for 1,2,4-TMB with an inlet concentration of 250 ppm and RH of 0%, 55%, 95% at 298.15 K. To reduce experiment time and resources, the experiment was conducted in a 3.5-cm fixed bed containing 4 g of BAC particles; all the other experimental conditions were maintained same as earlier. The inlet concentration of 1,2,4-TMB (250 ppm) was selected to analyse the impact of RH at low concentration levels, considering that at concentrations four times higher (1,000 ppm) no impact of RH was observed. At 55% RH, no effect of RH was felt on 1,2,4-TMB adsorption; however, at 95%RH, 1,2,4-TMB adsorption capacity decreased by 6.4% leading to a 7.6% reduction in bed service time and 4.6% water uptake. This is mainly due to the lower affinity of 1,2,4-TMB at 250 ppm compared to 1,000 ppm, against the competing water vapor molecules at 95% RH. The model predicted this behavior well with an overall MRAE of 1.6% and 5.1% for adsorption capacity and service time respectively. This signifies the robustness of the Manes method and the overall model in sensitivity analysis.

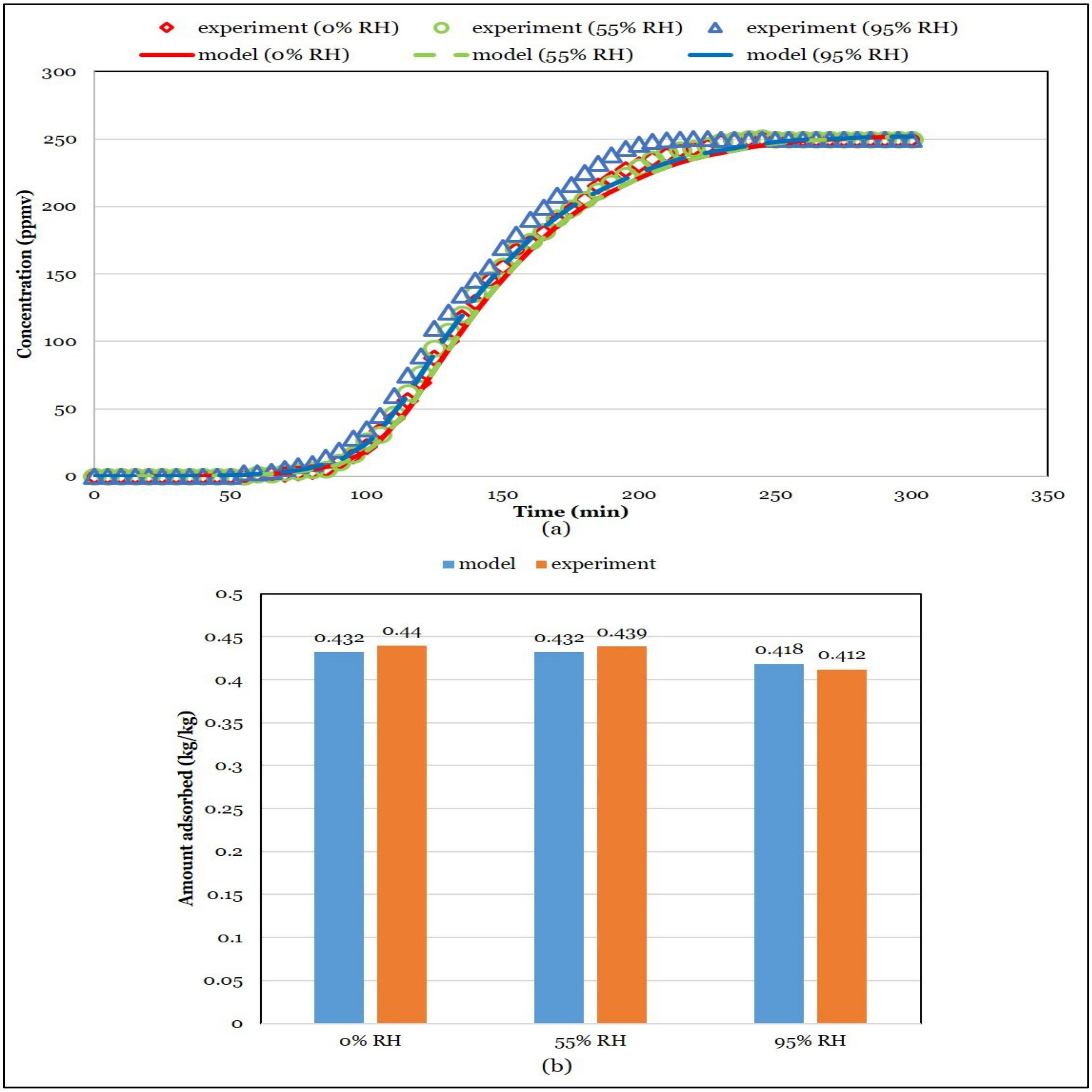

Figure 4-11. Competitive adsorption of water vapor and 1,2,4-TMB on BAC at 298.15 K: (a) comparison of experimental and modeled breakthrough curves; (b) comparison of experimental equilibrium adsorption capacity with modeled results.

4.6 References

Bruanuer, S., Emmett, P., & Teller, E. (1938). Adsorption of gases in multimolecular layers. *J. Am. Chem. Soc, 60*, 309-319.

Coker, R., Gomez, C., & Schunk, G. (2015). Multi-Dimensional Adsorption Model of CO2/H2O Sorbent Bed. *COMSOL Conference*. Boston: COMSOL.

Do, D., & Rice, R. (1987). On the relative importance of pore and surface diffusion in non-equilibrium adsorption rate processes. *Chem. Eng. Sci., 42*, 2269-2284.

Haynes, W. (2017). *CRC Handbook of Chemistry and Physics* (97th ed.). Boca Raton, Florida: CRC Press/Taylor & Francis.

Huasheng, G., Dahui, W., Yunchun, Y., & Tian'en, T. (2002). Binary Adsorption Equilibrium of Benzene-Water Vapor Mixtures on Activated Carbon. *Chinese J. Chem. Eng., 10*, 367-370.

Huggahalli, M., & Fair, J. (1996). Prediction of Equilibrium Adsorption of Water onto Activated Carbon. *Ind. Eng. Chem. Res., 35*, 2071-2074.

Kwapinski, W. (2009). Combined wall and thermal effects during nonisothermal packed bed adsorption. *Chem. Eng. J., 152*, 271-276.

Li, C., Xuemin, H., Fangning, F., & Fengli, J. (2010). Effect of relative humidity on adsorption capacity of organic vapors on activated carbon and prediction by the modified D-R equation. *International Conference on Digital Manufacturing & Automation* , (pp. 608-611). Changha, Hunan.

Linders, M., van den Broeke, L., Kapteijn, F., & Moulijn, J. A. (2001). Binary Adsorption Equilibrium of Organics and Water on Activated Carbon. *AIChE J., 47*, 1885-1892.

Marivoet, J., Teodoroiu, P., & Wajc, S. (1974). Porosity, velocity and temperature profiles in cylindrical packed beds. *Chem. Eng. Sci., 29*, 1836-1840.

Nastaj, J., Witkiewicz, K., & Chybowska, M. (2016). Modeling of multicomponent and multitemperature adsorption equilibria of water vapor and organic compounds on activated carbons. *Ads. Sci. Technol., 34*, 144-175.

Okazaki, M., Tamon, H., & Toei, R. (1978). Prediction of binary adsorption equilibria of solvent and water vapor on activated carbon. *J. Chem. Eng. Japan, 11*, 209-215.

Qi, N., Appel, W., & LeVan, M. (2006). Adsorption Dynamics of Organic Compounds and Water Vapor in Activated Carbon Beds. *Ind. Eng. Chem. Res., 45*, 2303-2314.

Schlüter, S., Hennig, T., Schieferstein, E., & Meller, K. (2016). Simulator for Automotive Evaporative Emissions Restraint Systems. *COMSOL Conference*. Munich: COMSOL.

Shaverdi, G. (2012). *Developing a Model for Mass Transfer in Adsorption Packed-bed Filters* . Montreal: Concordia University.

Taqvi, S., Appel, W., & LeVan, M. (1999). Coadsorption of Organic Compounds and Water Vapor on BPL Activated Carbon. 4. Methanol, Ethanol, Propanol, Butanol, and Modeling. *Ind. Eng. Chem. Res., 38*, 240-250.

Tefera, D., Hashisho, Z., Philips, J., Anderson, J., & Nichols, M. (2014). Modeling Competitive Adsorption of Mixtures of Volatile Organic Compounds in a Fixed-Bed of Beaded Activated Carbon. *Environ. Sci. Technol., 48*, 5108-5117.

Tefera, D., Lashaki, M., Fayaz, M., Hashisho, Z., Philips, J., Anderson, J., & Nichols, M. (2013). Two-Dimensional Modeling of Volatile Organic Compounds Adsorption onto Beaded Activated Carbon. *Environ. Sci. Technol., 47*, 11700-11710.

Chapter 5 CONCLUSIONS AND RECOMMENDATIONS

5.1 Thesis Overview

This research investigated the impact of water vapor on VOC adsorption onto AC and developed a suitable 2D thermodynamically consistent model to predict the multicomponent adsorption equilibria and the transfer kinetics during the competitive adsorption process involving a VOC and water vapor. The VOCs selected for this research work were selected based on their polarity and water solubility to evaluate different scenarios during competitive adsorption of polar or non-polar VOC with water vapor.

The model consists of two major components: VOC-water vapor multicomponent adsorption isotherm, and the adsorption transport phenomena. The multicomponent competitive adsorption isotherm was modeled using the Manes method, which was modified for its use with polar VOCs. It is thermodynamically consistent and requires only the single-component adsorption isotherms of the tested VOC and water vapor as inputs. Therefore, the accuracy of the single-component adsorption isotherms, modeled using the MDR and QHR isotherm equations, is highly critical to the success of the Manes method. The MDR and QHR isotherm equations were applied to fit the experimental data of VOC adsorption (type I) and water vapor adsorption (type V) on AC, with an overall r^2 value of 0.998 and 0.999 respectively. The Manes method then predicted the adsorption capacity for VOCs during competitive adsorption with water vapor with an overall MRAE of 5.2% and 1.9% for polar and non-polar VOCs respectively. The method also predicted the water uptake during competitive adsorption with VOC at about 95% RH with an overall MRAE of 40.1% for polar VOCs and 14.9% for non-polar VOCs.

The adsorption transport phenomena model used here is an extension of the model developed by Tefera et al., (2013, 2014). The transfer kinetics simulated here were the adsorbate mass balance in the gas and adsorbed phase, and the heat and momentum balance across the fixed-bed adsorber of BAC particles. The model predicted the VOC breakthrough profile curves during competitive adsorption with water vapor with an overall MRAE (non-zero data points only) of 14.8% for polar VOCs and 15.8% for non-polar VOCs. The experimental and modeled adsorbed bed temperature profiles at the centre of the fixed-bed (r = 0.0 cm, z = 7.5 cm) were also compared, and were found to have an overall MRAE of 2.6% and 1.9% for the tested polar and non-polar VOCs respectively. After the validations of the multicomponent competitive adsorption isotherm, breakthrough and adsorber bed temperature profiles, 2D adsorbed-phase concentration and temperature distribution was generated.

5.2 Conclusions

The model built in this study will help the industry to optimize adsorber design and operating conditions to minimize the severe impact of RH during adsorption of VOCs from gas streams, and will also reduce the number of pilot-scale tests required to optimize the effect of process parameters and variables. The model results were encouraging, especially because it is thermodynamically consistent and its main inputs were independently determined adsorbate and adsorbent properties, adsorber geometry and operating conditions. The work conducted here contributes to a better understanding of the mechanism of the competing polar or non-polar VOC with water vapor molecules during competitive adsorption.

The main conclusions from the VOC-water vapor competitive adsorption equilibria study and modeling are as follows:

- Appreciable impact of RH on VOC adsorption on BAC can only be observed at RH levels higher than 75% due to water vapor's low affinity towards BAC adsorption at RH below those levels.
- Polar VOCs were found to be highly susceptible to RH compared to non-polar VOCs, owing to their low affinity towards BAC and high water-miscibility.
- The impact of RH on a VOC adsorption decreases with higher adsorption affinity of the VOC towards BAC.
- In the case of water uptake during competitive adsorption with VOC on BAC, the amount of water adsorbed increased with the pure VOC adsorption potential and vice versa.

The main conclusions from the study and modeling of the transport processes during competitive adsorption between VOC and water vapor are as follows:

- The changes to the adsorption breakthrough profiles of VOC during competitive adsorption with water vapor on BAC follows the trend of adsorption affinity, with low adsorption-affinity VOCs such as polar VOCs experiencing a higher reduction in bed service time and thereby a faster movement of MTZ, compared to high adsorption-affinity VOCs such as non-polar VOCs.
- Polar VOCs, which experienced a more severe impact of water vapor than the non-polar VOCs during competitive adsorption, had a higher adsorber-bed temperature increase. This is mainly due to the adsorbate(s) loading, heat of adsorption and heat of dissolution (for polar VOCs in the VOC-water vapor mixture).

The extent of the impact of RH on VOC adsorption on BAC is also highly sensitive to the adsorption temperature and the inlet concentrations of the adsorbates in the VOC-water vapor mixture. The model developed here was found to be sensitive towards changes in adsorber bed temperature, inlet gas concentrations, and carrier gas RH simultaneously, signifying its overall utility in optimizing the adsorber service lifetime. The main conclusion from the sensitivity analysis is as follows:

- For a given inlet concentration of VOC and RH level, optimization of adsorber bed temperature is critically important to maintain the balance between the effect of temperature on carrier gas RH and its effect on the bed service time and VOC adsorption capacity.

5.3 Recommendations for Future Work

This research investigated and developed a multicomponent competitive adsorption model to predict the effect of RH on VOC adsorption in a fixed-bed adsorber. Based on the obtained results and conclusions, the following recommendations can be made for future research:

- Many VOC-laden gas streams contain mixtures of VOCs (polar and non-polar) together-with water vapor, which compete for the available adsorption sites. The model developed in this research could be extended further to account for more than one VOC in a VOC-water vapor mixture.
- The model developed here considers the gas mixture to be ideal. Activity coefficients models such as Wilson, UNIQUAC, therefore, can be used and applied to the existing model to generate better results and account for non-ideality of a mixture.

- Thermodynamically-consistent model such as VMC could be applied for predicting multicomponent competitive adsorption equilibria, as it does not need any extension, and the same model can be used for both VOC-VOC systems and VOC-water vapor systems for any number of adsorbates in a mixture. It is mathematically intensive, and needs to be revised for computer simulation.
- The VOC-water vapor competitive adsorption isotherm developed here using Manes method can be applied to different adsorber configurations such as fluidized bed, and moving bed. This could assist in selecting the best adsorber configuration for a particular contaminant capture application.
- The competitive adsorption model built here could also be applied to adsorbents other than AC such as molecular sieves, zeolites, etc., for any kind of single-VOC-water vapor mixtures.

5.4 References

Tefera, D., Hashisho, Z., Philips, J., Anderson, J., & Nichols, M. (2014). Modeling Competitive Adsorption of Mixtures of Volatile Organic Compounds in a Fixed-Bed of Beaded Activated Carbon. *Environ. Sci. Technol., 48*, 5108-5117.

Tefera, D., Lashaki, M., Fayaz, M., Hashisho, Z., Philips, J., Anderson, J., & Nichols, M. (2013). Two-Dimensional Modeling of Volatile Organic Compounds Adsorption onto Beaded Activated Carbon. *Environ. Sci. Technol., 47*, 11700-11710.

WORKS CITED

Aktas, O., & Cecen, F. (2006). Effect of type of carbon activation on adsorption and its reversibility. *J. Chem. Technol. Biot., 81*, 94-101.

Aktas, O., & Cecen, F. (2007). Competitive adsorption and desorption of a bi-solute mixture: Effect of activated carbon type. *Adsorption, 13*, 159-169.

Alcaniz-Monge, J., Linares-Solano, A., & Rand, B. (2002). Mechanism of Adsorption of Water in Carbon Micropores As Revealed by a Study of Activated Carbon Fibers. *J. Phys. Chem. B, 106*, 3209-3216.

Alvarez, P., Garcia-Araya, J., Beltran, F., Masaa, F., & Medina, F. (2005). Ozonation of activated carbons: Effect on the adsorption of selected phenolic compounds from aqueous solutions. *J. Colloid Interf. Sci., 283*, 503-512.

Appel, W., LeVan, M., & Finn, J. (1998). Nonideal adsorption equilibria described by pure component isotherms and virial mixture coefficients. *Ind. Eng. Chem. Res., 37*, 4774-4782.

Bansal, R., & Goyal, M. (2005). *Activated Carbon Adsorption*. Taylor & Francis Group.

Benjamin, M. (2009). New Conceptualization and Solution Approach for the Ideal Adsorbed Solution Theory (IAST). *Environ. Sci. Technol., 43*, 2530-2536.

Bey, O., & Eigenberger, G. (2001). Gas flow and heat transfer through catalyst filled tubes. *Int. J. Therm. Sci., 40*, 152-164.

Bruanuer, S., Emmett, P., & Teller, E. (1938). Adsorption of gases in multimolecular layers. *J. Am. Chem. Soc, 60*, 309-319.

Butler, J., & Ockrent, C. (1930). Studies in Electrocapillarity. Part III. *J. Phys. Chem., 34*, 2841-2859.

Cal, M., Rood, M., & Larson, S. (1996). Removal of VOCs from humidified gas streams using activated carbon cloth. *Gas Sep. Purif., 10*, 117-121.

Calvert, S., & Englund, H. (1984). *Handbook of Air Pollution Technology*. New York: John Wiley & Sons, Inc.

Chahbani, M., & Tondeur, D. (2000). Mass transfer kinetics in pressure swing adsorption. *Sep. Purif. Technol., 20*, 185-196.

Chen, J., Loo, L., & Wang, K. (2011). An Ideal Absorbed Solution Theory (IAST) Study of Adsorption Equilibria of Binary Mixtures of Methane and Ethane on a Templated Carbon. *J. Chem. Eng. Data, 56*, 1209-1212.

Chen, Y., Ritter, J., & Yang, R. (1990). Nonideal Adsorption from Multicomponent Gas Mixtures at Elevated Pressures on a 5A Molecular Sieve. *Chem. Eng. Sci., 45*, 2877-2894.

Chou, M., & Chiou, J. (1997). Modeling effects of moisture on adsorption capacity of activated carbon for VOCs. *J. Environ. Eng., 123*, 437-443.

Chuang, C., Chiang, P., & Chang, E. (2003). Modeling VOCs adsorption onto activated carbon. *Chemosphere, 53*, 17-27.

Cohen, Y., & Metzner, A. B. (1981). Wall effects in laminar flow of fluids through packed beds. *AIChE J., 27*, 705-715.

Coker, R., Gomez, C., & Schunk, G. (2015). Multi-Dimensional Adsorption Model of CO2/H2O Sorbent Bed. *COMSOL Conference*. Boston: COMSOL.

Dabrowski, A., Podkoscielny, P., Hubicki, Z., & Barczak, M. (2005). Adsorption of phenolic compounds by activated carbon - A critical review. *Chemosphere, 58*, 1049-1070.

Dantas, T., Luna, F., Silva Jr., I., Torres, A., de Azevedo, D., Rodrigues, A., & Moreira, R. (2011). Modeling of the fixed-bed adsorption of carbon dioxide and a carbon dioxide-nitrogen mixture on zeolite 13X. *Braz. J. Chem. Eng., 28*, 533-544.

Do, D. (1998). *Adsorption Analysis: Equilibria and Kinetics*. London: Imperial College Press.

Do, D., & Do, H. (2000). A model for water adsorption in activated carbon. *Carbon, 38*, 767-773.

Do, D., & Rice, R. (1987). On the relative importance of pore and surface diffusion in non-equilibrium adsorption rate processes. *Chem. Eng. Sci., 42*, 2269-2284.

Do, D., Junpirom, S., & Do, H. (2009). A new adsorption–desorption model for water adsorption in activated carbon. *Carbon, 47*, 1466-1473.

Dubinin, M., & Radushkevich, L. (1947). The equation of the characteristic curve of the activated charcoal. *Proc. Acad. Sci. USSR Phys. Chem. Sec., 55*, 331-337.

Dubinin, M., & Serpinsky, V. (1981). Isotherm equation for water vapor adsorption by microporous carbonaceous adsorbents. *Carbon, 19*, 402-403.

Efremenko, I., & Sheintuch, M. (2006). Predicting solute adsorption on activated carbon: phenol. *Langmuir, 22*, 3614-3621.

Environment and Climate Change Canada . (2016). *Volatile Organic Compounds in Consumer and Commercial Products*. Retrieved from http://www.ec.gc.ca/cov-voc/Default.asp?lang=En&n=BEE9D2C5-1

Environment and Climate Change Canada. (2016). *Volatile Organic Compound Emissions*. Retrieved from https://www.ec.gc.ca/indicateurs-indicators/default.asp?lang=en&n=64B9E95D-1

Environment and Climate Change Canada. (2016). *Volatile organic compounds that participate in atmospheric photochemical reactions*. Retrieved from http://www.ec.gc.ca/toxiques-toxics/Default.asp?lang=En&n=98E80CC6-1&xml=075320D0-CF6E-4261-890E-90725A29E3C4

Fletcher, A., Kennedy, M., Zhao, X., Bell, J., & Thomas, K. (2006). Adsorption of Organic Vapour Pollutants on Activated Carbon. *Recent Advances in Adsorption Processes for Environmental Protection and Security* (pp. 29-54). Kiev: NATO Science for Peace and Security.

Foo, K., & Hameed, B. (2010). Insights into the modeling of adsorption isotherm systems. *Chem. Eng. J., 156*, 2-10.

Fournel, L., Mocho, P., Brown, R., & Le Cloirec, P. (2010). Modeling breakthrough curves of volatile organic compounds on activated carbon fibers. *Adsorption, 16*, 147-153.

Freundlich, H. (1906). Over the adsorption in solution. *J. Phys. Chem., 57*, 385-471.

Fujisawa, M., Maeda, M., Takagi, S., & Kimura, T. (2002). Enthalpies of dilution of mono-, di- and poly-alcohols in dilute aqueous solutions at 298.15 K. *J. Therm. Anal. Calorim., 69*, 841-848.

Furmaniak, S., Gauden, P., Terzyk, A., & Rychlicki, G. (2008). Water adsorption on carbons — Critical review of the most popular analytical approaches. *Adv. Colloid Interface Sci., 137*, 82-143.

Giraudet, S., Pre´, P., Tezel, H., & Le Cloirec, P. (2006). Estimation of adsorption energies using the physical characteristics of activated carbons and the molecular properties of volatile organic compounds. *Carbon, 44*, 2413-2421.

Gothard, F., Clobanu, M., Breban, D., & Bucur, C. (1976). Predicting the Parameters in the Wilson Equations for Activity Coefficients in Binary Hydrocarbon Systems. *Ind. Eng. Chem. Process Des. Dev., 15*, 333-337.

Grant, R., & Manes, M. (1966). Adsorption of Binary Hydrocarbon Gas Mixtures on Activated Carbon. *Ind. Eng. Chem. Fund., 5*, 490-498.

Gregg, S., & Sing, K. (1982). *Adsorption, Surface Area and Porosity*. New York: Academic Press.

Guenther, A. (1995). A global model of natural volatile organic compound emissions. *J. Geophy. Res., 100*(D5), 8873-8892.

Gun'ko, V., Turov, V., & Kozynchenko, O. (2008). Characteristics of adsorption phase with water/organic mixtures at a surface of activated carbons possessing intraparticle and textural porosities. *App. Surf. Sci., 25*, 3220-3231.

Guo, P. (2012). Dependency of tortuosity and permeability of porous media on directional distribution of pore voids. *Transp. Porous Media, 95*, 285-303.

Gupta, V., & Verma, N. (2002). Removal of volatile organic compounds by cryogenic condensation followed by adsorption. *Chem. Eng. Sci., 57*, 2679-2696.

Haghseresht, F., & Lu, G. (1998). Adsorption characteristics of phenolic compounds onto coal-reject-derived adsorbents. *Energy Fuels, 12*, 1100-1107.

Hashisho, Z., Emamipour, H., Rood, M., Hay, K., Kim, B., & Thurston, D. (2008). Concomitant adsorption and desorption of organic vapor in dry and humid air streams using microwave and direct electrothermal swing adsorption. *Environ. Sci. Technol., 42*, 9317-9322.

Hashisho, Z., Rood, M., & Botich, L. (2005). Microwave-swing adsorption to capture and recover vapors from air streams with activated carbon fiber cloth. *Environ. Sci. Technol., 39*, 6851-6859.

Haynes, W. (2017). *CRC Handbook of Chemistry and Physics* (97th ed.). Boca Raton, Florida: CRC Press/Taylor & Francis.

Hefti, M., Marx, D., Joss, L., & Mazzotti, M. (2015). Adsorption equilibrium of binary mixtures of carbon dioxide and nitrogen on zeolites ZSM-5 and 13X. *Microporous Mesoporous Mater., 215*, 215-228.

Heinonen, J., Landa, H., Sainio, T., & Seidel-Morgenstern, A. (2012). Use of Adsorbed Solution theory to model competitive and co-operative sorption on elastic ion exchange resins. *Sep. Purif. Technol., 95*, 235-247.

Huasheng, G., Dahui, W., Yunchun, Y., & Tian'en, T. (2002). Binary Adsorption Equilibrium of Benzene-Water Vapor Mixtures on Activated Carbon. *Chinese J. Chem. Eng., 10*, 367-370.

Huggahalli, M., & Fair, J. (1996). Prediction of Equilibrium Adsorption of Water onto Activated Carbon. *Ind. Eng. Chem. Res., 35*, 2071-2074.

Hui, C., Chen, B., & McKay, G. (2003). Pore-surface diffusion model for batch adsorption processes. *Langmuir, 19*, 4188-4196.

Hung, C., & Bai, H. (2008). Adsorption behaviors of organic vapors using mesoporous silica particles made by evaporation induced self-assembly method. *Chem. Eng. Sci., 63*, 1997-2005.

Hung, H., & Lin, T. (2007). Prediction of the Adsorption Capacity for Volatile Organic Compounds onto Activated Carbons by the Dubinin–Radushkevich–Langmuir Model. *J. Air & Waste Manage. Assoc., 57*, 497-506.

Hutton, A. G. (2001). Quality and trust in industrial computational fluid dynamics. *Houille Blanche, 3-4*, 25-28.

Ilic, M., Flockerzi, D., & Seidel-Morgenstern, A. (2010). A thermodynamically consistent explicit competitive adsorption isotherm model based on second-order single component behaviour. *J. Chromatogr. A, 1217*, 2132-2137.

Jain, J., & Snoeyink, V. (1973). Adsorption from bisolute systems on active carbon. *J. Water Pollut. Control Fed., 45*, 2463-2479.

Jarvie, M. E., Hand, D. W., Bhuvendralingam, S., Crittenden, J. C., & Hokanson, D. R. (2005). Simulating the performance of fixed-bed granular activated carbon adsorbers: Removal of synthetic organic chemicals in the presence of background organic matter. *Water Res., 39*, 2407-2421.

Joly, A., & Perrard, A. (2009). Linear driving force models for dynamic adsorption of volatile organic compound traces by porous adsorbent beds. *Math. Comp. Sim., 79*, 3492-3499.

Kampa, M., & Castanas, E. (2008). Human health effects of air pollution. *Environ. Pollut., 151*, 362-367.

Kapoor, A., Ritter, J., & Yang, R. (1989). On the Dubinin-Radushkevich Equation for Adsorption in Microporous Solids in the Henry's Law Region. *Langmuir, 5*, 1118-1121.

Kawasaki, N., Kinoshita, H., Oue, T., Nakamura, T., & Tanada, S. (2004). Study on adsorption kinetic of aromatic hydrocarbons onto activated carbon in gaseous flow method. *J. Colloid Interface Sci., 275*, 40-43.

Keener, T., & Zhou, D. (1990). Prediction of Activated Carbon Adsorption Performance Under High Relative Humidity Conditions. *Environ. Progr., 9*, 40-46.

Khan, F., & Ghoshal, A. (2000). Removal of volatile organic compounds from polluted air. *J. Loss Prev. Process Ind., 13*, 527-545.

Kim, B. (2011). VOC emissions from automotive painting and their control: A review. *Environ. Eng. Res., 16*, 1-9.

Kim, P., & Agnihotri, S. (2008). Application of water–activated carbon isotherm models to water adsorption isotherms of single-walled carbon nanotubes. *J. Colloid Interface Sci., 325*, 64-73.

Kister, A., & Waldman, D. (1958). Heat of mixing of acetone with water and with methanol. *J. Phys. Chem., 62*, 245-246.

Kuwagaki, H., Meguro, T., Tatami, J., Komeya, K., & Tamura, K. (2003). An improvement of thermal conduction of activated carbon by adding graphite. *J. Mater. Sci., 38*, 3279-3284.

Kwapinski, W. (2009). Combined wall and thermal effects during nonisothermal packed bed adsorption. *Chem. Eng. J., 152*, 271-276.

Lama, R., & Lu, B.-Y. (1965). Excess Thermodynamic Properties of Aqueous Alcohol Solutions. *J. Chem. Eng. Data, 10*, 216-219.

Landa, H., & Flockerzi, D. (2013). A Method for Efficiently Solving the IAST Equations with an Application to Adsorber Dynamics. *AIChE J., 59*, 1263-1277.

Langmuir, I. (1916). The constitution and fundamental properties of solids and liquids. *J. Am. Chem. Soc., 38*, 2221-2295.

Lapkin, A., Joyce, L., & Crittenden, B. (2004). Framework for evaluating the “Greenness” of chemical processes: Case studies for a novel VOC recovery technology. *Environ. Sci. Technol., 38*, 5815-5823.

Lashaki, M., Atkinson, J., Hashisho, Z., Phillips, J., Anderson, J., & Nichols, M. (2016a). The role of beaded activated carbon's surface oxygen groups onirreversible adsorption of organic vapors. *J. Hazard. Mater., 317*, 284-294.

Lashaki, M., Atkinson, J., Hashisho, Z., Phillips, J., Anderson, J., Nichols, M., & Misovski, T. (2016b). Effect of desorption purge gas oxygen impurity on irreversible adsorption of organic vapors. *Carbon, 99*, 310-317.

Lashaki, M., Fayaz, M., Niknaddaf, S., & Hashisho, Z. (2012b). Effect of the adsorbate kinetic diameter on the accuracy of the Dubinin-Radushkevich equation for modeling adsorption of organic vapors on activated carbon. *J. Hazard. Mater., 241-242*, 154-163.

Lashaki, M., Fayaz, M., Wang, H., Hashisho, Z., Philips, J., Anderson, J., & Nichols, M. (2012a). Effect of Adsorption and Regeneration Temperature on Irreversible Adsorption of Organic Vapors on Beaded Activated Carbon. *Environ. Sci. Technol., 46*, 4083-4090.

Lee, J., Choi, D., Kwak, D., & Jung, H. (2005). Adsorption Dynamics of Water Vapor on Activated Carbon. *Adsorption, 11*, 437-441.

Leethochawalit, M., Bustard, M., Wright, P., & Meeyoo, V. (2001). Novel vapor-phase biofiltration and catalytic combustion of volatile organic compounds. *Ind. Eng. Chem. Res., 40*(23), 5334-5341.

Leslie, G. (2000). Health risks from indoor air pollutants: Public alarm and toxicological reality. *Indoor Built Environ., 9*, 5-16.

Li, C., Xuemin, H., Fangning, F., & Fengli, J. (2010). Effect of relative humidity on adsorption capacity of organic vapors on activated carbon and prediction by the modified D-R equation. *International Conference on Digital Manufacturing & Automation* , (pp. 608-611). Changha, Hunan.

Linders, M., van den Broeke, L., Kapteijn, F., & Moulijn, J. A. (2001). Binary Adsorption Equilibrium of Organics and Water on Activated Carbon. *AIChE J., 47*, 1885-1892.

Lodewyckx, P., & Vansant, E. (1999). Water Isotherms of Activated Carbons with Small Amounts of Surface Oxygen. *Carbon, 37*, 1647-1649.

Logan, D. (1997). Estimating physical properties for control equipment design. *Environ. Prog., 16*, 237-242.

Manes, M. (1984). Estimation of the effects of humidity on the adsorption onto activated carbon of the vapors of water-immiscible organic liquids. *Fundamentals of Adsorption* (pp. 335-344). New York: Engineering Foundation.

Mangano, E., Friedrich, D., & Brandani, S. (2015). Robust Algorithms for the Solution of the Ideal Adsorbed Solution Theory Equations. *AIChE J., 61*, 981-991.

Marivoet, J., Teodoroiu, P., & Wajc, S. (1974). Porosity, velocity and temperature profiles in cylindrical packed beds. *Chem. Eng. Sci., 29*, 1836-1840.

Murillo, R., García, T., Aylón, E., Callén, M., Navarro, M., López, J., & Mastral, A. (2004). Adsorption of Phenanthrene on Activated Carbons: Breakthrough Curve Modeling. *Carbon, 42*, 2009-2017.

Myers, A. (1983). Activity Coefficients of Mixtures Adsorbed on Heterogeneous Surfaces. *AIChE J., 29*, 691-693.

Myers, A. (2005). Prediction of Adsorption of Nonideal Mixtures in Nanoporous Materials. *Adsorption, 11*, 37-42.

Myers, A., & Prausnitz, J. (1965). Thermodynamics of Mixed-Gas Adsorption. *AIChE J., 11*, 121-126.

Myers, A., & Valenzuela, D. (1986). Computer Algorithm and Graphical Method for Calculating Adsorption Equilibria of Gas Mixtures. *J. Chem. Eng. Jap., 19*, 392-395.

Nastaj, J., Witkiewicz, K., & Chybowska, M. (2016). Modeling of multicomponent and multitemperature adsorption equilibria of water vapor and organic compounds on activated carbons. *Ads. Sci. Technol., 34*, 144-175.

National Toxicology Program. (2016). *14th Report on Carcinogens*. Retrieved from https://ntp.niehs.nih.gov/pubhealth/roc/index-1.html

Nemec, D., & Levec, J. (2005). Flowthrough packed bed reactors: 2. Two-phase concurrent downflow. *Chem. Eng. Sci., 60*, 6958-6970.

Nield, D., & Bejan, A. (2006). *Convection in Porous Media*. New York: Springer.

Oberkampf, W., & Trucano, T. (2002). Verification and validation in computational fluid dynamics. *Prog. Aerospace Sci., 38*, 209-272.

O'Brien, J., & Myers, A. (1985). Rapid Calculations of Multicomponent Adsorption Equilibria from Pure Isotherm Data. *Ind. Eng. Chem. Process Des. Dev., 24*, 1188-1191.

Okazaki, M., Tamon, H., & Toei, R. (1978). Prediction of binary adsorption equilibria of solvent and water vapor on activated carbon. *J. Chem. Eng. Japan, 11*, 209-215.

Oliemans, R. (2000). ERCOFTAC's role in promoting computational fluid dynamics. *Houille Blanche, 7-8*, 43-46.

Papasavva, S., Kia, S., Claya, J., & Gunther, R. (2001). Characterization of automotive paints: An environmental impact analysis. *Prog. Org. Coat., 43*, 193-206.

Pelekani, C., & Snoeyink, V. (1999). Competitive adsorption in natural water: role of activated carbon pore size. *Water Res., 33*, 1209-1219.

Piccot, S. D., Watson, J. J., & Jones, J. W. (1992). A global inventory of volatile organic compound emissions from anthropogenic sources. *J. Geophy. Res., 97*(D9), 9897-9912.

Popescu, M., Joly, J. P., Carre, J., & Danatoiu, C. (2003). Dynamical adsorption and temperature-programmed desorption of VOCs (toluene, butyl acetate and butanol) on activated carbons. *Carbon, 41*, 739-748.

Pramar, G., & Rao, N. (2009). Emerging control technologies for volatile organic compounds. *Cri. Rev. Environ. Sci. Technol., 39*, 41-78.

Puértolas, B., López, M., Navarro, M., López, J., Murillo, R., García, T., & Mastral, A. (2010). Modelling the breakthrough curves obtained from the adsorption of propene onto microporous inorganic solids. *Ads. Sci Technol., 28*, 761-775.

Qi, N., & LeVan, M. (2005a). Coadsorption of Organic Compounds and Water Vapor on BPL Activated Carbon. 5. Methyl Ethyl Ketone, Methyl Isobutyl Ketone, Toluene, and Modeling. *Ind. Eng. Chem. Res., 44*, 3733-3741.

Qi, N., & LeVan, M. (2005b). Adsorption equilibrium modeling for water on activated carbons. *Carbon, 43*, 2258-2263.

Qi, N., Appel, W., & LeVan, M. (2006). Adsorption Dynamics of Organic Compounds and Water Vapor in Activated Carbon Beds. *Ind. Eng. Chem. Res., 45*, 2303-2314.

Qi, S., Hay, K., & Cal, M. (2000b). Predicting humidity effect on adsorption capacity of activated carbon for water-immiscible organic vapors. *Adv. Environ. Res., 4*, 357-362.

Qi, S., Hay, K., & Rood, M. (1998). Isotherm Equation for Water Vapor Adsorption onto Activated Carbon. *J. Environ. Eng., 124*, 1130-1134.

Qi, S., Hay, K., Rood, M., & Cal, M. (2000a). Equilibrium and Heat of Adsorption for Water Vapor and Activated Carbon. *J. Environ. Eng., 126*, 267-271.

Ramos, M., Bonelli, P., Cukierman, A., Ribeiro Carrott, M., & Carrott, P. (2010). Adsorption of volatile organic compounds onto activated carbon cloths derived from a novel regenerated cellulosic precursor. *J. Hazard. Mater., 177*, 175-182.

Richter, E., Schutz, W., & Myers, A. (1989). Effect of Adsorption Equation on Prediction of Multicomponent Adsorption Equilibria by the Ideal Adsorbed Solution Theory. *Chem. Eng. Sci., 44*, 1609-1616.

Russell, B., & LeVan, M. (1997). Coadsorption of Organic Compounds and Water Vapor on BPL Activated Carbon. 3. Ethane, Propane, and Mixing Rules. *Ind. Eng. Chem. Res., 36*, 2380-2389.

Sakuth, M., Meyer, J., & Gmehling, J. (1998). Measurement and prediction of binary adsorption equilibria of vapors on dealuminated Y-zeolites (DAY). *Chem. Eng. Process, 37*, 267-277.

Salame, I., & Bandosz, T. (1999). Experimental Study of Water Adsorption on Activated Carbons. *Langmuir, 15*, 587-593.

Schlüter, S., Hennig, T., Schieferstein, E., & Meller, K. (2016). Simulator for Automotive Evaporative Emissions Restraint Systems. *COMSOL Conference*. Munich: COMSOL.

Shaverdi, G. (2012). *Developing a Model for Mass Transfer in Adsorption Packed-bed Filters* . Montreal: Concordia University.

Shi, Y., Lee, Y., & Kim, A. (2012). Knudsen Diffusion Through Cylindrical Tubes of Varying Radii: Theory and Monte Carlo Simulations. *Transp. Porous Media, 93*, 517-541.

Shonnard, D., & Hiew, D. (2000). Comparative environmental assessments of VOC recovery and recycle design alternatives for a gaseous waste stream. *Environ. Sci. Technol., 34*, 5222-5228.

Simon, C., Smit, B., & Haranczyk, M. (2016). pyIAST: Ideal adsorbed solution theory (IAST) Python package. *Comput. Phys. Commun., 200*, 364-380.

Siperstein, F., & Myers, A. (2001). Mixed-Gas Adsorption. *AIChE J., 47*, 1141-1159.

Sircar, S., & Hufton, J. R. (2000). Why does the linear driving force model for adsorption kinetics work? *Adsorption, 6*, 137-147.

Slasli, A., Jorge, M., Stoeckli, F., & Seaton, N. (2003). Water adsorption by activated carbons in relation to their microporous structure. *Carbon, 41*, 479-486.

Sontheimer, H., Crittenden, J., & Summers, S. (1988). *Activated carbon for water treatment* (2nd ed.). Karlsruhe: DVGW-Forschungsstelle, Engler-Bunte-Institut, Universität Karlsruhe.

Stoeckli, F. (2002). Water adsorption in activated carbons of various degrees of oxidation described by the Dubinin equation. *Carbon, 40*, 969-971.

Stoeckli, F., Jakubov, T., & Lavanchy, A. (1994). Water Adsorption in Active Carbons described by the Dubinin-Astakhov Equation. *J. Chem. Soc. Faraday. Trans., 90*, 783-786.

Sullivan, P., Stone, B., Hashisho, Z., & Rood, M. (2007). Water adsorption with hysteresis effect onto microporous activated carbon fabrics. *Adsorption, 13*, 173-189.

Suwanayuen, S., & Danner, R. (1980). A gas adsorption isotherm equation based on vacancy solution theory. *AIChE J., 26*, 68-76.

Suzuki, M. (1990). *Adsorption Engineering*. Amsterdam: Elsevier Science Publishing Company, Inc.

Talu, O., & Meunier, F. (1996). Adsorption of Associating Molecules in Micropores and Application to Water on Carbon. *AIChE J., 42*, 809-819.

Talu, O., & Zwiebel, I. (1986). Multicomponent Adsorption Equilibria of Nonideal Mixtures. *AIChE J., 32*, 1263-1276.

Talu, O., & Zwiebel, I. (1987). Spreading Pressure Dependent Equation for Adsorbate Phase Acitivity Coefficients. *React. Polym., 5*, 81-91.

Talu, O., Li, J., & Myers, A. (1995). Activity Coefficients of Adsorbed Mixtures. *Adsorption, 1*, 103-112.

Tao, W., Yang, T., Chang, Y., Chang, L., & Chung, T. (2004). Effect of Moisture on the Adsorption of Volatile Organic Compounds by Zeolite 13X. *J. Environ. Eng., 130*, 1210-1216.

Taqvi, S., & LeVan, M. (1997). Virial Description of Two-Component Adsorption on Homogeneous and Heterogeneous Surfaces. *Ind. Eng. Chem. Res., 36*, 2197-2206.

Taqvi, S., Appel, W., & LeVan, M. (1999). Coadsorption of Organic Compounds and Water Vapor on BPL Activated Carbon. 4. Methanol, Ethanol, Propanol, Butanol, and Modeling. *Ind. Eng. Chem. Res., 38*, 240-250.

Tefera, D., Hashisho, Z., Philips, J., Anderson, J., & Nichols, M. (2014). Modeling Competitive Adsorption of Mixtures of Volatile Organic Compounds in a Fixed-Bed of Beaded Activated Carbon. *Environ. Sci. Technol., 48*, 5108-5117.

Tefera, D., Lashaki, M., Fayaz, M., Hashisho, Z., Philips, J., Anderson, J., & Nichols, M. (2013). Two-Dimensional Modeling of Volatile Organic Compounds Adsorption onto Beaded Activated Carbon. *Environ. Sci. Technol., 47*, 11700-11710.

The European Union. (2004). *Directive 2004/42/CE of the European Parliament and the Council*. Retrieved from http://eur-lex.europa.eu/LexUriServ/LexUriServ.do?uri=OJ:L:2004:143:0087:0096:EN:PDF

Thomas, W., & Crittenden, B. (1998). *Adsorption Technology and Design*. Boston: Butterworth Publishers.

Tien, C. (2013). *Adsorption Calculations and Modelling*. Butterworth-Heinemann.

Underhill, D., & Kawar, K. (1999). Effect of Relative Humidity on the Adsorption of Selected Water-Miscible Organic Vapors by Activated Carbon. *AIHA J., 60*, 730-736.

United States Environmental Protection Agency. (2016). *Volatile Organic Compounds' Impact on Indoor Air Quality*. Retrieved from https://www.epa.gov/indoor-air-quality-iaq/volatile-organic-compounds-impact-indoor-air-quality#Sources

United States Environmental Protection Agency. (2017). *Technical Overview of Volatile Organic Compounds*. Retrieved from https://www.epa.gov/indoor-air-quality-iaq/technical-overview-volatile-organic-compounds#5

Vahabi, M., Mehdizadeh, E., Kabganian, M., & Barazandeh, F. (2011). Experimental identification of IPMC actuator parameters through incorporation of linear and nonlinear least squares methods. *Sens. Actuators A Phys., 168*, 140-148.

Van Ness, H. (1969). Adsorption of gases on solids: Review of the role of thermodynamics. *Ind. Eng. Chem. Fundam., 8*, 464-473.

Wang, H., Lashaki, M., Fayaz, M., Hashisho, Z., Phillips, J., Anderson, J., & Nichols, M. (2012). Adsorption and Desorption of Mixtures of Organic Vapors on Beaded Activated Carbon. *Environ. Sci. Technol., 46*, 8341-8350.

Weber, W., & Smith, E. (1987). Simulation and design models for adsorption processes. *Environ. Sci Technol., 21*, 1040-1050.

WHO. (1989). Indoor air quality: organic pollutants. Report on a WHO meeting. *EURO Rep Stud, 111*, 1-70.

Willmott, C., & Matsuura, K. (2005). Advantages of the mean absolute error (MAE) over the root mean square error (RMSE) in assessing average model performance. *Clim. Res., 30*, 79-82.

Wood, G. (2000). *Review of Models for Adsorption of Single Vapors, Mixtures of Vapors, and Vapors at High Humidities on Activated Carbon for Applications including Predicting Service Lives of Organic Vapor Respirator Cartridges*. Washington, D.C.: Los Alamos National Laboratory.

Xu, Z., Cai, J., & Pan, B. (2013). Mathematically modeling fixed-bed adsorption in aqueous systems. *J. Zhejiang Univ. Sci. A, 16*, 147-153.

Yang, R. (1987). *Gas Separation by Adsorption Processes*. Stoneham, Massachusetts: Butterworth Publishers.

Yang, R. (2003). *Adsorbents: Fundamentals and Application*. New Jersey: John Wiley & Sons, Inc.

Ye, X., Qi, N., & LeVan, M. (2003). Prediction of adsorption equilibrium using a modified D-R equation: organic-water vapor mixtures on BPL carbon. *Carbon, 41*, 2519-2525.

Yun, J., Park, H., & Moon, H. (1996). Multicomponent Adsorption Calculations Based on Adsorbed Solution Theory. *Korean J. Chem. Eng., 13*, 246-254.

APPENDIX A MATLAB CODE FOR MANES METHOD

```
%%
%Imranul Islam Laskar
%Content first created: 1 July 2016
%% Declaring global variables for the program
tic
global R T P C
R = 8.314; %Gas constant in J/K/mol
T = 298.15; %Adsorption temperature in Kelvin
P = 101.325; %Adsorption pressure in kPa, 101.325 kPa = 1 atm
C = R*T;

%% **Modified Dubinin-Raduskevich (MD-R) Curve Fitting for 2- Propanol**

Psv = 5.866; %Saturated pressure of 2- Propanol in kPa at 25degC and P (From Sigma
Aldrich)
MWv = 60.095; %Molecular weight of 2- Propanol in g/mol (HCP)
Dv = 0.772; %Liquid Density of 2- Propanol in g/cc at T and P (From Sigma Aldrich)
MVv = MWv/Dv; %Molar volume of 2- Propanol at T and P

erpv = [0.00 0.01 0.02 0.03 0.04 0.05 0.10 0.20 0.30 0.40 0.50 0.60 0.70...
   0.80 0.90]; %p/ps, relative pressure
eqsv = [0 0.231687679 0.284011059 0.313108692 0.329777718 0.340868721...
    0.3635075 0.376392517 0.38177494 0.385461082 0.389114571...
    0.391626358 0.393583603 0.395638695 0.397791595];
   %experimental maximum 2- Propanol adsorbed per gram of adsorbent,g/g

calcqsv = @(c,erpv) (1-exp(-(c(1).*erpv))).*(c(2).*(exp(-(((C/c(3)).^2)...
     .*((log(erpv)).^2)))))+(exp(-(c(1).*erpv))).*(c(4).*erpv);
%calculated maximum 2- Propanol adsorbed per gram of adsorbent,g/g
c0 = [10,0.55,2000,0.2]; %Initial guesses of D-R parameters, c(1),c(2),c(3),c(4)
c = lsqcurvefit(calcqsv,c0,erpv,eqsv); %MD-R parameters optimization
Z=c(2).*(0.775./0.785);
```

```
%% **Qi-Hay-Rood Water Isotherm Curve Fitting**

Psw = 3.17; %Saturated pressure of Water in kPa at T and P (From HCP)
MWw = 18.015; %Molecular weight of Water in g/mol (From HCP)
Dw = 0.90; %Solid Density of Water in g/cc at T and P (From HCP)
MVw = MWw/Dw; %Molar volume of Water at T and P

erpw = [0.0006 0.0489 0.1010 0.1494 0.1999 0.2502 0.2995 0.3499 0.3992...
    0.4491 0.4990 0.5488 0.5990 0.6497 0.7007 0.7497 0.7998 0.8493...
    0.8993]; %p/ps, relative pressure
eqsw = [0.0000 0.0003 0.0006 0.0013 0.0021 0.0028 0.0037 0.0052 0.0074...
    0.0113 0.0164 0.0247 0.0618 0.1516 0.2963 0.4135 0.4324 0.4384...
    0.4425];
%experimental maximum water adsorbed per gram of adsorbent,g/g

calcqsw = @(k,erpw) (k(1)./(1 + exp(k(2).*(((k(3)./Psw)-erpw)))));
%calculated maximum water adsorbed per gram of adsorbent,g/g
k0 = [0.3,15,1]; %Initial guesses of Q-H-R parameters, c(1),c(2), and c(3)
k = lsqcurvefit(calcqsw,k0,erpw,eqsw); %Q-H-R parameters optimization

%% **Competitive adsorption of carrier gas humidity with 2- Propanol, Polanyi-based model**
i=1;
j=1;
for rpv = 0:0.0006:0.012     %reduced iterations
  for rpw = 0.95 %reduced iterations
    T1=298.15;
    B = R*T1;
    qv = (1-exp(-(c(1).*rpv))).*(Z.*(exp(-(((B/c(3)).^2)...
      .*((log(rpv)).^2)))))+(exp(-(c(1).*rpv))).*(c(4).*rpv);

    Vv = qv./Dv;
```

```
qw = (k(1)./(1 + exp(k(2).*(((k(3)./3)-rpw)))));
Vw = qw./Dw;

if (rpv==0.0000 & rpw==0.0000)
   Qv(i,j) = 0;
   Qw(i,j) = 0;
   plot3(rpv,rpw,Qv(i,j),'mo',rpv,rpw,Qw(i,j),'bo')
   xlabel('Relative vapor pressure of 2- Propanol')
   ylabel('Relative vapor pressure of Water')
   zlabel('Amount Adsorbed,(g/g)')
   legend('2- Propanol Loading','Water Loading')
   j=j+1;
   grid on
   grid minor
   hold on
   continue
elseif (rpv==0.0000 & (Vw>Vv))
   Qv(i,j) = 0;
   Qw(i,j) = qw;
   plot3(rpv,rpw,Qv(i,j),'mo',rpv,rpw,Qw(i,j),'bo')
   grid on
   grid minor
   hold on
   j=j+1;
   continue
elseif ((Vv>Vw))
   Qw(i,j) = 0;
   Qv(i,j) = qv;
   plot3(rpv,rpw,Qv(i,j),'mo',rpv,rpw,Qw(i,j),'bo')
   grid on
   grid minor
   hold on
```

```
  j=j+1;
  continue
elseif ((Vw>Vv))
  for g2 = rpv:-0.000001:0.0000001
    qv1 = (1-exp(-(c(1).*g2))).*(Z.*(exp(-(((C/c(3)).^2)...
      .*((log(g2)).^2)))))+(exp(-(c(1).*g2))).*(c(4).*g2);
    Vv1 = qv1./Dv;
    Av = C.*(log(1./g2));
    J1 = Av./MVv;
    rpw1 = (k(3)./Psw)-((1./k(2)).*(log((k(1)./Vv1)-1)));
    Aw = C.*(log(1./rpw1));
    J2 = Aw./MVw;
    J3 = (C./MVw).*(log(rpw));
    J = J1-J2-J3;
    J4 = ((J.*MVv)./C);
    J5 = exp(J4);
    g3 = (1./J5);
    Qv(i,j) = qv1;
    Qw(i,j) = (Dw.*(Vw-Vv1));
    if ((g3-rpv)<=0.00000001)

      break

    else continue
    end
  end

  plot3(rpv,rpw,Qv(i,j),'k*',rpv,rpw,Qw(i,j),'y*')

      grid on
      grid minor
      hold on
```

```
                    j=j+1;
                    continue

        end
    end
    i=i+1;
end
toc
```